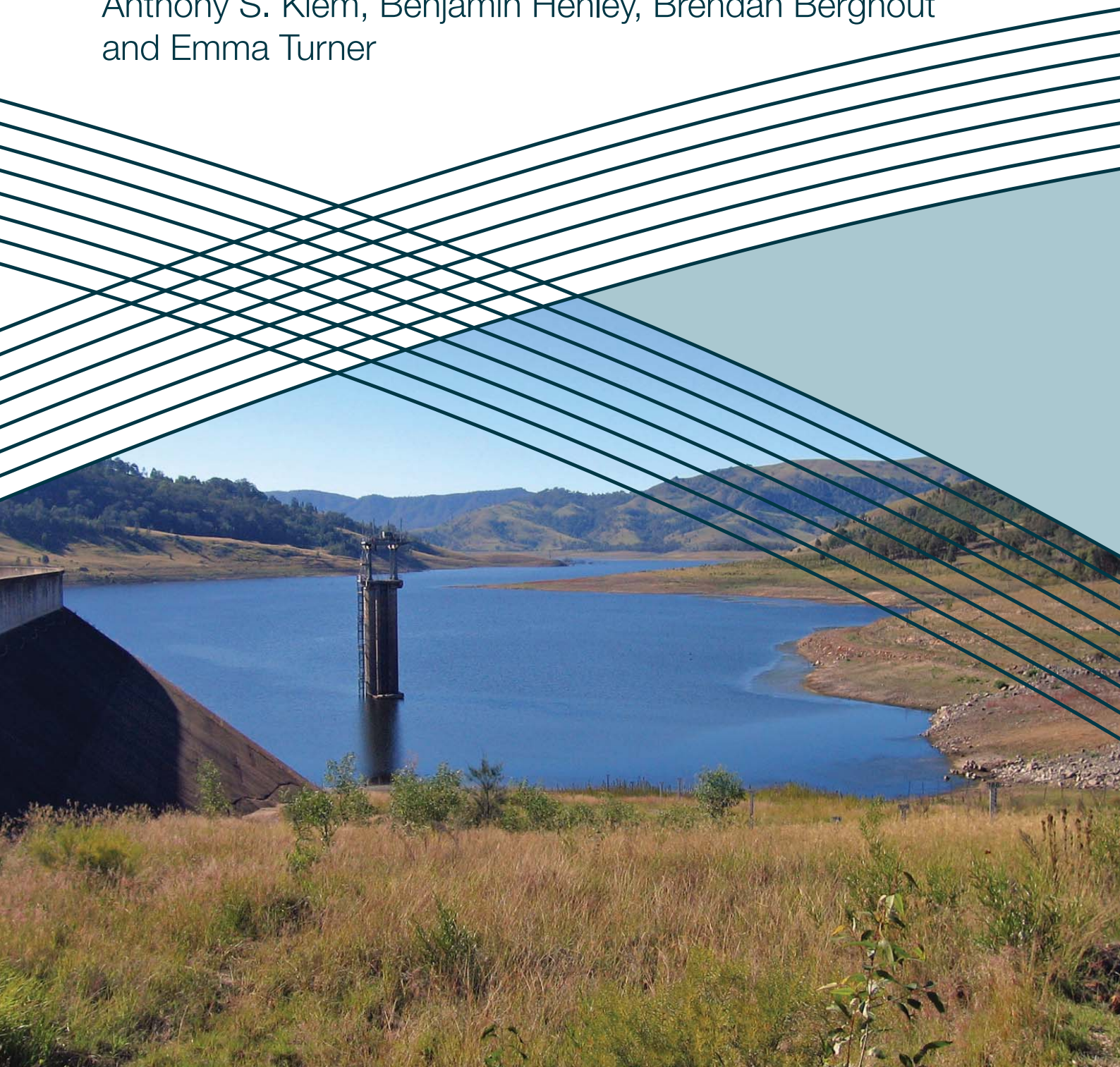


Robust optimisation of urban drought security for an uncertain climate

Final Report

Mohammad Mortazavi-Naeini, George Kuczera,
Anthony S. Kiem, Benjamin Henley, Brendan Berghout
and Emma Turner



Robust optimisation of urban drought security for an uncertain climate

University of Newcastle

AUTHORS

Mohammad Mortazavi-Naeini (University of Newcastle)

George Kuczera (University of Newcastle)

Anthony S. Kiem (University of Newcastle)

Benjamin Henley (University of Newcastle)

Brendan Berghout (Hunter Water Corporation)

Emma Turner (Hunter Water Corporation)



Published by the National Climate Change Adaptation Research Facility

ISBN: 978-1-925039-68-9

NCCARF Publication 97/13

© 2013 University of Newcastle

This work is copyright. Apart from any use as permitted under the Copyright Act 1968, no part may be reproduced by any process without prior written permission from the copyright holder.

Please cite this report as:

Mortazavi, M, Kuczera, G, Kiem, AS, Henley, B, Berghout, B, Turner, E, 2013 *Robust optimisation of urban drought security for an uncertain climate*. National Climate Change Adaptation Research Facility, Gold Coast, pp.74.

Acknowledgement

This work was carried out with financial support from the Australian Government (Department of Climate Change and Energy Efficiency) and the National Climate Change Adaptation Research Facility.

The role of NCCARF is to lead the research community in a national interdisciplinary effort to generate the information needed by decision-makers in government, business and in vulnerable sectors and communities to manage the risk of climate change impacts.

Disclaimer

The views expressed herein are not necessarily the views of the Commonwealth or NCCARF, and neither the Commonwealth nor NCCARF accept responsibility for information or advice contained herein.

Á
Ô[ç^!Á æ ^Á| ^} } a•Á! ^\ Áæ Á[] ^!ã @ÁÁ ÁS^^* æ ÉQa! Á! ^æ Á! { { [] •Á

TABLE OF CONTENTS

ABSTRACT	1
EXECUTIVE SUMMARY	2
1. OBJECTIVES OF THE RESEARCH	4
2. RESEARCH ACTIVITIES AND METHODS	5
2.1 <i>Robust Multi-Criterion Optimisation</i>	<i>5</i>
2.1.1 <i>Motivation</i>	<i>5</i>
2.1.2 <i>A Generic Formulation</i>	<i>8</i>
2.1.3 <i>Multi-Objective Evolutionary Algorithms</i>	<i>9</i>
2.2 <i>Overview of Lower Hunter Case Study</i>	<i>13</i>
2.3 <i>Stochastic Generation of Historic and Future Climate Scenarios</i>	<i>15</i>
2.3.1 <i>Stochastic generation of daily rainfall and evapotranspiration scenarios</i>	<i>16</i>
2.3.2 <i>Rainfall-Runoff Modelling</i>	<i>21</i>
2.4 <i>Lower Hunter Bulk Water System Simulation Model</i>	<i>26</i>
2.4.1 <i>Current HWC Model</i>	<i>26</i>
2.4.2 <i>Overview of WATHNET5</i>	<i>26</i>
2.4.3 <i>Daily WATHNET5 Model of Current Lower Hunter Bulk Water System</i>	<i>29</i>
2.4.4 <i>Validation of Daily WATHNET5 Model</i>	<i>34</i>
2.4.5 <i>Monthly WATHNET5 Model</i>	<i>36</i>
2.5 <i>Formulation of the Robust Optimisation Problem for the Lower Hunter System</i>	<i>40</i>
2.5.1 <i>Generalising the monthly WATHNET5 model</i>	<i>40</i>
2.5.2 <i>Decisions</i>	<i>42</i>
2.5.3 <i>Objective Functions</i>	<i>45</i>
2.5.4 <i>Constraints</i>	<i>48</i>
2.5.5 <i>Improving Computational Performance</i>	<i>48</i>
3. RESULTS AND OUTPUTS	50
3.1 <i>No-Climate-Change Optimisation</i>	<i>50</i>
3.1.1 <i>No-Climate-Change 2060 Demand Scenario</i>	<i>50</i>
3.1.2 <i>No-Climate-Change 2 x Current Demand Scenario</i>	<i>53</i>
3.1.3 <i>Sensitivity to Restriction Social Costs</i>	<i>55</i>
3.2 <i>Robust Optimisation for an Uncertain Future Climate</i>	<i>58</i>
3.2.1 <i>Uncertain-2070-Climate, 2060-Demand Scenario</i>	<i>58</i>
3.2.2 <i>Uncertain-2070-Climate, 2 x Current Demand Scenario</i>	<i>61</i>

3.3	<i>Concluding Remarks</i>	64
4.	END USER PERSPECTIVE ON THE OPTIMISATION METHODOLOGY	65
4.1	<i>Define the study area</i>	66
4.2	<i>Develop a bulk water system simulation model</i>	66
4.3	<i>Augment the bulk water system simulation model with decision variables (e.g. water supply or demand management options)</i>	66
4.4	<i>Derive climate data</i>	66
4.5	<i>Define objective functions</i>	66
4.6	<i>Environmental objectives</i>	67
4.7	<i>Define constraints</i>	68
4.8	<i>Select an optimiser software package</i>	68
4.9	<i>Run the optimiser</i>	68
4.10	<i>Further analysis</i>	69
5.	GAPS AND FUTURE RESEARCH DIRECTIONS	70
	REFERENCES	72

List of figures

Figure 1	<i>Trade-off between expected cost and spread of costs across scenarios.</i>	6
Figure 2	<i>Schematic of ϵ-dominance concept</i>	10
Figure 3	<i>Illustration of ϵ-dominance concept for minimising f_1 and f_2</i>	10
Figure 4	<i>Illustration of Pareto front in conjunction with the ϵ-dominance concept</i>	11
Figure 5	<i>Schematic of ϵMOEA</i>	12
Figure 6	<i>Map of existing Lower Hunter bulk water system</i>	14
Figure 7	<i>Schematic of Lower Hunter water sources</i>	15
Figure 8	<i>Map of Lower Hunter catchments</i>	17
Figure 9	<i>SimHyd schematic</i>	222
Figure 10	<i>Multi-year overlapping aggregated totals for Seaham Residual runoff for historic and stochastically generated data using stochastic model calibrated to historic data</i>	24
Figure 11	<i>Annual autocorrelograms for Seaham Residual runoff for historic and stochastically generated data using stochastic model calibrated to historic data</i>	25
Figure 12	<i>A simple network in WATHNET5</i>	28
Figure 13	<i>Full network including hidden arcs and nodes for network shown in Figure 12</i>	28
Figure 14	<i>Carryover arcs input box</i>	29
Figure 15	<i>Schematic of current Hunter water supply modeled by WATHNET5</i>	29
Figure 16	<i>Schematic of Chichester subsystem</i>	30
Figure 17	<i>Tomago Sandbeds subsystem</i>	32
Figure 18	<i>Demand subsystem</i>	33
Figure 19	<i>Comparison of Chichester reservoir volumes simulated by daily WATHNET5 and HWC models</i>	34
Figure 20	<i>Comparison of Grahamstown reservoir volumes simulated by daily WATHNET5 and HWC models</i>	35
Figure 21	<i>Comparison of Tomago total bucket volumes simulated by daily WATHNET5 and HWC models</i>	35

Figure 22 Scatter plot of monthly Seaham weir inflow volume and maximum possible monthly volume pumped to Grahamstown	36
Figure 23 Schematic of monthly WATHNET5 model	37
Figure 24 Chichester reservoir volume distributions derived from daily and monthly WATHNET5 models	38
Figure 25 Grahamstown reservoir volume distributions derived from daily and monthly WATHNET5 models.	38
Figure 26 Tomago upper bucket volume distributions derived from daily and monthly WATHNET5 models	39
Figure 27 Tomago lower bucket volume distributions derived from daily and monthly WATHNET5 models	39
Figure 28 WATHNET5 schematic of the generalized Lower Hunter model	41
Figure 29 Pareto optimal solutions for the no-climate-change 2060 demand scenario (92GL/year)	51
Figure 30 Time series plot of supplied demand for the worst 50-year replicate: Top panel corresponds to solution 1; bottom panel corresponds to solution 4	53
Figure 31 Pareto optimal solutions for the no-climate-change 2 x current demand scenario	54
Figure 32 Pareto optimal solutions for different restriction cost factors for the no-climate-change 2 x current demand scenario (144GL/year)	56
Figure 33 Pareto optimal solutions for different emergency restriction social cost ranges for the no-climate-change 2 x current demand scenario (144GL/year)	57
Figure 34 Robust Pareto optimal solutions for the 2060 demand scenario (92GL/year)	58
Figure 35 Total storage (%) time series for worst-drought replicate in solution 1 of Figure 34	60
Figure 36 Robust Pareto optimal solutions for the 2060 demand scenario (92GL/year) for two cases	60
Figure 37 Robust Pareto optimal solutions for the 2 x current demand scenario (144GL/year)	61
Figure 38 Time series plots for worst-drought replicate for solution 1 of Figure 37: Top panel – total storage (%); middle panel – desalination production (ML/month); bottom panel – supplied demand (ML/month)	63
Figure 39 Process for applying the optimisation methodology	65

List of tables

Table 1 Ratio of statistic calculated on historical data (122 years) to the average of the same statistic for stochastically generated data (mean of 100 replicates of 122 years)	18
Table 2 Ratio (mean of 100 replicates of 122 years divided by 122 year history) of Lag 0 cross correlation in annual (sum of three month seasons) total rainfall and PET	19
Table 3 Climate change factors (% change to 1990 baseline mean) used in this study	20
Table 4 Description of SimHyd model parameters and initial states	21
Table 5 SimHyd model parameters and initial states for each functional unit of the nine HWC sub catchments	23
Table 6 Chichester Trunk Gravity Main Restrictions (SKM, 2003)	31
Table 7 Possible restriction policy for Lower Hunter water system	33
Table 8 List of decision variables	44
Table 9 Capital cost summary	47
Table 10 Summary of operating costs	47
Table 11 Restriction cost summary	47
Table 12 Costs associated with emergency rationing	47
Table 13 Summary of labelled solutions on Pareto front in Figure 29	52
Table 14 Summary of labelled solutions on Pareto front in Figure 31	55
Table 15 Summary of three solutions with similar expected emergency restriction costs on Pareto fronts in Figure 30	57
Table 16 Summary of labelled solutions on Pareto front in Figure 34	59
Table 17 Summary of labelled solutions on Pareto front in Figure 37	62

ABSTRACT

Recent experience with drought and a shifting climate has highlighted the vulnerability of urban water supplies to “running out of water” in Perth, south-east Queensland, Sydney, Melbourne and Adelaide and has triggered major investment in water source infrastructure which ultimately will run into tens of billions of dollars. With the prospect of continuing population growth in major cities, the provision of acceptable drought security will become more pressing particularly if the future climate becomes drier.

Decision makers need to deal with significant uncertainty about future climate and population. In particular the science of climate change is such that the accuracy of model predictions of future climate is limited by fundamental irreducible uncertainties. It would be unwise to unduly rely on projections made by climate models and prudent to favour solutions that are robust across a range of possible climate futures.

This study presents and demonstrates a methodology that addresses the problem of finding “good” solutions for urban bulk water systems in the presence of deep uncertainty about future climate. The methodology involves three key steps: 1) Build a simulation model of the bulk water system; 2) Construct replicates of future climate that reproduce natural variability seen in the instrumental record and that reflect a plausible range of future climates; and 3) Use multi-objective optimisation to efficiently search through potentially trillions of solutions to identify a set of “good” solutions that optimally trade-off expected performance against robustness or sensitivity of performance over the range of future climates.

A case study based on the Lower Hunter in New South Wales demonstrates the methodology. It is important to note that the case study does not consider the full suite of options and objectives; preliminary information on plausible options has been generalised for demonstration purposes and therefore its results should only be used in the context of evaluating the methodology. “Dry” and “wet” climate scenarios that represent the likely span of climate in 2070 based on the A1F1 emissions scenario were constructed. Using the WATHNET5 model, a simulation model of the Lower Hunter was constructed and validated. The search for “good” solutions was conducted by minimising two criteria, 1) the expected present worth cost of capital and operational costs and social costs due to restrictions and emergency rationing, and 2) the difference in present worth cost between the “dry” and “wet” 2070 climate scenarios. The constraint was imposed that solutions must be able to supply (reduced) demand in the worst drought. Two demand scenarios were considered, “1.28 x current demand” representing expected consumption in 2060 and “2 x current demand” representing a highly stressed system. The optimisation considered a representative range of options including desalination, new surface water sources, demand substitution using rainwater tanks, drought contingency measures and operating rules.

It was found the sensitivity of solutions to uncertainty about future climate varied considerably. For the “1.28 x demand” scenario there was limited sensitivity to the climate scenarios resulting in a narrow range of trade-offs. In contrast, for the “2 x demand” scenario, the trade-off between expected present worth cost and robustness was considerable. The main policy implication is that (possibly large) uncertainty about future climate may not necessarily produce significantly different performance trajectories. The sensitivity is determined not only by differences between climate scenarios but also by other external stresses imposed on the system such as population growth and by constraints on the available options to secure the system against drought.

EXECUTIVE SUMMARY

Recent experience with drought and a shifting climate has highlighted the vulnerability of urban water supplies to “running out of water” in Perth, south-east Queensland, Sydney, Melbourne and Adelaide and has triggered major investment in water source infrastructure which ultimately will run into tens of billions of dollars. With the prospect of continuing population growth in major cities, the provision of acceptable drought security will become more pressing particularly if the future climate becomes drier.

Decision makers need to deal with significant uncertainty about future climate (which affects supply) and population pressures (which affect the demand placed on the system). In particular the science of climate change is such that the accuracy of model predictions of future climate is limited by fundamental irreducible uncertainties such as knowledge limitations (e.g., cloud physics and sub-grid variability), the inherent chaotic nature of climate and uncertainty about human behaviour to reduce greenhouse gas emissions. It would be unwise to unduly rely on projections made by climate models and prudent to favour solutions that are robust across a range of possible climate futures.

This study presents and demonstrates a methodology that addresses the problem of finding “good” solutions for urban bulk water systems in the presence of deep uncertainty about future climate. The methodology involves three key steps:

1. Build a simulation model of the bulk water system: This entails validating the model against historic performance and extending its capability to simulate a future solution or portfolio consisting of a mix of operating rules, infrastructure investments and policy settings and to evaluate the economic, social and environmental consequences of adopting a particular solution.
2. Construct replicates of future climate: The replicates are times series of climate variables such as rainfall and potential evapotranspiration that a) reproduce natural variability seen in the instrumental record and b) reflect a plausible range of changes to future climate. The climate variables would typically input to calibrated rainfall-runoff models to produce streamflow time series at multiple sites.
3. Use multi-objective optimisation: Robust algorithms exist to efficiently search through potentially trillions of solutions to identify a set of “good” or Pareto-optimal solutions. A Pareto-optimal solution belongs to the set of solutions that optimally trade-off expected performance against robustness or sensitivity of performance over the range of future climates. These solutions cannot be improved upon without the expression of value judgments about the trade-offs. In a democratic society this requires the exercise of a legitimate political process which includes *inter alia* involvement of stakeholders in the water planning process and trade-off decisions.

A case study based on the Lower Hunter in New South Wales demonstrates the methodology. It is important to note that the case study does not consider the full suite of options and objectives; preliminary information on plausible options has been generalised for demonstration purposes and therefore its results should only be used in the context of evaluating the methodology. The three methodological steps were implemented as follows:

1. Build a simulation model of the bulk water system: After satisfactory validation the WATHNET5 model of the Lower Hunter was extended to simulate a representative range of possible future options including desalination (pre-built or triggered by a

drought), a new surface water source, demand substitution using domestic rainwater tanks, drought contingency measures that trigger restrictions and emergency rationing and desalination, and operating rules that balance storage and trigger transfers.

2. Construct replicates of future climate: A best-practice approach was adopted to derive climate change factors that defined “dry” and “wet” scenarios to represent the likely span of climate in 2070. The climate change factors were based on the subset of GCMs considered close to realistic for Australian hydro-climatology and on the A1F1 emissions scenario. These climate change factors were used to perturb historical records of rainfall and potential evapotranspiration. Stochastic models were calibrated to the perturbed historical records and used to generate long climate sequences that reproduce both the natural variability found in the historical record and plausible changes to future climate. These sequences were used to generate streamflow time series at multiple sites.
3. Use multi-objective optimisation: Two objectives were adopted: 1) minimise the expected present worth cost of capital and operational costs and social costs due to restrictions and emergency rationing, and 2) maximise robustness by minimising the difference in present worth cost between the “dry” and “wet” 2070 climate scenarios. The constraint was imposed that a feasible solution must be able to supply (restricted) demand in the worst drought encountered in 500,000 years – this is nominally taken to represent a policy of avoiding catastrophic failure in the event of an extreme drought. Two demand scenarios were considered: a) “1.28 x current demand” representing expected consumption in 2060; and b) “2 x current demand” representing a highly stressed system.

It was found the robustness (or conversely the sensitivity) of solutions to uncertainty about future climate varied considerably between the two demand scenarios. For the “1.28 x demand” scenario there was limited sensitivity to the “2070 “dry” and “wet” climate scenarios resulting in a narrow range of trade-offs between expected present worth cost and robustness – in the worst case, the difference in present worth cost between the “dry” and “wet” scenarios was less than 4% of the expected present worth cost of \$360m (averaged over the two scenarios). However, if the option of a new surface water source was excluded from the set of available options, the expected present worth costs and robustness markedly deteriorated – in the worst case, the difference in present worth cost between the climate scenarios was over 12% of the expected present worth cost of \$812m. In all solutions pre-built desalination was adopted. For the “2 x demand” scenario, the trade-off was considerably greater – in the worst case, the difference in present worth cost between the climate scenarios was over 40% of the expected present worth cost of \$1092m.

The main policy implication is that (possibly large) uncertainty about future climate may not necessarily produce significantly different performance trajectories. The sensitivity is determined not only by differences between climate scenarios but also by other external stresses imposed on the system such as population growth and by constraints on the available options to secure the system against drought.

Finally, while the case study focussed on economic and social costs and a limited range of options, the methodology and supporting technology is general and capable of handling a wide range of objectives, constraints and options. However, to realise its full and substantial potential, there is a pressing need develop more experience over a range of applications.

1. OBJECTIVES OF THE RESEARCH

The majority of Australians live in large urban centres which cannot function without adequate water supply. Bulk water systems represent a network of surface and groundwater storages, desalination and reclamation plants, water treatment plants and transfer infrastructure that harvest, store and transfer water to urban areas. Failure of bulk water systems to supply minimum water needs for an extended period would most likely result in disastrous social and economic losses. For example, closing down commercial and industrial activity in Sydney would result in losses of the order of a billion dollars per day; given that severe drought can persist over extended periods, such closure could conceivably last for months, possibly years, and threaten the very existence of the city¹. Recent experience with drought and a shifting climate has highlighted the vulnerability of urban water supplies to “running out of water” in Perth, south-east Queensland, Sydney, Melbourne and Adelaide and has triggered major investment in water source infrastructure which ultimately will run into tens of billions of dollars. With the prospect of rapid population growth in major cities, the provision of acceptable drought security will become more pressing particularly in the face of considerable uncertainty about future climate.

The identification of solutions for urban bulk water systems that are both optimal and robust in the presence of uncertainty presents a difficult challenge. In particular, decision makers need to deal with significant uncertainty about future climate (which affects supply) and anthropogenic forcing (which affects the demand placed on the system). Much of this uncertainty can be described using probability distributions that have been inferred from past data on system behaviour. However, in some cases, while the future events are identifiable, there is insufficient data and prior knowledge to meaningfully assign probabilities to such events. In such cases, there is almost complete reliance on the assignment of subjective probabilities. Such uncertainty is referred to as “deep” uncertainty to emphasise that traditional probability approaches are not likely to be meaningful.

In the context of urban water resources, one such uncertainty is future climate change. Dessai *et al.* (2009) argued that the accuracy of model predictions of future climate is limited by “fundamental irreducible uncertainties” such as knowledge limitations (e.g., cloud physics and sub-grid variability), the inherent chaotic nature of climate and uncertainty about human behaviour to reduce greenhouse gas emissions. They argued that such uncertainties may be extremely difficult to quantify. Nonetheless, decisions will and must continue to be made even “in the absence of accurate and precise climate predictions”. Dessai *et al.* (2009) recommend against overreliance on projections made by climate models and favour solutions that are robust across a range of possible futures.

The primary objective of this study is to address the problem of finding “good” solutions for urban bulk water systems in the presence of deep uncertainty about future climate change. The study will develop and demonstrate a methodology that identifies planning and operational decisions that can be characterised as being optimal and also robust in the face of uncertain knowledge about future climate change.

¹ This estimate is based on the GDP contribution of the Sydney region and assumes that complete closure of commerce and industry for x% of the year will result in a proportionate loss of GDP.

2. RESEARCH ACTIVITIES AND METHODS

This section describes the development and application of the concept of robust optimisation for urban bulk water systems in the face of “deep” uncertainty about future climate change. It is organised as follows: First, the robust multi-criterion optimisation problem is formally defined. Then the Lower Hunter case study is introduced after which the construction of future climate change scenarios is described. Following this the Lower Hunter bulk water simulation model is described. This then leads to the formulation of the robust optimisation problem for the Lower Hunter system describing the decisions, objective functions, constraints and strategies to improve computational performance.

2.1 *Robust Multi-Criterion Optimisation*

2.1.1 *Motivation*

Urban water agencies are tasked with the responsibility of planning and operating bulk water systems in a way that minimises economic, social and environmental costs while providing an acceptable level of drought security. The management of urban drought security typically involves a two-pronged strategy:

Risk mitigation: This involves development of long-term strategies that affect water use efficiency and behaviours and long-lead time water source infrastructure associated with surface and subsurface water storage, harvesting and recycling to manage the risk exposure to severe drought; and

Drought contingency: Once a drought develops, trigger events, whose probability of occurrence is determined by the risk mitigation strategy, initiate short-term responses such as restrictions/rationing and short-lead time (and usually very expensive) source augmentation.

The urban water sector typically uses ad hoc trial-and-error approaches to search the solution space of drought security options in pursuit of “good” solutions. The number of potentially feasible solutions is huge, and trial-and-error search, even by experienced engineers and planners, cannot adequately explore this space. Good solutions may be missed, particularly under future climates that are different to the past, resulting in possibly large opportunity costs to the community.

Multi-criterion optimisation offers a quantum improvement over trial-and-error search and more closely reflects actual decision making. In the context of this study, we are looking for solutions which maximise drought security, minimise operating and investment costs and minimise social impacts. There is no one best solution. Multi-criterion optimisation identifies the Pareto set of solutions, which expresses the optimal trade-offs between competing objectives. This Pareto set provides the best set of solutions for negotiation, something trial-and-error search cannot guarantee.

However, this in itself is not sufficient. Risk-averse decision makers will shun solutions that are optimal in an average sense but produce significantly different results depending on which of the assumed scenarios actually occur. Indeed Mahmoud *et al.* (2009) observe that “scenario results are of limited value if the involved uncertainty is not properly considered”.

In the context of this project, interest focuses on robust solutions where a solution is deemed more robust if its performance is less sensitive to the choice of scenario

describing possible future states. The pressing need is to identify solutions/strategies that are robust as well as efficient across these scenarios.

A natural way to characterise robustness is to minimise the spread or difference in performance between the worst and best scenario. The core idea is to introduce the minimisation of performance spread into the multi-criterion optimisation problem. This is best illustrated by a simple example involving minimisation of expected cost. Figure 1 shows how the introduction of a second objective, namely the minimisation of spread, leads to an optimal trade-off set of solutions. In this example, solution A is the most efficient (smallest expected present worth cost) but least robust (greatest cost spread), while solution B is the most robust but least efficient. Decision makers will be interested in exploring the trade-offs between robustness and efficiency. For example, solution C may interest decision makers as it is slightly more costly than A but substantially less sensitive to differences between worst and best scenarios.

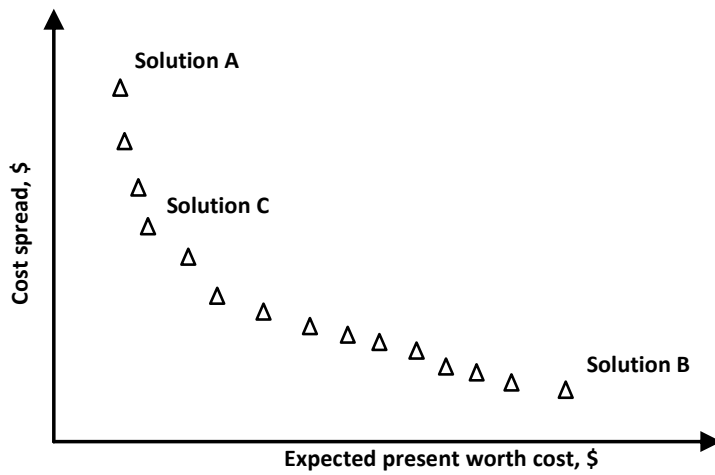


Figure 1 Trade-off between expected cost and spread of costs across scenarios.

The multi-objective optimisation problem can be formulated as:

$$\begin{aligned}
 & \min_x f_i(x) \quad i = 1, 2, \dots, M \\
 & \text{subject to} \\
 & g_i(x) \geq 0 \quad i = 1, 2, \dots, I \\
 & h_j(x) = 0 \quad j = 1, 2, \dots, J \\
 & x_k^L \leq x_k \leq x_k^U \quad k = 1, 2, \dots, K
 \end{aligned} \tag{1}$$

where x is a solution defined as a vector of K decision variables with lower and upper bounds x^L and x^U respectively and $f(x)$ is a vector of M objective functions. The problem is subject to I inequality constraints $g_i(x) \geq 0$ and J equality constraints $h_j(x) = 0$. If all objective functions are minimised, a feasible solution x is said to dominate another feasible solution y , if and only if

$$\begin{aligned}
 & f_i(x) \leq f_i(y) \text{ for } i=1, \dots, M \\
 & f_j(x) < f_j(y) \text{ for at least one } j \in \{1, \dots, M\}
 \end{aligned} \tag{2}$$

A solution is said to be Pareto optimal if it is not dominated by any other solution in the feasible solution space. A Pareto optimal solution cannot be improved with respect to any objective without worsening at least one other objective. The set of all feasible non-dominated solutions in x is referred to as the Pareto optimal set. For a given Pareto optimal set, the corresponding objective function values in the objective space are called the Pareto front.

An important practical advantage of multi-criterion optimisation is that it does not require the decision-maker to specify *a priori* weights on different objectives and thus defers the need to make explicit value judgments on trade-offs until after the optimisation has been conducted (Deb, 2001).

As already noted, urban water managers, like other decision makers, are frequently confronted with the need to make major decisions in the face of poorly defined uncertainty about future states of the system. The pursuit of optimal solutions needs to be tempered by the need to find solutions that are robust in the presence of poorly defined uncertainty about future states or assumptions. Considering the risks posed by global climate change, Matalas and Fiering (1977) introduced the concept of robustness to the water resources field, describing it as 'the insensitivity of a system design to errors, random or otherwise, in the estimate of those parameters affecting design choice'. Robust solutions should be found so that they can be adaptable to a range of "wait and see" strategies "with some economic efficiency or optimality traded in favour of adaptability and robustness" (Matalas and Fiering, 1977). Dessai et al. (2009) argued that decisions will and must continue to be made even "in the absence of accurate and precise climate predictions". In the face of deep uncertainty, they argue that overreliance on predictions made by climate models is unwise. Consequently, solutions should be robust across a range of possible futures.

In the water resource field, Watkins and McKinney (1997) reviewed a considerable literature on making decisions that hedge against risk. Watkins and McKinney (1997) presented a framework that formally incorporated risk aversion into the optimisation problem, thus enabling trade-offs to be made between expected performance and robustness. They applied the robust optimisation framework of Mulvey *et al.* (1995) to two water resource problems. By assigning probabilities to different scenarios defined as possible model parameters, they explored two types of robustness, optimality-robustness which identifies solutions that are "close" to optimal for all scenarios, and feasibility-robustness which identifies solutions that remain "almost" feasible for all scenarios. The principal limitation of the Watkins and McKinney approach was the restrictive nature of the classical mathematical program that simulated the water resource system and that defined the objectives.

Recent advances in evolutionary multi-criterion optimisation have overcome many of the limitations of classical mathematical programming (Deb, 2001). Deb and Gupta (2006) provide a review of robust multi-criterion optimisation. They interpret robustness as some measure of insensitivity to disturbances in the environment or in the design variables. Specifically, they suggested robust optimisation of type II, in which the original objectives are optimised subject to an additional constraint which limits changes in the objective function values arising from uncertainty. However, a significant practical limitation of this approach is that the parameter defining the neighbourhood of acceptable objective function perturbations must be specified *a priori* by the decision-maker. Barrico and Antunes (2006) extended these ideas to classify Pareto-optimal solutions according to their degree of robustness, rather than just classifying solutions as robust or not robust. Jin and Sendhoff [2003] characterised robust optimisation as a multi-objective optimisation with two generic objectives: expected performance and robustness. Luo and Zheng [2008] presented a

methodology for robust Pareto optimisation which converts multi-objective optimisation problems into a bi-objective optimisation problem with the first objective optimising solution's quality (based on some measure involving the original objectives), and the second optimising the solution's robustness.

In this study, we follow the approach described by Cui and Kuczera (2010) which combines an adaptation of the Watkins and McKinney formulation with an evolutionary multi-criterion algorithm to create a tool capable of solving complex water resource problems.

2.1.2 A Generic Formulation

The common theme that emerges from review of robust optimisation approaches is the need to explore the Pareto-optimal trade-off between measures of expected performance and sensitivity of the performance measures to future events or states. Our formulation of the robust optimisation problem exploits the generality offered by evolutionary multi-criterion optimisation algorithms.

The starting point is the scenario which describes a plausible future state of the system (Mahmoud et al, 2009). It describes variables (such as model parameters or forcing time series) that are external (or exogenous) to the system. The defining feature of a scenario is that its variables affect system performance but cannot be changed by the system.

In this study, each scenario will describe m replicates of n -year time series of hydro-climate and demand data corresponding to a future climate state. Suppose there are N future scenarios $\{S_j, j = 1, \dots, N\}$ with probability of occurrence $\{p_j, j = 1, \dots, N\}$. Although probabilities are assigned to each scenario, they are likely to be subjectively determined with little reliance on data.

Let $h(\cdot)$ be a simulation model of the urban bulk water system

$$Z_j = h[x, S_j] \quad (3)$$

where x is a decision vector describing operating and infrastructure variables that can be changed by the evolutionary optimisation algorithm, S_j is the system input consisting of streamflow, rainfall, water demand and model parameters for m replicates of length an n -year period conditioned on the j^{th} scenario and Z_j is the system response conditioned on scenario j .

These considerations lead to the following specification of the robust multi-objective optimisation problem:

$$\begin{aligned} \min_x & \left\{ \sum_{j=1}^N p_j f_i(x | Z_j), R[f_i(x | Z_1), \dots, f_i(x | Z_N)], i = 1, \dots, M \right\} \\ \text{subject to } & Z_j = h[x, S_j], j = 1, \dots, N \\ & g(x) \leq 0 \end{aligned} \quad (4)$$

where $f_i(x | Z_j)$ is the score for the i^{th} objective (or criterion) function for a given decision x and output Z_j conditioned on the j^{th} scenario, and

$R[f_i(x | Z_1), \dots, f_i(x | Z_N)]$ is some robustness measure expressed as a function of the

criterion scores evaluated for the N scenarios. The term $g(x)$ is some function of the decision variables used to constrain the decisions – for example, in bulk urban water supply, one may impose the constraint that the system does not run out of water in any scenario.

The robustness measure would express some measure of variability or sensitivity of the criterion scores with respect to the scenarios. For example, it may be the standard deviation of the criterion scores over the N scenarios. For more risk averse decision makers, measures based on worst case outcomes may be used such as the spread defined as

$$R[f_i(x|Z_1), \dots, f_i(x|Z_N)] = \left| \max_j f_i(x|Z_j) - \min_j f_i(x|Z_j) \right| \quad (5)$$

or the maximum criterion score defined as

$$R[f_i(x|Z_1), \dots, f_i(x|Z_N)] = \left| \max_j f_i(x|Z_j) \right| \quad (6)$$

It is worth noting that the standard deviation depends on scenario probabilities while the spread and worst case measures are independent of the scenario probabilities. In cases where there is little confidence in the probabilities assigned to scenarios (as is the case with future climate change) the use of “probability-free” robustness measures seems particularly warranted.

The Cui and Kuczera (2010) formulation given by equation (4) is conceptually similar to that of Watkins and McKinney (1997). The main difference is the use of multi-objective evolutionary algorithms (MOEAs) which impose virtually no restrictions on the mathematical form of the simulation model of equation (3), criterion functions and constraints. The WATHNET5 simulation and optimisation model (Kuczera *et al.*, 2009; Mortazavi *et al.*, 2012) exploits this generality to provide a system-independent tool that makes possible application of robust optimisation to complex urban bulk water systems.

2.1.3 Multi-Objective Evolutionary Algorithms

The solution of equation (4) exploits recent developments in optimisation that have substantially expanded the scope and capability of optimisation approaches. The term “evolutionary algorithm” (EA) represents a class of stochastic optimisation methods that is based on the process of natural evolution. The origins of EAs were proposed in the late 1950s, and since the 1970s several classes of evolutionary methods have been developed such as genetic algorithms, evolutionary programming, and evolution strategies. EAs have been employed in a variety of engineering applications and these algorithms have proven themselves as general, robust and powerful methods (Deb 2001; Coello *et al.* 2007)..

In this study the ϵ -multi-objective optimisation evolutionary algorithm (ϵ MOEA) is used to solve equation (4). The distinguishing feature of ϵ MOEA is the use of the ϵ -dominance concept which divides the objective space into hyperboxes of size ϵ and allows only one non-dominated solution to reside in each box (Laumanns *et al.* 2002). Inclusion of this concept in a genetic algorithm (GA) framework produces a method capable of maintaining a diverse and well-distributed set of solutions with a small algorithmic computational cost (Deb *et al.* 2003).

As before, without loss of generality, it is assumed there are M objectives, all of which are to be minimised. A solution x_1 is said to ε -dominate the solution x_2 for some $\varepsilon_j > 0$ if the following conditions are true (Coello *et al.* 2007):

$$\begin{aligned} f_j(x_1) &\leq f_j(x_2) + \varepsilon_j \text{ for all } j \in \{1, \dots, M\} \\ f_j(x_1) &< f_j(x_2) + \varepsilon_j \text{ for at least one } j \in \{1, \dots, M\} \end{aligned} \quad (7)$$

To gain more insight consider Figure 2 which shows two non-dominated solutions, x_1 and x_2 . To check if x_1 ε -dominates x_2 , x'_2 is found by adding ε_1 and ε_2 to the objective function values of x_2 . Since x'_2 is dominated by x_1 , it follows that x_1 ε -dominates x_2 .

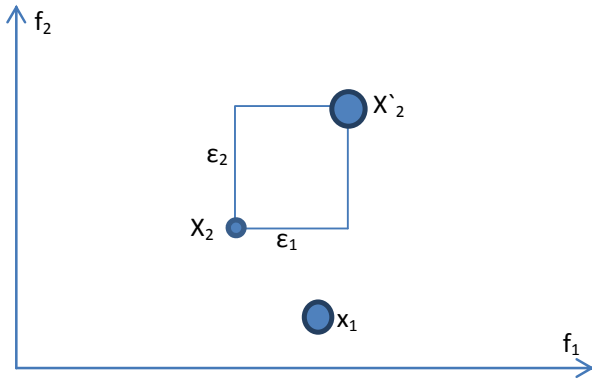


Figure 2 Schematic of ε -dominance concept

The box formed in Figure 2 leads to the idea of dividing objective space into hyperboxes to facilitate checking if solutions are ε -dominated. Figure 3 illustrates hyperboxes for an objective space with two objectives. It shows that the solution P ε -dominates the entire region ABCDA while P only dominates the region PECFP. Indeed, any solution in the ABCDA area except the box area in which P is located, would be ε -dominated by P because if ε_1 and ε_2 are added to the objective values of such a solution it would lay in the hatched area. However, all the solutions which share the same box with solution P ε -dominate each other. In this case the solution which has shortest Euclidean distance to the bottom left corner of the box dominates other solutions. This situation is illustrated in Figure 3 for solutions 1 and 2. Since solution 1 is closer to the bottom left corner of the box, it is retained and solution 2 is discarded.

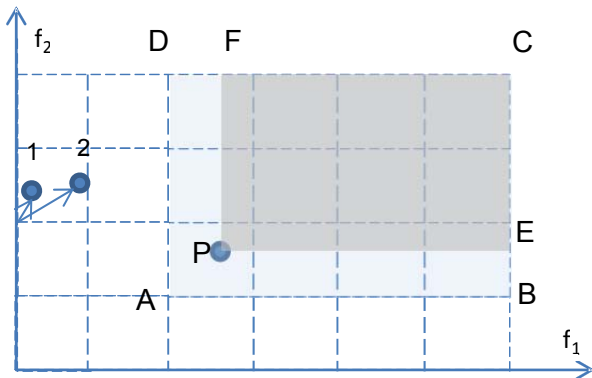


Figure 3 Illustration of ε -dominance concept for minimizing f_1 and f_2 (adapted from Deb *et al.*, 2003)

Figure 4 demonstrates application of the ϵ -dominance concept. In the left panel, a number of hyperboxes host one or more solutions. The second panel illustrates the solutions that remain after ϵ -dominance sorting. In hyperboxes containing more than one solution the solution which is closer to the bottom left corner of the hyperbox (for minimisation) is preserved while the other solutions are discarded. For instance, in two of the hyperboxes, there are two solutions occupying the hyperbox - those marked by a cross are discarded to produce the set of ϵ non-dominated solutions. The next step is to implement ϵ -dominance sorting. Thus, the solutions to the right of it are dominated and hence discarded. This results in the final ϵ -dominance Pareto front.

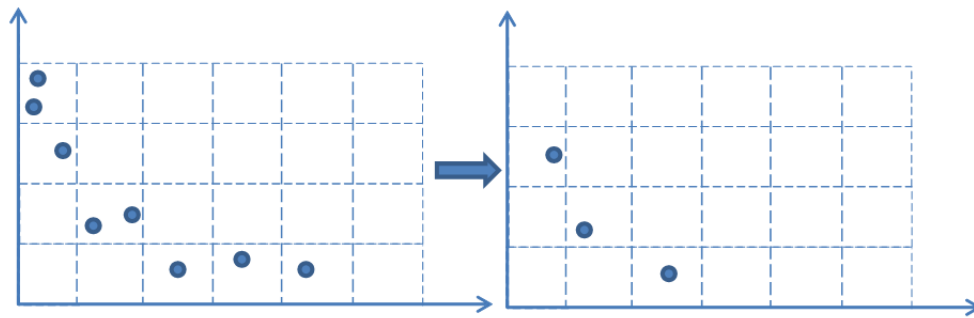


Figure 4 Illustration of Pareto front in conjunction with the ϵ -dominance concept (adapted from Kollat and Reed, 2006)

ϵ MOEA uses two co-evolving archives: the current population $P(t)$ and the current ϵ non-dominated solutions $E(t)$, where t is the iteration counter. The initial population $P(0)$ is selected randomly and the initial archive $E(0)$ is assigned the ϵ -non-dominated solutions of $P(0)$. Thereafter, two solutions, referred as parents, one each from the current and the archive population are selected for mating. To select a parent from $P(t)$, two solutions are chosen randomly. Then, if one of the solutions dominates the other one, that solution is chosen. Otherwise, the two solutions are non-dominated and one of the solutions is selected randomly. The parent from $E(t)$ is simply chosen at random among the archive members. Applying crossover and mutation operations on the two parents produces two offspring solutions. This procedure is illustrated in Figure 5.

Each of the offspring solutions is evaluated and then compared with the current and archive populations for possible inclusion. First, tests are conducted to determine if an offspring should be accepted into the $E(t)$ archive:

1. If the offspring solution is ϵ -dominated by any solution in $E(t)$, it is rejected.
2. If the offspring ϵ -dominates any solution in $E(t)$, that solution is deleted and the offspring added to $E(t)$.
3. If both of the above cases fail, it indicates that the offspring solution is ϵ -non-dominated. In that case, the following tests apply:
 - a. If the offspring solution does not share the same hyperbox with any solution in $E(t)$, the offspring is added to $E(t)$.
 - b. If the offspring shares the same hyperbox with a solution, strict non-domination is applied. If the offspring solution strictly dominates the archive

solution or it does not strictly dominate the archive solution but is closer to bottom left corner of the hyperbox (for minimisation problems), then it is accepted into $E(t)$ and the archived solution rejected.

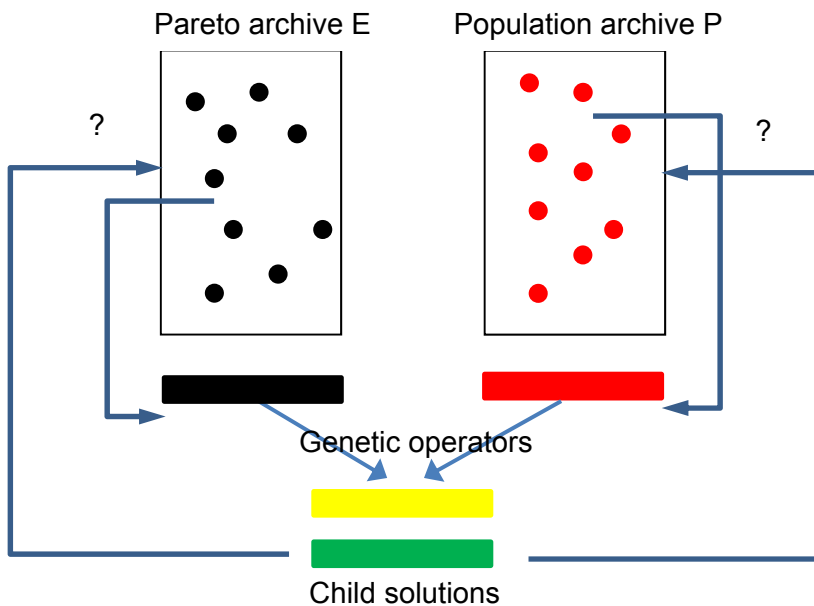


Figure 5 Schematic of ϵ MOEA (adapted from Deb *et al.*, 2003)

If an offspring is not accepted into $E(t)$, then tests are conducted to determine if the offspring is to be accepted into $P(t)$. To include the new offspring in $P(t)$, three tests are conducted:

1. If the offspring solution is dominated by any existing member of the population, it is rejected.
2. If the offspring solution dominates one or more solutions in the current population, it replaces one at random.
3. If both of the above cases fail, it indicates the offspring solution is a non-dominated solution with respect to the current population. As a result, it replaces a random member of the population.

ϵ MOEA and other heuristic search methods cannot guarantee finding Pareto optimal solutions. For that reason it is usual practice to rerun these algorithms multiple times with different random seed numbers.

The search is terminated when:

1. There is no improvement in non-dominated solutions after a certain number of iterations.
2. A maximum number of iterations have been reached.
3. A prescribed accuracy or diversity in non-dominated solutions has been achieved.

2.2 Overview of Lower Hunter Case Study

The Lower Hunter system has been chosen for the case study. Unlike other major Australian urban systems, the Lower Hunter system harvests water from high yielding catchments and thus has relied on comparatively small annual carryover storage. As a result, it is considered more vulnerable to severe drought because the comparatively low storage capacity reduces the lead-time to respond to severe drought.

Hunter Water Corporation, hereafter referred to as HWC, provides water services for the Lower Hunter region in NSW. Its area of operations covers 5,366 km² in the local government areas of Cessnock, Lake Macquarie, Maitland, Newcastle, Port Stephens, Dungog and small parts of Singleton. Over 200,000 properties are connected to its water supply network (HWC, 2012).

The Lower Hunter's drinking water supply is drawn from a combination of surface storages and groundwater resources. Major components of the current supply and distribution system include:

- Chichester Dam on the Williams River;
- Chichester Trunk Gravitational Main (CTGM);
- Seaham Weir on the Williams River;
- Balickera Diversion Channel off Seaham Weir;
- Grahamstown Dam - an off river storage; and
- Tomago and Tomaree groundwater sources.

The location of these components is shown in Figure 6, while Figure 7 presents a detailed schematic of the Lower Hunter bulk water system showing catchments, aquifers and major fluxes.

The Williams River is a major surface water source. Flows within the Williams River have been regulated with the construction of Chichester Dam and Seaham Weir. HWC currently extracts water from the Williams River via Chichester Dam and pumps from the Seaham Weir pool to Grahamstown Dam.

The Tomago Sandbeds is the major groundwater source, providing about 20% of the Lower Hunter's drinking water. The Sandbeds are strategically important for both ongoing and backup water supply. Ongoing supply from the Sandbeds reduces the load on surface water sources (Chichester Dam and Grahamstown Dam) and thereby allows greater overall yield from the total water supply system. This large storage volume can also be used as a reserve supply during drought, and is available as a backup supply in the event of water quality issues in the surface storages.

The Tomaree Sandbeds is an unconfined aquifer consisting of four small groundwater catchments on the Tomaree Peninsula. It is used for localised supply at relatively minor volumes compared with other the overall system supply requirements. The Paterson and Allyn Rivers provide localised water for the small township of Gresford. As these demand centres are small and independent of the primary system, they were excluded from this study.

The Metropolitan Water Directorate, within the NSW government Department of Finance and Services, is leading a whole-of-government approach to developing a Lower Hunter Water Plan (LHWP) in close consultation with the lower Hunter community.

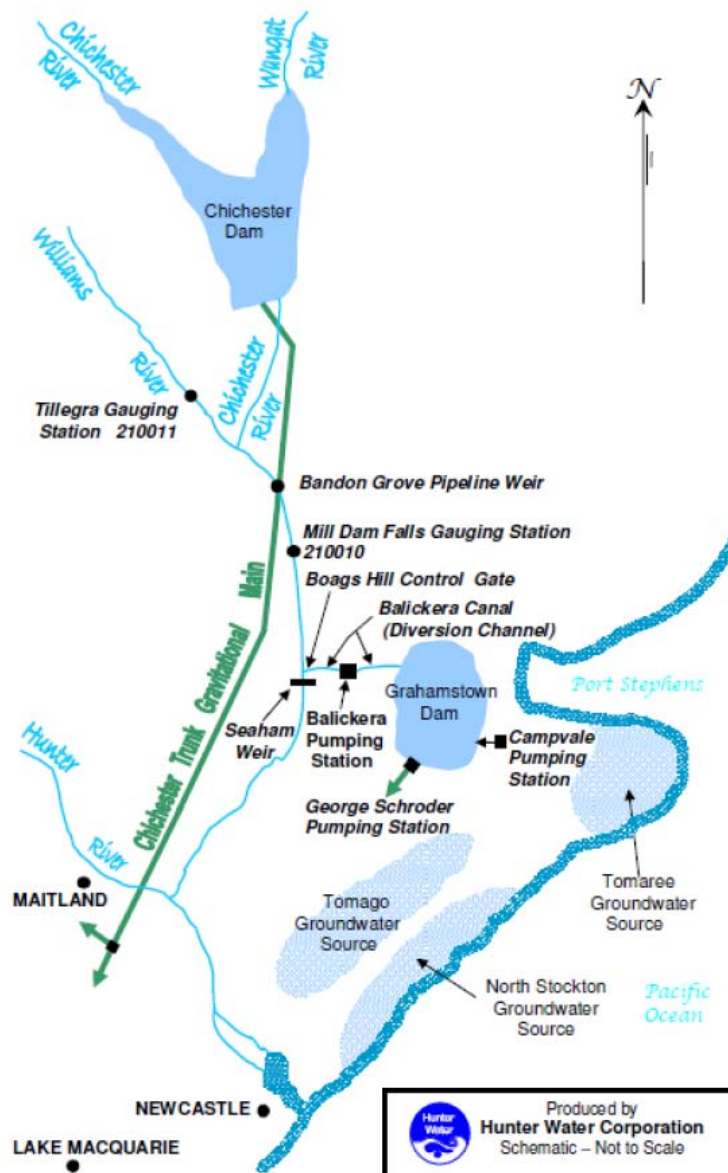


Figure 6 Map of existing Lower Hunter bulk water system (reproduced with permission)

The LHWP is to identify measures to:

- provide water security during drought
- ensure reliable water supplies to meet growing water demand due to a growing population and increased business and industry activity
- help protect aquatic ecosystems
- maximise net benefits to the community.

Whilst there may superficially appear to be some similarities between this case study and elements of the LHWP, there are some significant differences. The purpose of this case study is to demonstrate a methodology in an end user context, with plausible but generalised decision variables. It is not intended to provide a comprehensive review of the full spectrum of decision variables nor does it purport to include the level of community/stakeholder engagement covered by the LHWP.

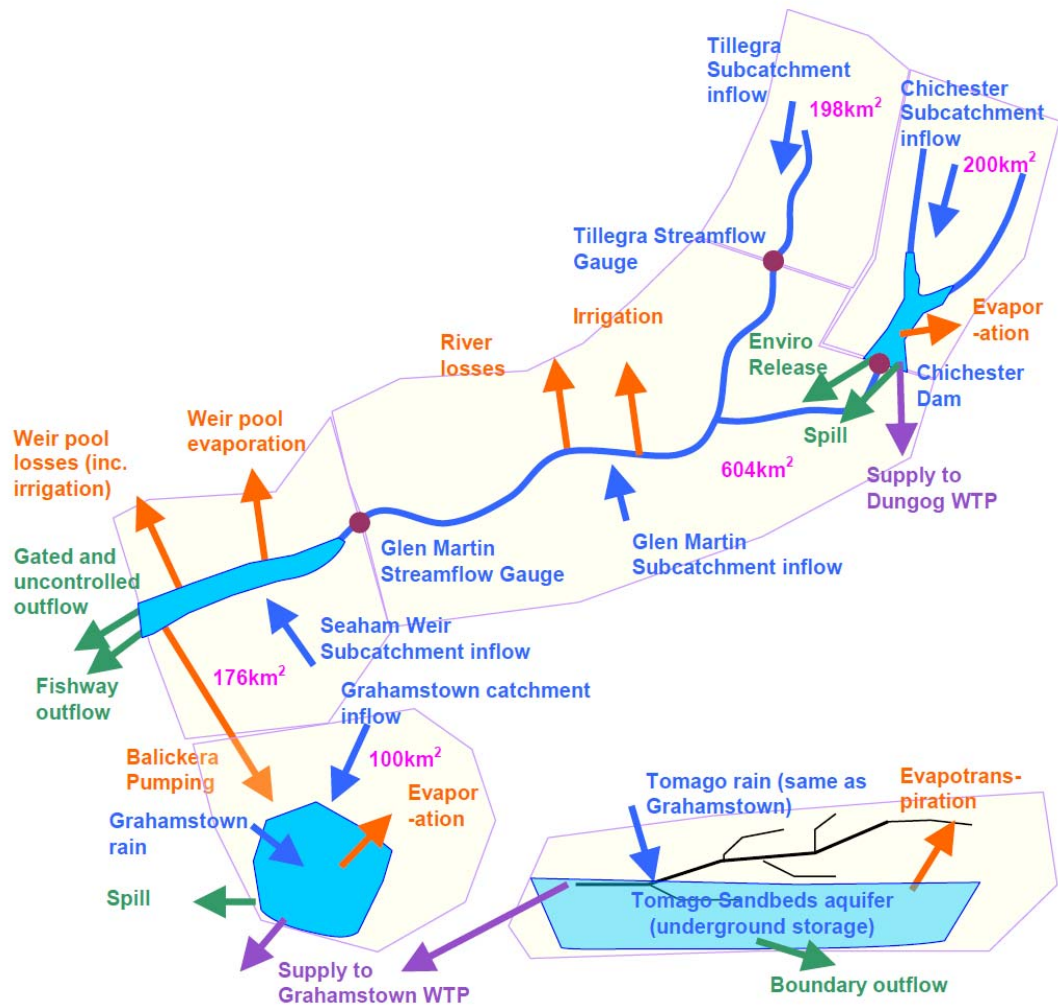


Figure 7 Schematic of Lower Hunter water sources (reproduced with permission)

2.3 Stochastic Generation of Historic and Future Climate Scenarios

The construction of future climate scenarios is a challenging task. In addition to the influence of natural climate variability and the problems associated with the brevity (in climatological terms) of instrumental hydro-climatological records, there is also serious concern about how human-induced climate change may increase the frequency and severity of extreme events, including droughts and floods, in the future. Accordingly, there have been attempts to utilise climate model outputs to determine how anthropogenic climate change may affect water resources and, on the basis of this information, to develop water resource management strategies to deal with the projected risks. However, the uncertainty associated with future climate projections is known to be significant (e.g. Parry *et al.*, 2007; Randall *et al.*, 2007; Koutsoyiannis *et al.*, 2008, 2009; Blöschl and Montanari, 2010; Montanari *et al.*, 2010; Kiem and Verdon-Kidd, 2011) and is magnified further when attempting to make inferences at the regional (i.e., catchment) scale (e.g., differentiating between coastal and inland processes). This is especially the case for precipitation (e.g., Lim and Roderick, 2009) and hydro-climatic extremes (see <http://ipcc-wg2.gov/SREX/>). The uncertainty is so high that projections of future drought risk, on either the short (seasonal up to 5 years) or long (more than 10 years into the future) term, currently have limited practical usefulness for water resource managers and/or government policy makers [National Climate Change Adaptation Research Facility, 2010].

However, methods do exist to quantify risks associated with climate variability and/or change that do not rely solely on climate model outputs (e.g., McMahon *et al.*, 2008; Verdon-Kidd and Kiem, 2010). These methods involve utilising stochastic modelling approaches that replicate the important statistics associated with historical data (e.g. interannual to multidecadal natural climate cycles, dry spells, wet epochs, extreme high and low rainfall etc.) and then utilising the best available climate modelling information to provide a range of plausible future scenarios.

This study focuses on the future climate around 2070 (i.e. the average climate during 2060-2079 or the 20 years centred on 2070). To simulate the performance of the Lower Hunter system it is necessary to develop streamflow replicates representative of the 2070 climate.

The methodology used in this study involves the following steps:

1. Select two 2070 climate scenarios representing the range in likely 2070 climate conditions – these scenarios will be referred to as ‘dry’ 2070 and ‘wet’ 2070 scenarios.
2. For each future scenario, perturb observed historic rainfall and potential evapotranspiration (PET) time series using the selected 2070 climate change factors.
3. Calibrate a stochastic multi-site model of rainfall and PET to the perturbed historic data.

Generate 10,000 50-year replicates of daily rainfall and PET representative of the “perturbed” climate.

Using calibrated rainfall-runoff models produce 10,000 50-year replicates of monthly streamflow at multiple sites.

2.3.1 *Stochastic generation of daily rainfall and evapotranspiration scenarios*

Historic data source

Historic rainfall and evaporation data for the Lower Hunter catchments was obtained from the SILO gridded rainfall and potential evapotranspiration (PET) datasets (<http://www.longpaddock.qld.gov.au/silo/>). The daily rainfall and PET data were calculated to be the area-weighted average of data from SILO point data sites that lie within each of the five catchment areas identified in Figure 8. Daily PET data was also obtained for the Grahamstown Dam area for the purpose of estimating evaporative losses from the lake surface. In this study, rainfall and PET stations are denoted R1 to R5 and E1 to E5, respectively (each corresponding to the Glen Martin, Tillegra, Chichester, Grahamstown Dam, and Seaham Weir catchments respectively), and E6 refers to PET from Grahamstown reservoir itself

All daily rainfall and PET data was available for a continuous period from January 1889 to January 2012.

The daily data for each of the five rainfall and six PET sites was aggregated into three-monthly totals based on traditional seasons (i.e. winter is June, July, August; spring is September, October, November; etc.). This was done for the period winter 1889 to autumn 2010 (i.e. March, April, May 2011) resulting in 11 time series of three-month totals based on 122 historical water years.

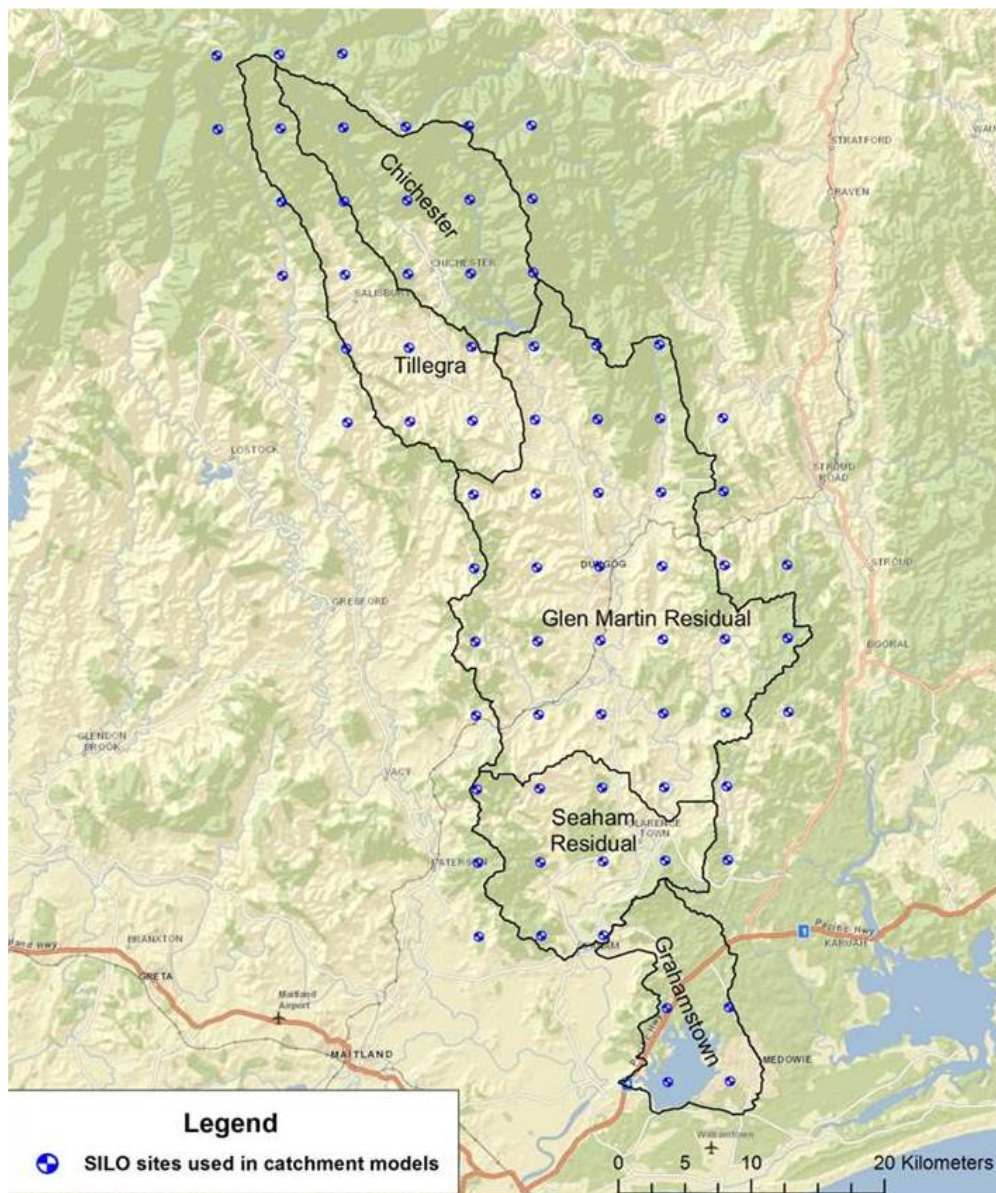


Figure 8 Map of Lower Hunter catchments (reproduced with permission)

Stochastic generation – historical climate

The seasonal (three month) rainfall and PET totals for the 11 sites required by the HWC rainfall-runoff models were then used as input into a multi-site stochastic generation model, based on Matalas (1967). The Matalas (1967) model was originally developed for application at the annual timescale but previous work (e.g. McMahon *et al.*, 2008) has confirmed it is also applicable to six or three month totals. The Matalas model uses an autoregressive lag-one model that preserves the lag-zero and lag-one cross correlations between the four seasons and across the five rainfall and six PET sites.

To verify the stochastic generation model, one hundred replicates, each of 122 years duration (i.e. the same length as the observed or unperturbed historical input data), were generated for each season and at each of the five rainfall and six PET sites to produce replicates of historical climate conditions (i.e. no climate change factors applied). Descriptive statistics for the replicates were compared with the same

descriptive statistics calculated for the historical observations to confirm that spatial and temporal variability was preserved by the multi-site stochastic generation process - see Tables 1 and 2.

Table 1 Ratio of statistic calculated on historical data (122 years) to the average of the same statistic for stochastically generated data (mean of 100 replicates of 122 years)

Site	Season	Mean	StDev	CoVar	Max	Min	Range	Min 10 yr total
R1	Winter	1.00	1.03	1.02	1.25	18.18	1.22	1.20
	Spring	1.00	1.01	1.02	1.02	8.83	0.96	1.00
	Summer	1.00	1.03	1.03	1.16	3.42	1.09	0.86
	Autumn	1.00	1.02	1.02	1.02	6.06	0.95	1.12
R2	Winter	1.01	1.03	1.03	1.27	17.54	1.20	1.21
	Spring	0.99	1.02	1.02	0.98	5.13	0.93	0.98
	Summer	1.00	1.02	1.04	1.14	2.72	1.07	0.83
	Autumn	1.00	1.02	1.02	1.18	10.05	1.10	1.12
R3	Winter	1.01	1.03	1.02	1.19	13.03	1.12	1.22
	Spring	0.99	1.02	1.02	0.95	6.25	0.87	0.96
	Summer	0.99	1.03	1.03	1.17	2.84	1.10	0.84
	Autumn	1.00	1.02	1.03	1.17	11.43	1.09	1.09
R4	Winter	1.00	1.02	1.02	1.22	9.83	1.16	1.15
	Spring	1.00	1.01	1.01	1.02	6.86	0.94	1.07
	Summer	1.00	1.03	1.02	1.00	1.08	1.00	0.87
	Autumn	1.00	1.02	1.03	1.00	3.01	0.95	1.02
R5	Winter	1.00	1.04	1.02	1.26	16.62	1.23	1.21
	Spring	1.00	1.01	1.01	1.04	10.88	0.96	1.03
	Summer	1.00	1.03	1.02	1.23	3.11	1.19	0.87
	Autumn	1.00	1.02	1.03	0.97	7.54	0.89	1.10
E1	Winter	1.00	1.02	1.10	0.98	1.01	0.88	0.99
	Spring	1.00	1.01	0.97	1.01	1.01	0.98	1.00
	Summer	1.00	1.01	1.11	1.00	1.04	0.86	0.99
	Autumn	1.00	1.01	0.99	1.00	1.02	0.94	1.00
E2	Winter	1.00	1.02	1.06	0.99	1.00	0.95	0.98
	Spring	1.00	1.01	1.08	1.01	1.03	0.94	1.00
	Summer	1.00	1.01	1.07	1.00	1.05	0.87	1.00
	Autumn	1.00	1.01	0.94	1.00	1.03	0.89	0.99
E3	Winter	1.00	1.02	1.01	0.99	0.99	0.97	0.98
	Spring	1.00	1.01	1.03	1.00	1.03	0.92	1.00
	Summer	1.00	1.01	1.06	1.00	1.04	0.88	1.01
	Autumn	1.00	1.01	1.05	1.00	1.02	0.93	0.99
E4	Winter	1.00	1.03	0.96	0.97	1.01	0.85	0.99
	Spring	1.00	1.02	1.01	1.00	1.00	0.99	1.00
	Summer	1.00	1.01	0.94	1.00	1.05	0.84	0.99
	Autumn	1.00	1.02	1.05	1.00	1.03	0.90	1.00
E5	Winter	1.00	1.02	0.94	0.98	1.01	0.87	0.98
	Spring	1.00	1.02	0.99	1.00	1.01	0.98	1.00
	Summer	1.00	1.01	0.93	1.00	1.05	0.86	0.99
	Autumn	1.00	1.01	1.02	1.01	1.03	0.93	1.00
E6	Winter	1.00	1.03	0.94	0.97	1.01	0.85	0.99
	Spring	1.00	1.02	1.00	1.00	1.00	1.00	1.00
	Summer	1.00	1.01	1.11	1.00	1.04	0.87	0.99
	Autumn	1.00	1.02	1.02	1.00	1.03	0.89	1.00

Table 2 Ratio (mean of 100 replicates of 122 years divided by 122 year history) of Lag 0 cross correlation in annual (sum of three month seasons) total rainfall and PET

Site	R1	R2	R3	R4	R5	E1	E2	E3	E4	E5	E6
R1	1.00	1.00	1.00	1.00	1.00	1.00	1.00	1.00	1.00	1.00	1.00
R2		1.00	1.00	1.00	1.00	1.00	1.00	1.00	1.00	1.00	1.00
R3			1.00	1.00	1.00	1.00	1.00	1.00	1.00	1.00	1.00
R4				1.00	1.00	1.00	1.00	1.00	1.00	1.00	1.00
R5					1.00	1.00	1.00	1.00	1.00	1.00	1.00
E1						1.00	1.00	1.00	1.00	1.00	1.00
E2							1.00	1.00	1.00	1.00	1.00
E3								1.00	1.00	1.00	1.00
E4									1.00	1.00	1.00
E5										1.00	1.00
E6											1.00

The three month seasonal totals generated via the multi-site stochastic generation process described above were then disaggregated to a daily time step using the method of fragments. Method of fragments is a process whereby the generated three month totals are compared to the historic three month totals at a key site. The daily pattern from the historic period with the closest total rainfall or evaporation (in the equivalent three month period) is used to create a daily time series from the three month generated data. The equivalent daily time series for the same three month period as the key site are then used to create daily time series for the other sites.

Once the stochastic generation process was verified (based on the 100 replicates of historical conditions, each of 122 years length) and it was confirmed that the important statistics were being preserved the process was repeated to generate 10,000 replicates which were each 50 years long. The resulting rainfall and PET sequences were then input into the Hunter Water SimHyd models to produce 10,000 replicates of 50 years of daily flow.

Stochastic generation – future climate

The process described above was repeated for two plausible 2070 climate scenarios. Climate change impacts were obtained from the Climate Change in Australia website (<http://climatechangeinaustralia.com.au/>; CSIRO-BoM, 2007) for the 'best estimate' projection for 2070 under the high emissions scenario (i.e. Intergovernmental Panel on Climate Change (IPCC) Special Report on Emission Scenarios A1FI emissions scenario). These projections were undertaken as part of the Australian Climate Change Science Program, a joint initiative of the Department of Climate Change and Energy Efficiency, the Bureau of Meteorology and CSIRO.

Other possible emission scenarios include the B1 (low) and A1B (medium) emission scenarios. However, in this case the A1FI (high) emission scenario was chosen because (a) the projections under A1FI encompass projections under the lower emission scenarios and (b) as of the time of writing, actual greenhouse gas emissions look to be tracking at (or even above) the A1FI scenario with the best available evidence suggesting that the low to medium greenhouse gas emission scenarios are increasingly unlikely.

Projections are expressed via change factors (summarized in Table 3) and are given relative to the period 1980-1999 (referred to as the 1990 baseline). The projections give an estimate of the average climate around 2070 (i.e. 2060-2079), taking into account consistency among climate models and the fact that individual years will show

variation from this average. More than 20 different general circulation models (or global climate models or GCMs), each run several times for each of the different emission scenarios, result in a distribution of plausible projected future impacts. The 50th percentile (the mid-point of the spread of model results) provides a ‘best estimate’ result while the 10th and 90th percentiles (lowest 10% and highest 10% of the spread of model results) provide a range of uncertainty. In this study the 50th percentile (‘best estimate’) was used in recognition of the numerous studies that have demonstrated that of the 23 GCMs used to develop future climate projections (i.e. utilised by Climate Change in Australia) only a select few (i.e. less than eight) can be considered close to realistic for Australian hydro-climatology and that current best practice is to use the projections where there is most agreement across the models rather than the extremes (which as mentioned are likely due to model biases rather than reality). To view the full range of climate model projections refer to <http://climatechangeinaustralia.com.au/> (CSIRO-BoM, 2007).

The climate change factors for the Lower Hunter are reported as a range in Table 3. The rationale for this range is fully described in the Climate Change in Australia website. Briefly this range was derived as follows:

1. For the A1F1 emission scenario, the projected range for global warming based on all GCM models, run several times, is 1.74 to 4.64 C° in 2070.
2. Using the 50th percentile estimate of local change in rainfall and PET per degree of global warming, a range of climate change factors for the Lower Hunter are obtained. In this study, the upper bound of the projected range was used to develop a ‘wet’ 2070 scenario and the lower bound was used to develop a ‘dry’ 2070 scenario.

Table 3 Climate change factors (% change to 1990 baseline mean) used in this study (obtained from <http://climatechangeinaustralia.com.au/> using the 2070 ‘best estimate’ (50th percentile) high emissions scenario).

Rainfall	Winter	Spring	Summer	Autumn
2070 wet	-10	-10	+2	-2
2070 dry	-20	-20	-2	-5
PET	Winter	Spring	Summer	Autumn
2070 wet	+12	+4	+8	+12
2070 dry	+16	+8	+12	+16

It should be noted that for a number of reasons it is possible for it to be wetter than the upper bound or drier than the lower bound (e.g. emission scenario exceeds A1FI, natural variability exceeds that which has been observed historically or which has been simulated by the GCM, some physical process(es) is(are) missed or underestimated in the GCMs, the small number of models simulating a 10th or 90th percentile scenario turn out to be right and the ‘best estimate’ or ‘consensus’ model results are wrong etc.). In any case, this study has employed the ‘best estimate’ projections which are in line with best practice. It should also be noted that significant variability around the average change factors presented in Table 3 is also implicitly incorporated via the stochastic approach describe above. Therefore, while it is possible that the future (i.e. average climate around 2070) could turn out to be drier or wetter than what any of the climate change scenarios produced here suggest, such an occurrence would be unlikely based on the climate modelling output and scientific understanding available at the time of performing this work.

The change factors obtained from the Climate Change in Australia website (shown in Table 3) were then used to perturb the historical time series of observed three month totals resulting in two further sets of multi-site stochastic replicates that incorporated

historical variability and also were indicative of the range of potential climate change impacts projected for around 2070.

The 'wet' 2070 perturbation of history was then input into the multi-site stochastic generation model to obtain 10,000 replicates of 50 years of climate change impacted seasonal rainfall and PET totals. The seasonal totals were then disaggregated to the daily time step, again using method of fragments as described above.

The same was done for the 'dry' 2070 scenario.

Verification of multi-site stochastic generation process

The statistics of the stochastically generated replicates of historical (i.e. unperturbed) three month totals were compared to the statistics of the observed historical data with the results summarised in Table 2 and Table 3. Overall, the multi-site stochastic generation technique is performing well at preserving the important statistics with the majority of bias within a 10% error range.

2.3.2 Rainfall-Runoff Modelling

The stochastically generated daily rainfall and evaporation are used as inputs to calibrated rainfall-runoff models to produce daily runoff simulations for each catchment in the Lower Hunter system. The rainfall-runoff model selected in this study is SimHyd (Chiew and Siriwardena, 2005) which is a lumped conceptual daily model for simulating daily runoff using daily rainfall and evapotranspiration as inputs. The model operates by accounting for water that is stored in, transferred between or overflowing from three conceptual stores: an interception store, a soil moisture store and a groundwater store. These processes are illustrated in the schematic of Figure 9, whereas Table 4 provides a description of the SimHyd model parameters.

Calibration

BMT WBM (2012) and HWC (2012) developed a methodology for rainfall-runoff modelling of the five HWC sub catchments. The methodology and models developed by BMT WBM (2012) are used in this study to simulate runoff from the HWC sub catchments. Each sub catchment is divided into one or more functional units (FU), based on soil type and land use, resulting in a total of nine functional units. BMT WBM (2012) and HWC (2012) calibrated a SimHyd model for each functional unit. Table 5 presents the SimHyd model parameters used to generate stochastic simulations of sub catchment runoff.

In keeping with the recommendations of the BMT WBM (2012) study, Laurenson flow routing was applied to the Tillegra and Chichester catchments for the routing of flows along river reaches. The Laurenson routing parameters used were $k_c = 75754$ and 387036 and $m = 0.8$ and 0.69 for the Tillegra and Chichester catchments respectively. Contributing flows from multiple functional units within each sub catchment are summed at the daily time step. Daily runoff data is aggregated to a monthly time step for use in the bulk water system simulation model.

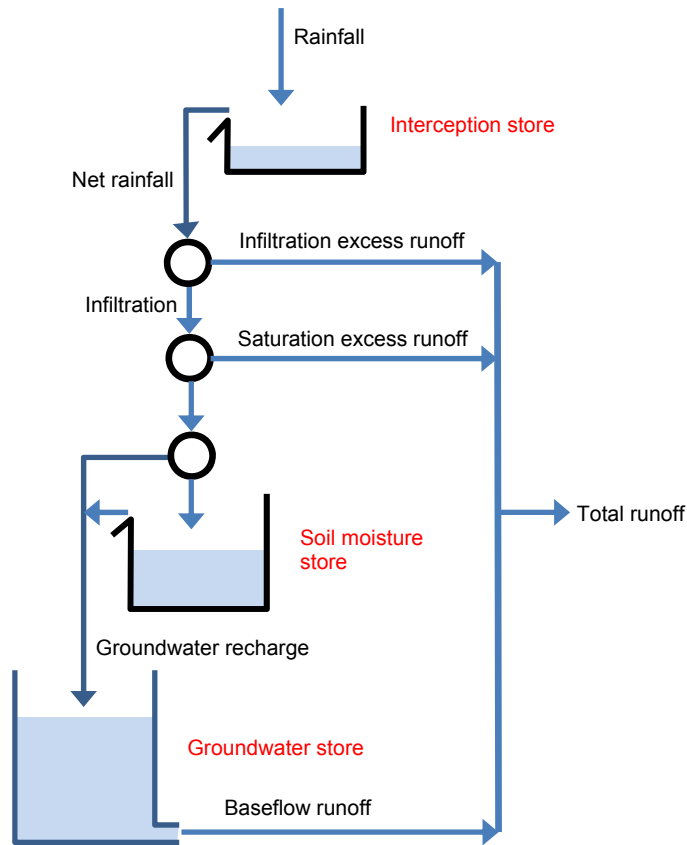


Figure 9 SimHyd schematic [adapted from Argent et. al. (2007)]

Table 4 Description of SimHyd model parameters and initial states [after Cinque (2009)]

Parameters/Initial states	Description
FUfract	Fraction of the subcatchment apportioned to this functional unit
Intcap	Interception store capacity (mm)
Coeff	Maximum infiltration loss (mm)
sq	Infiltration loss exponent
smsCap	Soil moisture store capacity (mm)
sub	Constant of proportionality in interflow equation
crak	Constant of proportionality in groundwater recharge equation
k	Baseflow linear recession parameter
initSFrac	Initial soil moisture store fraction
initGW	Initial groundwater store fraction

Table 5 SimHyd model parameters and initial states for each functional unit (Graz=Grazing, For=Forest) of the nine HWC sub catchments.

Parameter	Glen Martin		Tillegra			Chichester	Grahamstown	Seaham	
	Graz 1	For 1	Graz 1	Graz 2	For 1	For 1	For 1	Graz 1	For 1
FUfract	0.75	0.25	0.42	0.28	0.3	1	1	0.75	0.25
Intcap	3.97	4.79	4.76	4.68	4.92	0.5	2.28	3.97	4.79
Coeff	363	338	318	337	293	85	200	363	338
sq	10	3	4.8	0.4	9.6	3.6	1.5	10	3
smsCap	266	316	71	63	239	435	332	266	316
sub	0.029	0.088	0.003	0.003	0.003	0.167	0.311	0.029	0.088
crak	0.379	0.109	0.828	0.06	0.534	0.728	0.828	0.379	0.109
k	0.06	0.53	0.042	0.293	0.151	0.061	0.292	0.06	0.53
initSFrac	0.001	0.001	0.001	0.001	0.001	0.001	0.001	0.001	0.001
initGW	0.22	0.22	0.22	0.22	0.22	0.22	0.173	0.22	0.22

Validation of runoff simulation

The SimHyd runoff based on rainfall and PET generated by stochastic models calibrated to historical data is compared against historic runoff. For the purposes of long-term drought risk planning, the focus here is on the models' ability to produce realistic stochastic replicates that capture the characteristics of the data that have the greatest influence on water supply drought risk, namely the autocorrelogram of annual flows and the distributions of multi-year overlapping aggregated totals. Figure 10 compares multi-year overlapping aggregated runoff distributions for the observed runoff at the Seaham Residual catchment against the sampling distribution produced by the stochastic model calibrated to historic data. Similar results, not shown, were obtained for the remaining catchments.

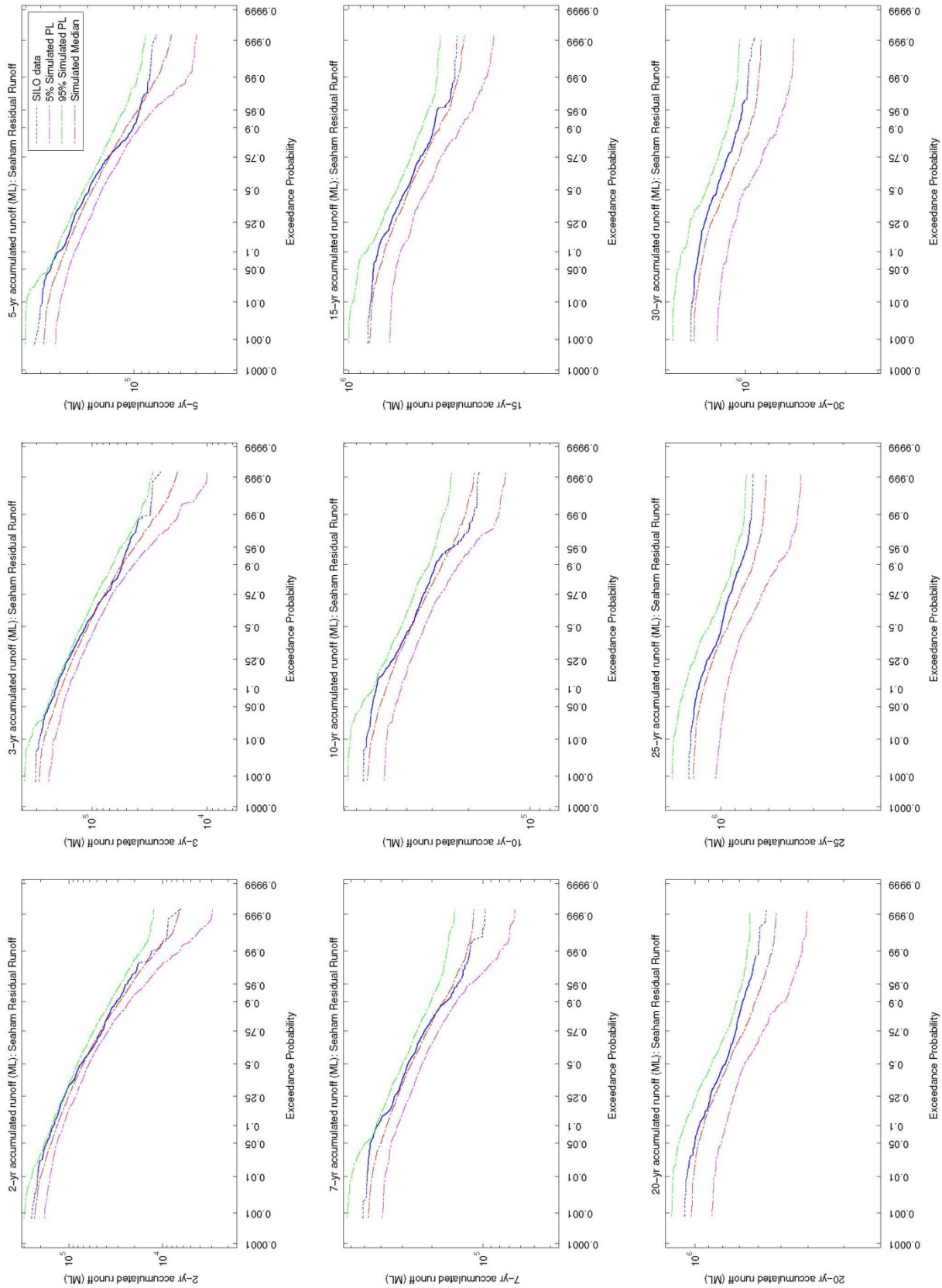


Figure 10 Multi-year overlapping aggregated totals for Seaham Residual runoff for historic and stochastically generated data using stochastic model calibrated to historic data

Figure 11 compares annual autocorrelograms for the five HWC sub catchments against the sampling distributions produced by the stochastic model.

The Figures show that the observed statistics largely fall within the 90% confidence limits implying that the differences between the observed and simulated statistics can be accounted for by sampling error alone. It is therefore concluded that the stochastically-generated rainfall and evapotranspiration time series routed through calibrated SimHyd models produce drought-relevant statistics that are statistically consistent with observed data.

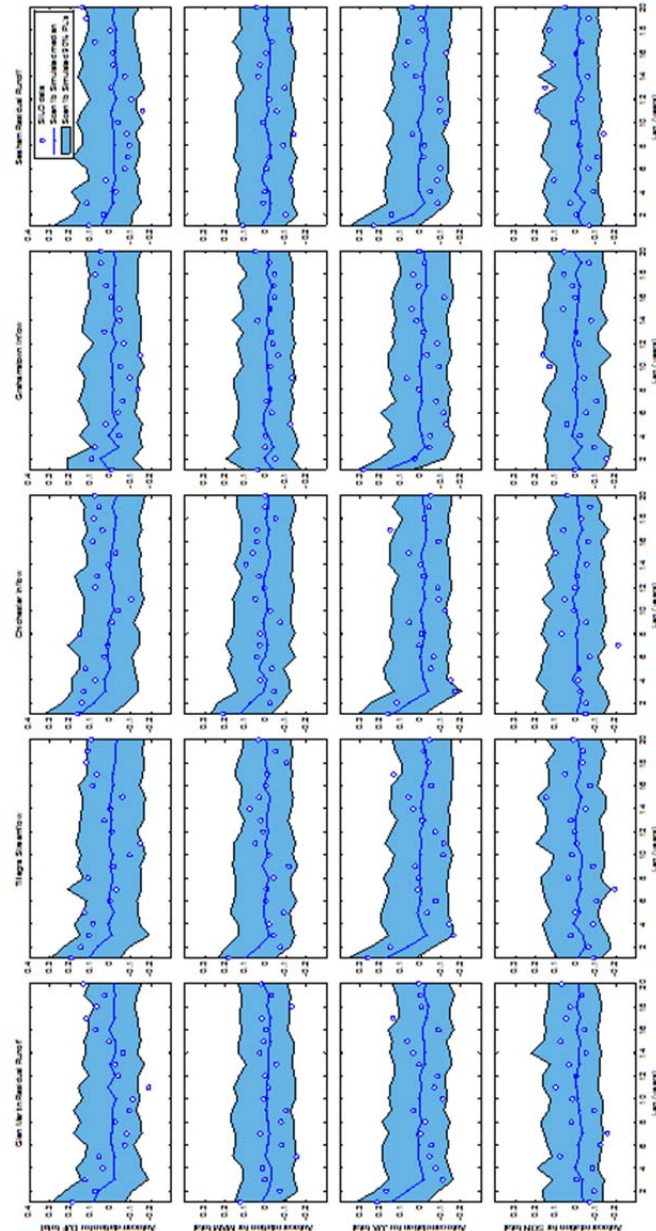


Figure 11 Annual autocorrelograms for Seaham Residual runoff for historic and stochastically generated data using stochastic model calibrated to historic data

2.4 *Lower Hunter Bulk Water System Simulation Model*

This section describes the implementation of equation (3), namely the simulation model of the Lower Hunter bulk water system.

2.4.1 *Current HWC Model*

The current simulation model used by HWC is a custom built FORTRAN model which uses a mass balance approach for simulating the supply system (HWC, 2012). A series of modules is used to simulate the demand, supply elements, transfer systems and capacity as well as the supply sources. The model was reviewed by SKM (2003) which is used as the reference document in this study.

The three major sources including Tomago Sandbeds, Grahamstown and Chichester reservoirs were described by mass balance models. The two major reservoirs were modelled in the same general manner, with the inflow calculated from catchment runoff and stream inflow data. Grahamstown, being an off-river storage, also received pumped transfers from Balickera Pump Station based upon stream flow in the Williams River and available capacity within the reservoir. Natural outflows from Chichester included environmental releases, evaporation and spills. Evaporation and spills were the only natural outflows accounted for in the Grahamstown module. Although spills were permitted these were not desirable due to the cost of pumping the water from the Williams river into the reservoir (SKM, 2003).

The Tomago Sandbeds were modelled as a complex system of natural processes including recharge, evapotranspiration and baseflow. The model comprised of two buckets, each representing half of the capacity of the Sandbeds, one representing the low lying areas and the other the higher areas. Recharge and evapotranspiration occur at each bucket. The differences between the two buckets were represented using different parameters. However, baseflow which represents the natural flow of water towards the ocean only occurs from the low lying bucket (SKM, 2003).

While the HWC model is computationally very quick, its architecture is not well suited for configuring new solutions and interfacing with an evolutionary search algorithm. As a result, a WATHNET5 model of the Lower Hunter system was developed. Before describing the Lower Hunter WATHNET5 model, a brief overview of WATHNET5 is presented.

2.4.2 *Overview of WATHNET5*

WATHNET5 (Kuczera, 2009) is a generalised simulation model using a network flow program (NFP) to allocate water within the system. The bulk water system is represented as a directed graph which is collection of nodes and a set of unidirectional arcs. The nodes represent source, demand or transfer points in the network. The arcs represent flow paths from one node to another. In WATHNET5, two types of arcs are defined, namely stream arcs which represent rivers and conduit arcs which represent pipes or channels. Six different nodes are defined in WATHNET5, namely stream, reservoir, demand, waste, harvest and junction nodes. Stream nodes represent a source of water to the system such as inflow to reservoirs or rainfall over a catchment. Reservoir nodes represent reservoirs and carryover storage from one time step to the next. Demand nodes represent sink points in the network. Junction nodes represent transfer points. Harvest nodes enable application of stochastic transfer functions such as in the modelling of domestic rainwater tank savings or run-of-river diversions at monthly time scales. Waste nodes act as a sink points to collect any water leaving the network.

In a network flow program, transfer costs are assigned to all arcs. In order to force flow through an arc, for instance an environmental flow, a high negative cost needs to be assigned.

At each time step WATHNET5 solves the following NFP:

$$\min_z c^T(x|Q_t, D_t, \theta)z \quad (8)$$

subject to

$$Az = b(x|Q_t, D_t, \theta) \quad (9)$$

$$0 \leq z \leq u(x|Q_t, D_t, \theta) \quad (10)$$

where Q_t and D_t are inflow and demand for time t respectively, θ is a vector of parameters assigned by the user, A is a node-arc incidence matrix and z is a vector of arc flows, x is a vector of decision variables (which can be optimised), $c(x|Q_t, D_t, \theta)$ is a vector of costs assigned to the arcs, $b(x|Q_t, D_t, \theta)$ is a vector of nodal requirements, either restricted demand or supply and $u(x|Q_t, D_t, \theta)$ is a vector of maximum flow capacity in each arc. It is noted that $c(x|Q_t, D_t, \theta)$, $b(x|Q_t, D_t, \theta)$ and $u(x|Q_t, D_t, \theta)$ are specified by the user using a FORTRAN-like script.

The formulation of the NFP in WATHNET5 is best described using an example based on the network shown in Figure 12. This network has two reservoirs and two demand nodes. Reservoir spill is collected by the waste node. The stream nodes provide stream inflow to the reservoirs. Figure 13 shows the full network including hidden arcs and the hidden balancing node. Without these hidden elements it would not be possible to simulate the system in Figure 12. The balance node ensures a mass balance for the network. The demand shortfall arc is assigned a very high cost and only conveys flow to the demand node if the demand cannot be satisfied by any other means. This ensures the NFP always returns a feasible solution even when demand cannot be satisfied by the real system. Waste nodes are connected to the balance node via waste arcs.

To simulate carryover of storage, one or more carryover arcs connect each reservoir to the balance node. By assigning sufficiently large gains (negative costs) to the carryover arcs, the NFP will assign flows to the carryover arcs in preference to assigning flows to a waste node.

WATHNET5 offers several options to assign carryover gains. These are illustrated in Figure 14 which shows the dialog box to assign carryover gains. All but one option involve some form of manual assignment of gains to individual carryover arcs. The remaining option, which is the one used in this study, automates the assignment of gains using the following equation:

$$Gain(i) = BG + (i - 1) * IG, i = 1, \dots, N \quad (11)$$

where $Gain(i)$ is the gain assigned to the i^{th} carryover arc, BG is the base gain, IG is incremental gain, and N is the number of carryover arcs. The capacity of each carryover arc is set as follows:

$$u_i = \frac{\text{ResCap}}{N}, i = 1, \dots, N \quad (12)$$

where u_i is the capacity of i^{th} carryover arc for the reservoir and ResCap is the reservoir capacity.

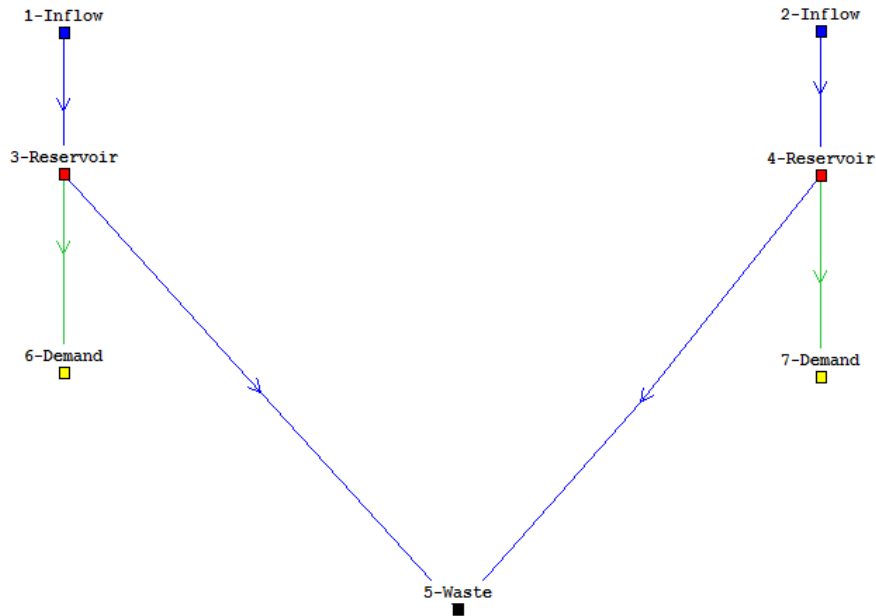


Figure 12 A simple network in WATHNET5[adapted from Kuczera (1992)]

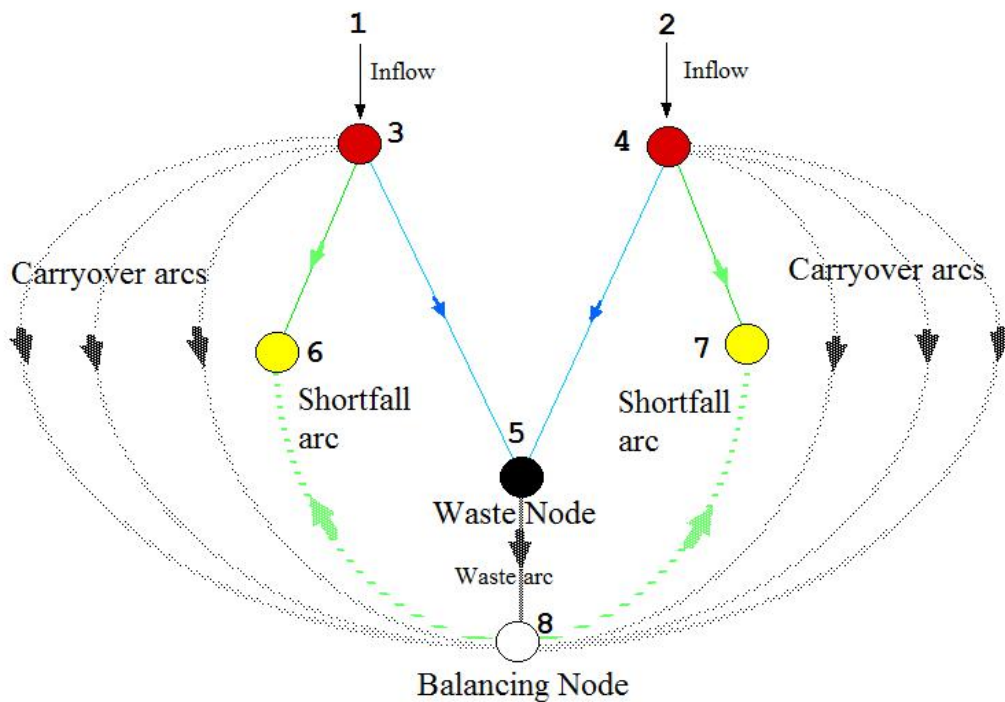


Figure 13 Full network including hidden arcs and nodes for network shown in Figure 12 (modified from Figure 12 (Kuczera 1992))

Carryover gains

Number of carryover arcs
20

Carryover gain option:

☒ Base gain
10000
and incremental gain
100
with carryover storage in:

☒ Equal increments
☐ Non-uniform increments
Edit

☐ Edit
non-uniform gain increments with offset
0
and scaling
1.000

Figure 14 Carryover arcs input box

2.4.3 Daily WATHNET5 Model of Current Lower Hunter Bulk Water System

The WATHNET5 schematic of the current Hunter System is shown in Figure 15. The layout was designed to spatially resemble Figure 6 to allow the components to be easily identified. Each subsystem within the schematic is briefly described. The model was configured to run at a daily time step.

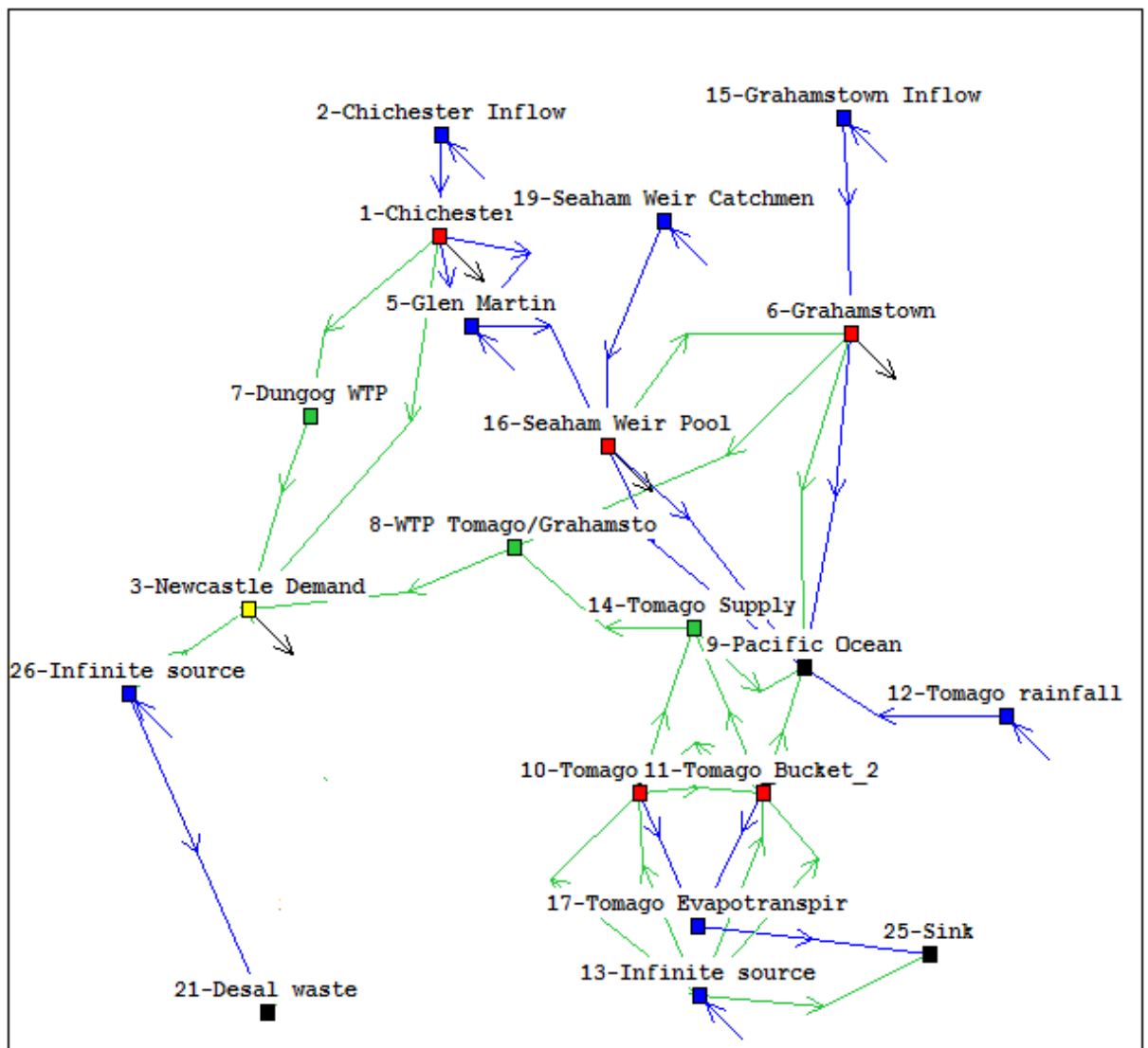


Figure 15 Schematic of current Hunter water supply modelled by WATHNET5

Chichester Subsystem

The configuration of the Chichester subsystem is shown in Figure 16. This includes the reservoir itself, inflow node and stream, as well as outflow arcs to simulate evaporation, spill, environmental flows and supply.

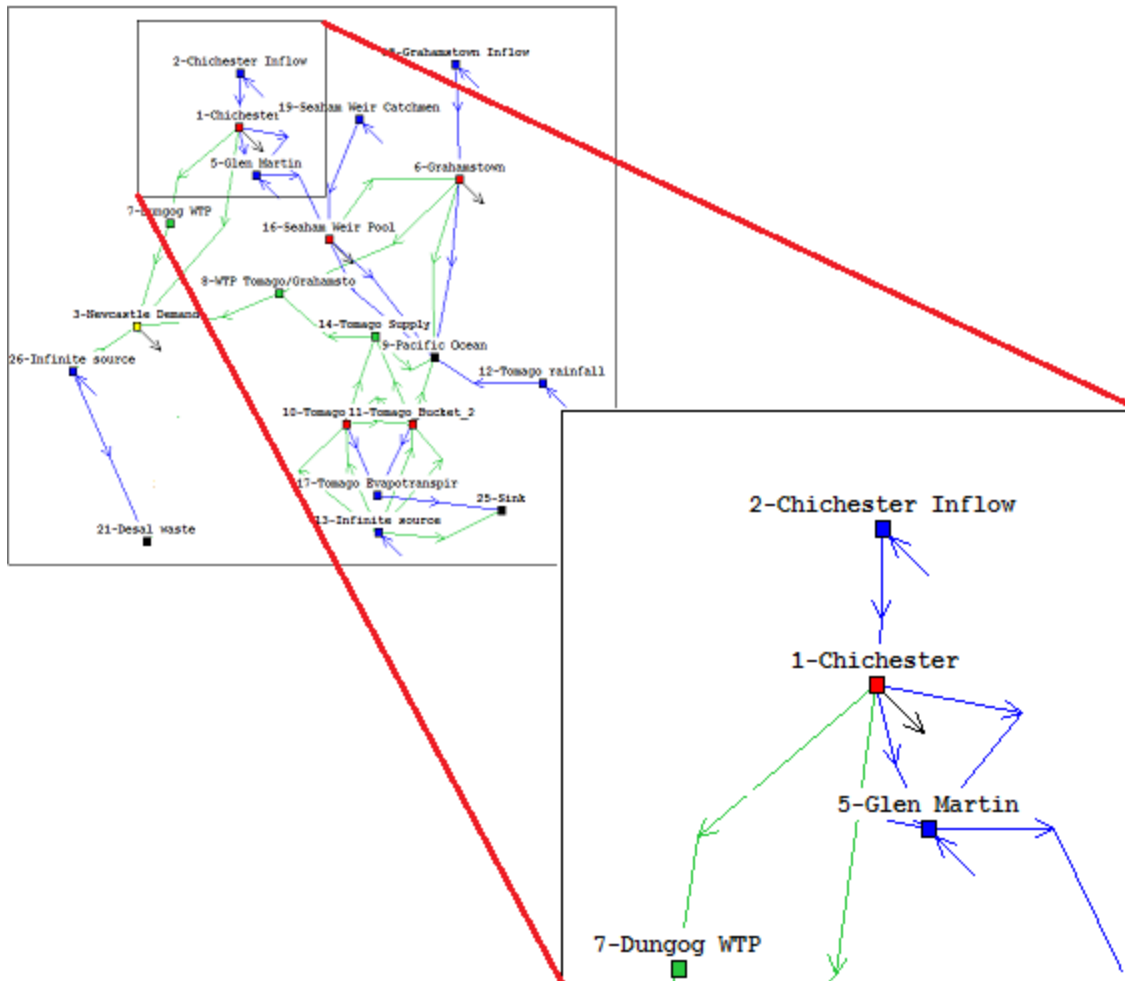


Figure 16 Schematic of Chichester subsystem

The active capacity of Chichester reservoir is 21,500 ML.

The two blue arcs (1, 5)² enable environmental flows and natural spill to occur. The environmental flows are equal to the lesser of the natural flow or 14 ML/d. This relationship determines the capacity of the arc according to the value of the environmental flow at a given time step. In order to ensure that these flows occur, one arc is loaded with a large negative cost. The other arc, the spill arc, is present merely to facilitate any excess flow that exceeds the capacity of the dam and other outflow mechanisms. This arc has a large capacity to enable it to transfer any volume of spill in excess of the reservoir volume. It also has a neutral cost to enable the model to access it when required.

² The arc notation (f,t) means the arc flows from node f to node t.

The Chichester system is connected to the supply network by the Chichester Trunk Gravity Main (CTGM). This is represented by the green conduit arc, (1, 7). This has a maximum flow capacity of 90 ML/d which is also limited by the amount of water which can be treated by the Dungog Water Treatment Plant. Table 6 documents the hydraulic constraints which restrict the amount of water that can be contributed to the system by this source.

Table 6 Chichester Trunk Gravity Main Restrictions (SKM, 2003)

Chichester Storage	Capacity
%	ML/d
> 60 %	83
> 45 %	60
> 20 %	27
< 20 %	5

There is an additional physical constraint on the pipe arising from the possibility of damage to the pipe if there are no flows being carried. For this reason it is desirable that at least 30 ML are transported each day when possible. The low flow conditions where storage is below 20% are to be avoided if possible.

Grahamstown Subsystem

The Grahamstown subsystem consists of Grahamstown reservoir and Seaham Weir.

The capacity of the Grahamstown reservoir was increased to 192,350 ML in 2005 following upgrades to the spillway. As Grahamstown reservoir is an off-river storage, the simulation of the inflow must include pumping from the Williams River at Balickera Pump Station and runoff from the catchment area. The dead storage (i.e. water that is stored below the elevation of the offtake from the dam) in Grahamstown Dam is estimated to be 9,950 ML and the accessible storage is 183,300 ML.

Up to 280 ML/day can be extracted from Grahamstown reservoir and treated by the Grahamstown/Tomago Water Treatment Plant. This, however, has the potential to be increased if the current supply system should be unable to meet the demand.

Although Seaham weir is not a supply source, it is modelled as a reservoir to control the water levels and allow pumping to occur from the Williams River. The weir pool is represented in the model as a reservoir with a constant surface area of 2 km² and capacity of 360 ML. The inflow to the weir includes the residual flow down the Williams River which is derived by the upstream arcs and runoff from the Glen Martin and Seaham catchments.

It is assumed that pumping from the weir pool to Grahamstown reservoir occurs when the Grahamstown storage is more than 5,000 ML below its full capacity, which reflects HWC operating practices. The purpose of allowing a 5,000 ML freeboard in the dam is to provide space in the dam to catch local runoff and thereby minimise the risk that pumped water will contribute to spills from the dam. The pumping volume is set equal to 90% of flow in the Williams river to reflect the average proportion of flow that can be harvested in terms of the available water quality, with the maximum pumping capacity of 1440 ML/day.

Tomago Subsystem

The Tomago aquifer subsystem shown in Figure 17 is comparatively complex. The aquifer is represented by two buckets, nodes 10 and 11. Node 10 represents the higher parts of the aquifer, while node 11 represents the lower part which is connected to the ocean. Each bucket represents half of the 130 km² surface area which forms the

Tomago Sandbeds. The water level in the Tomago aquifer is taken as the average of the water level simulated in each of the two buckets. The accessible storage in the Tomago aquifer is estimated to be 60,000ML when the aquifer is full. The storage is nominally full when the average water level is 4.8m above sea level, and the storage is empty when the average level drops below 1.8m above sea level.

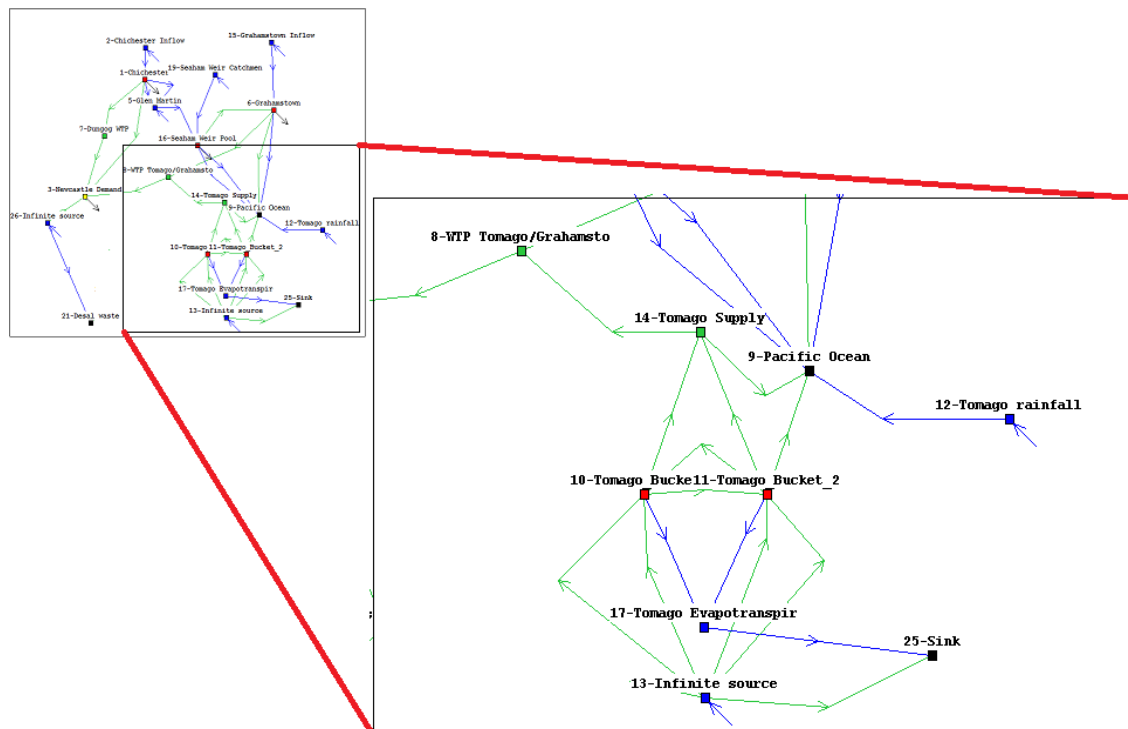


Figure 17 Tomago Sandbeds subsystem

Arcs (14,10) and (14,11) convey recharge to the buckets. This is accomplished by setting costs for (14,10) and (14,11) to very high negative values and using an arc script to set the required recharge equal to the arc capacity. The high negative arc cost induces a flow from node 14, an infinite source node, equal to the arc capacity.

The algorithm for recharge is described by SKM (2003). First, interception by the unsaturated zone (ML/day) is calculated as a function of the current bucket volume. If the interception is greater than the rainfall on a particular day then no recharge occurs. However, if the rainfall exceeds interception, the recharge to the aquifer is the lesser of the maximum recharge capacity and the difference between rainfall and interception.

The moisture deficit is used to simulate the unsaturated zone in the aquifer (SKM, 2003). If the interception is greater than the rainfall then the deficit is calculated by subtracting the interception from the daily rainfall value; otherwise, the deficit is set to zero.

Evapotranspiration represents uptake of water from the aquifer by plants as well as evaporation from the water table. It is simulated in a manner similar to recharge using arcs (11,17) and (12,17). The evapotranspiration is a function of potential evapotranspiration, current bucket volume and moisture deficit.

The flow between the buckets and between the lower bucket and ocean is determined by a Darcy law equation. Noting that the volume in the Tomago buckets represents the available water above sea level and the specific yield is constant, it follows that the difference in water table height between buckets is proportional to the difference in bucket volumes. Hence the flow between buckets is proportional to the volume

difference. Likewise the flow between the lower bucket and ocean is proportional to the volume in the lower bucket.

The supply from the Sandbeds is limited by HWC to 90 ML/d to reflect current operation of the borefield. The conduits leaving the buckets each have large capacities to allow the supply rate to be manipulated. This variable needs to be managed appropriately because if the available supply is over drawn, salt water intrusion and decreased water quality can occur. A trigger volume, which can also be adapted, has been established to prevent over extraction of the water. This prevents pumping whilst still allowing the processes of evaporation and recharge to occur below the trigger volume.

Demand and Restriction Policy

All industrial and residential demand is simulated as one demand node in the WATHNET5 model. The demand configuration is shown in Figure 18. The demand is mainly supplied by Dugong and Tomago water treatment plants.

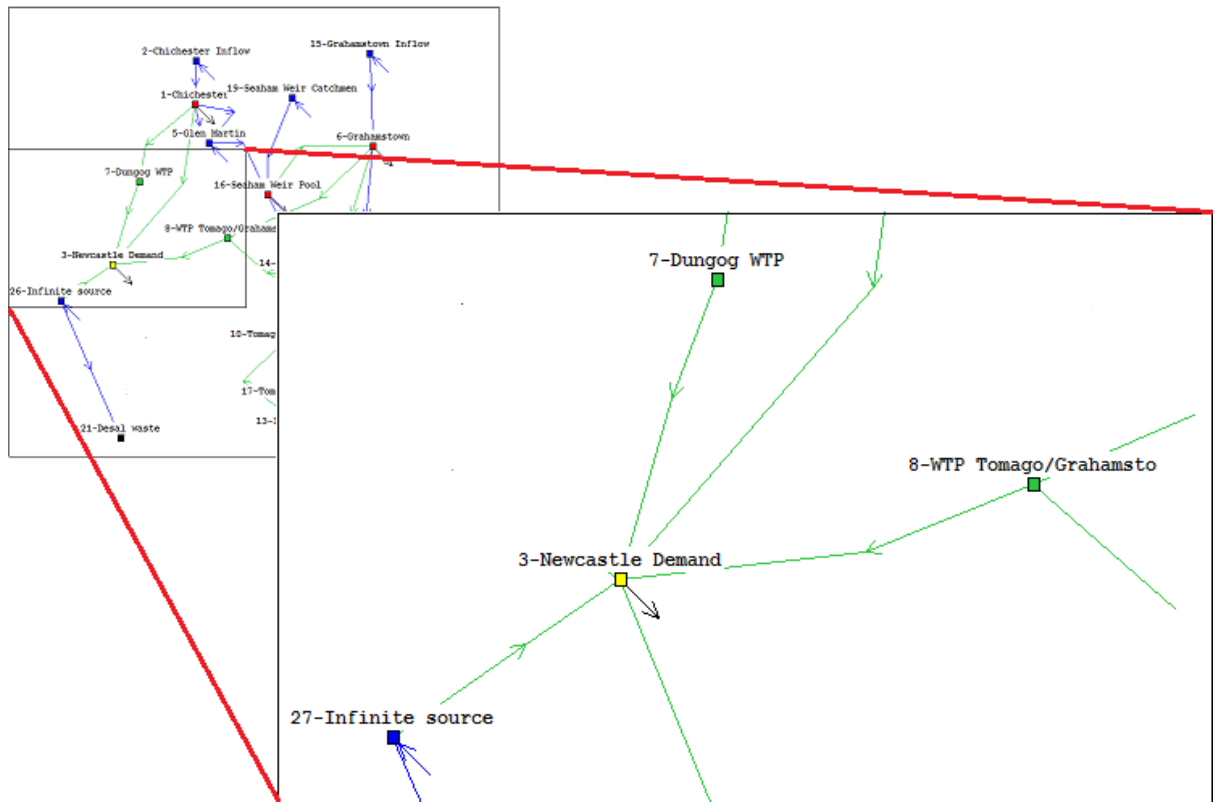


Figure 18 Demand subsystem

Table 7 summarises a possible drought water restriction policy for the Lower Hunter. The restriction level is determined by storage triggers. For example, if the storage is between 50 and 60% then level 2 restrictions apply and demand is reduced by 3%.

Table 7 Possible restriction policy for Lower Hunter water system

Restriction level	Storage trigger (%)	Demand reduction (%)
Level 1	70	0
Level 2	60	3
Level 3	50	10
Level 4	40	20
Level 5	30	28

Note: Level 1 relates to restriction readiness activities, so costs are incurred but no water savings are relied upon.

2.4.4 Validation of Daily WATHNET5 Model

The daily WATHNET5 model of the Lower Hunter was validated against the HWC model. The daily WATHNET5 model and the HWC model were run using historic streamflows for the period 1931 to 2010 with annual demand set to 73 GL. Figure 19, Figure 20 and Figure 21 compare time series of reservoir volumes simulated by the daily WATHNET5 and HWC models. The agreement is very good suggesting the daily WATHNET5 model produces results consistent with the HWC model.

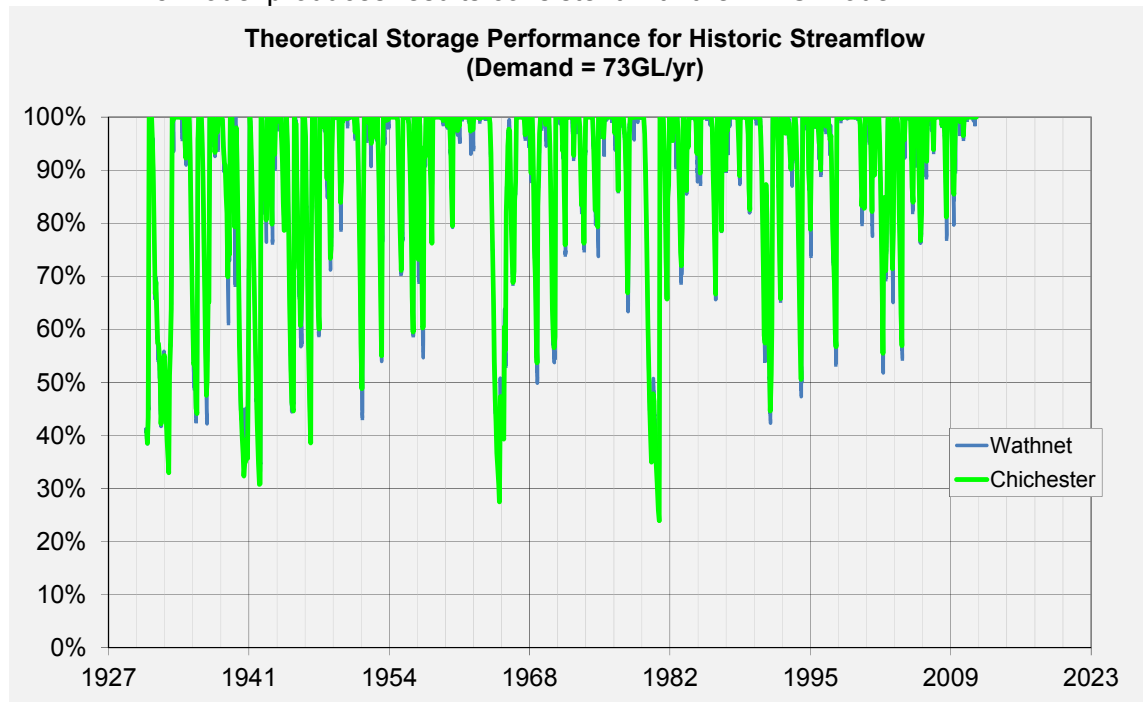


Figure 19 Comparison of Chichester reservoir volumes simulated by daily WATHNET5 and HWC models

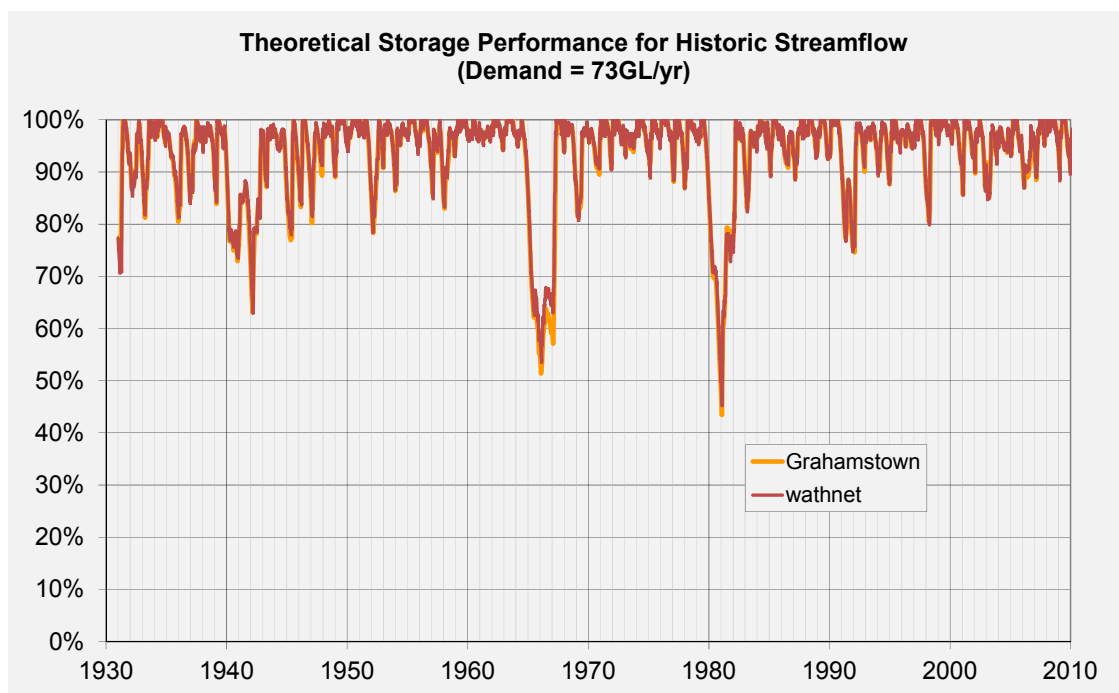


Figure 20 Comparison of Grahamstown reservoir volumes simulated by daily WATHNET5 and HWC models

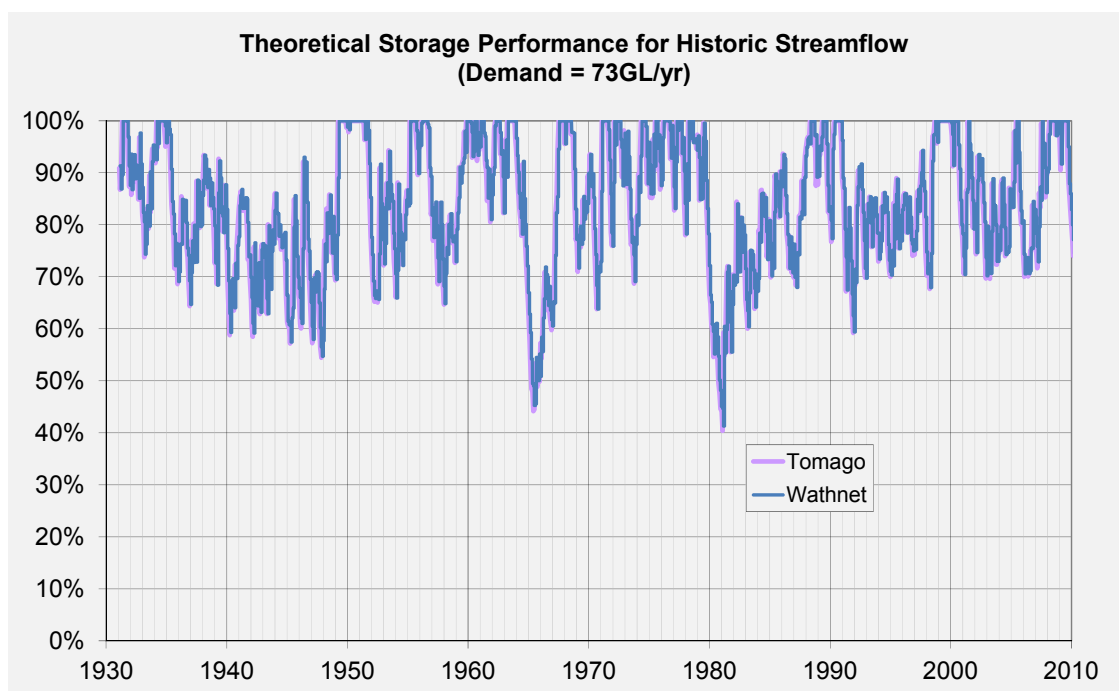


Figure 21 Comparison of Tomago total bucket volumes simulated by daily WATHNET5 and HWC models

2.4.5 Monthly WATHNET5 Model

The use of the daily WATHNET5 model in optimisation is not computationally feasible with the 72-core parallel cluster available for this study. To make the optimisation problem tractable, the daily WATHNET5 model was adapted to run at a monthly time step.

The conversion of the daily WATHNET5 model to a monthly model is straightforward for all but the Grahamstown subsystem. This is because the drawdown times of the reservoirs are sufficiently long to be insensitive to daily variations in streamflow and consumption. However, in the case of the Grahamstown subsystem, the transfer of water from Seaham weir to Grahamstown reservoir is sensitive to variations in daily flows. Figure 22 shows a scatter plot of monthly inflow volume to Seaham weir and the maximum volume that can be pumped in the month. During periods of high inflow into Seaham weir, the daily inflow volume exceeds the capacity of the Balickera pumps to transfer water to Grahamstown. Therefore, during high flow periods, simple scaling of the Balickera pump capacity to a monthly volume would result in a gross overestimate of the transfer capacity of the Balickera pumps.

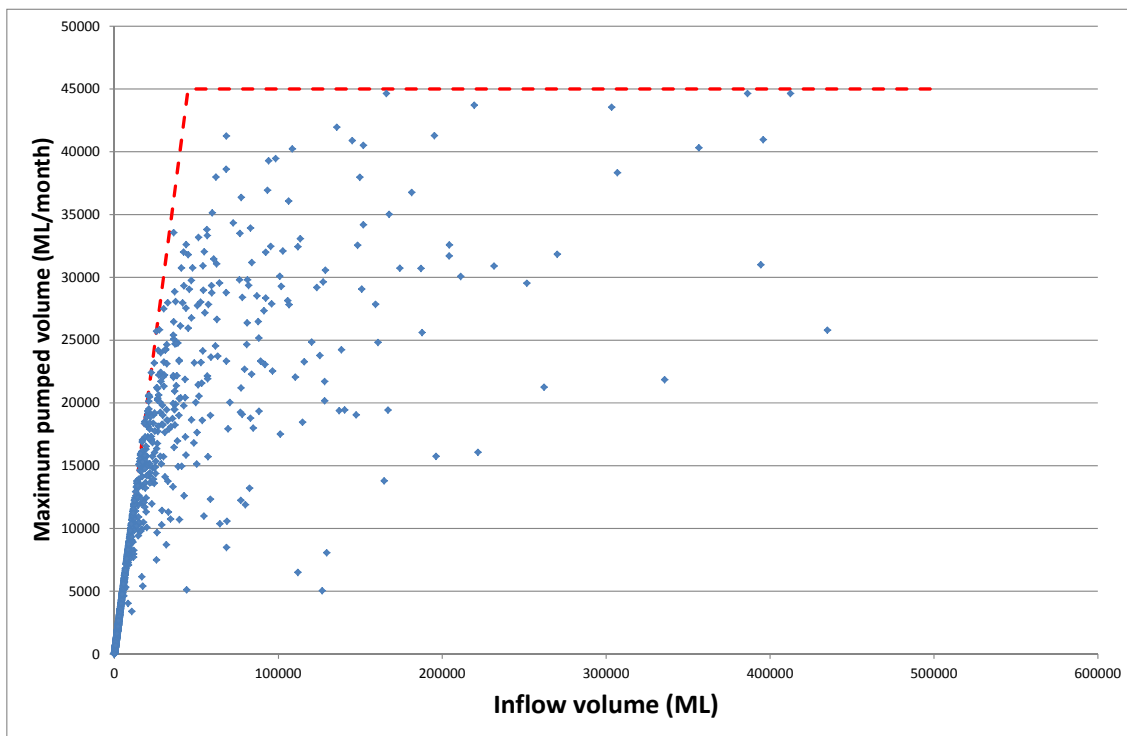


Figure 22 Scatter plot of monthly Seaham weir inflow volume and maximum possible monthly volume pumped to Grahamstown

To deal with this type of temporal scaling problem, WATHNET5 has a harvest node which uses a k-nearest neighbour algorithm to randomly sample the actual volume pumped to Grahamstown. This is accomplished by importing the data shown in Figure 22 into WATHNET5. At every month of the simulation the inflow into Seaham weir is determined. Then the k^{th} nearest neighbour pumped volume is randomly sampled from the imported database and assigned as the capacity of the Balickera pumps for that month.

A similar approach is required when introducing domestic rainwater tanks as an alternative supply source. Because rainwater tanks can spill and empty several times in a month, a monthly water balance would produce misleading yields. Use of a harvest node using monthly rainfall as the input will deal with this problem.

Figure 23 presents a schematic of the monthly WATHNET5 model with the addition of a harvest node 24 to properly allow for the variation in transfer capacity shown in Figure 22.

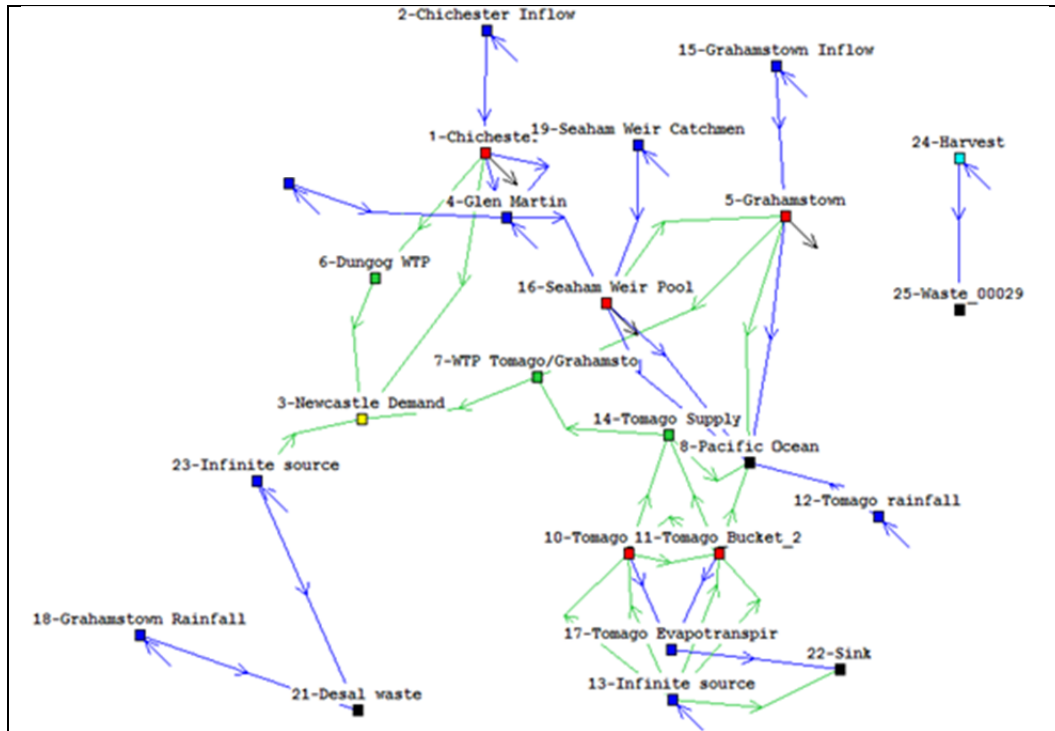


Figure 23 Schematic of monthly WATHNET5 model

To ensure the monthly WATHNET5 model produces results consistent with the daily WATHNET5 model, the two models were run for the historic period between 1931 and 2010 with an annual demand of 73 GL. The distributions of reservoir volumes derived from the daily and monthly WATHNET5 models are shown in Figure 23 to Figure 27. All plots show a close correspondence between the distributions derived from the daily and monthly models. Given that use of the monthly model will reduce computation time by a factor of 30, any minor loss of accuracy is more than offset by the capability to perform optimisation.

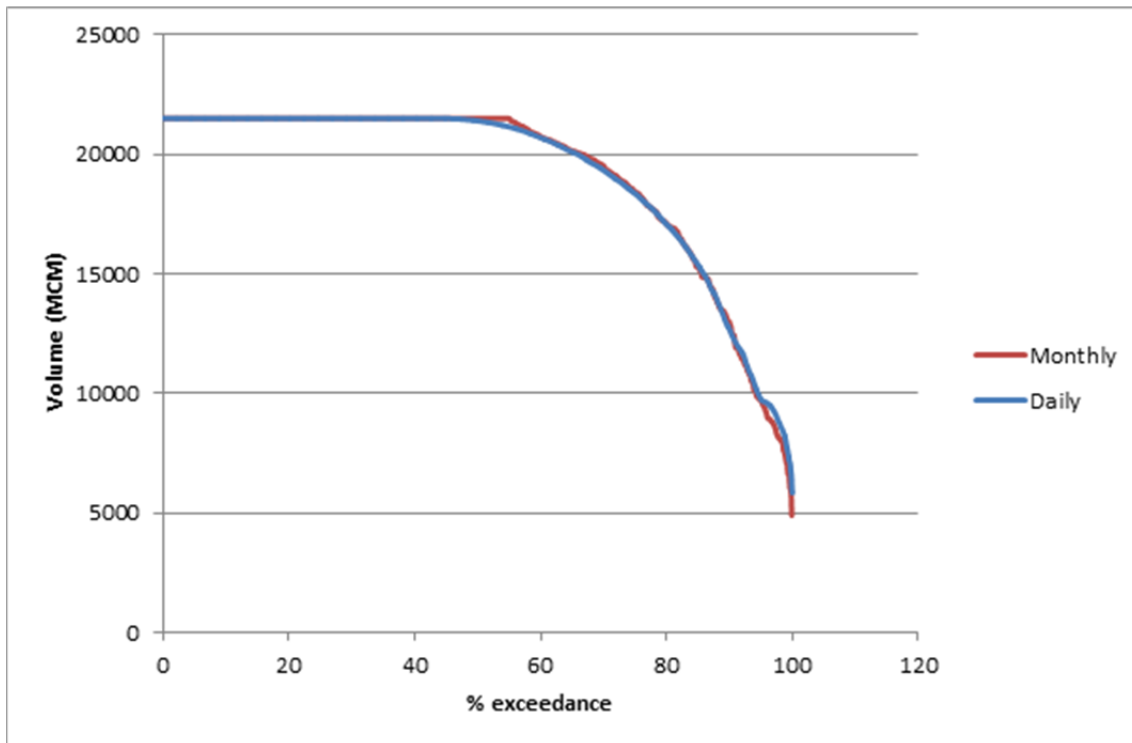


Figure 24 Chichester reservoir volume distributions derived from daily and monthly WATHNET5 models

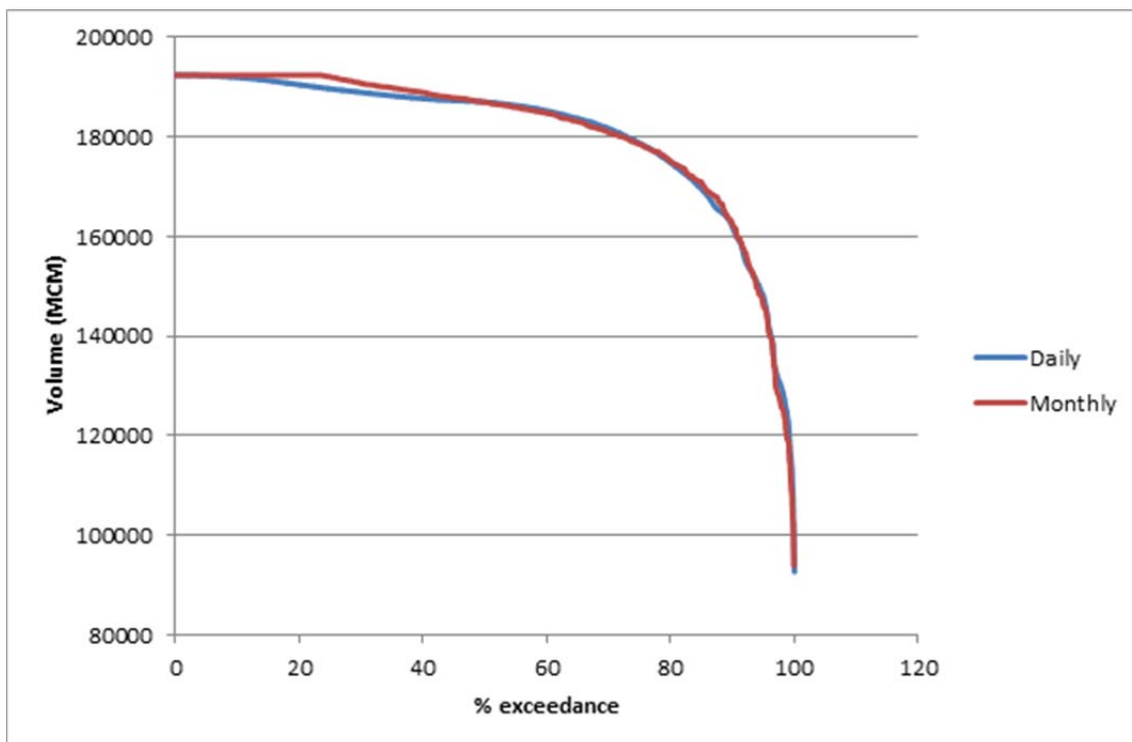


Figure 25 Grahamstown reservoir volume distributions derived from daily and monthly WATHNET5 models

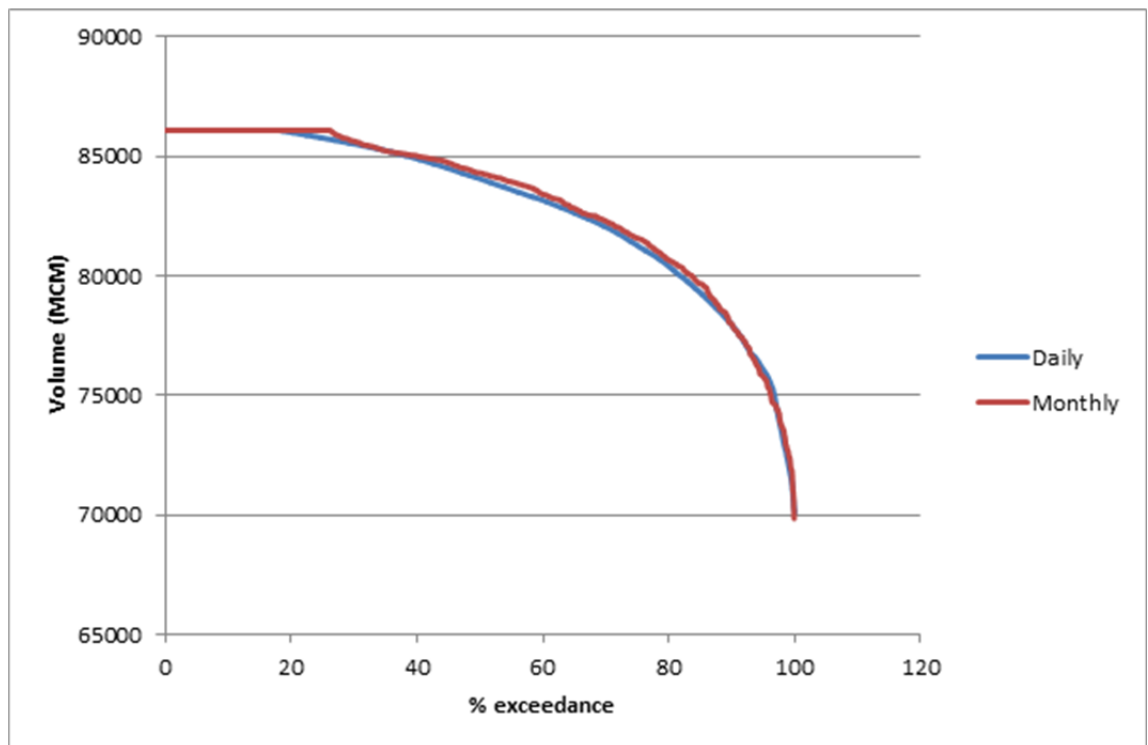


Figure 26 Tomago upper bucket volume distributions derived from daily and monthly WATHNET5 models

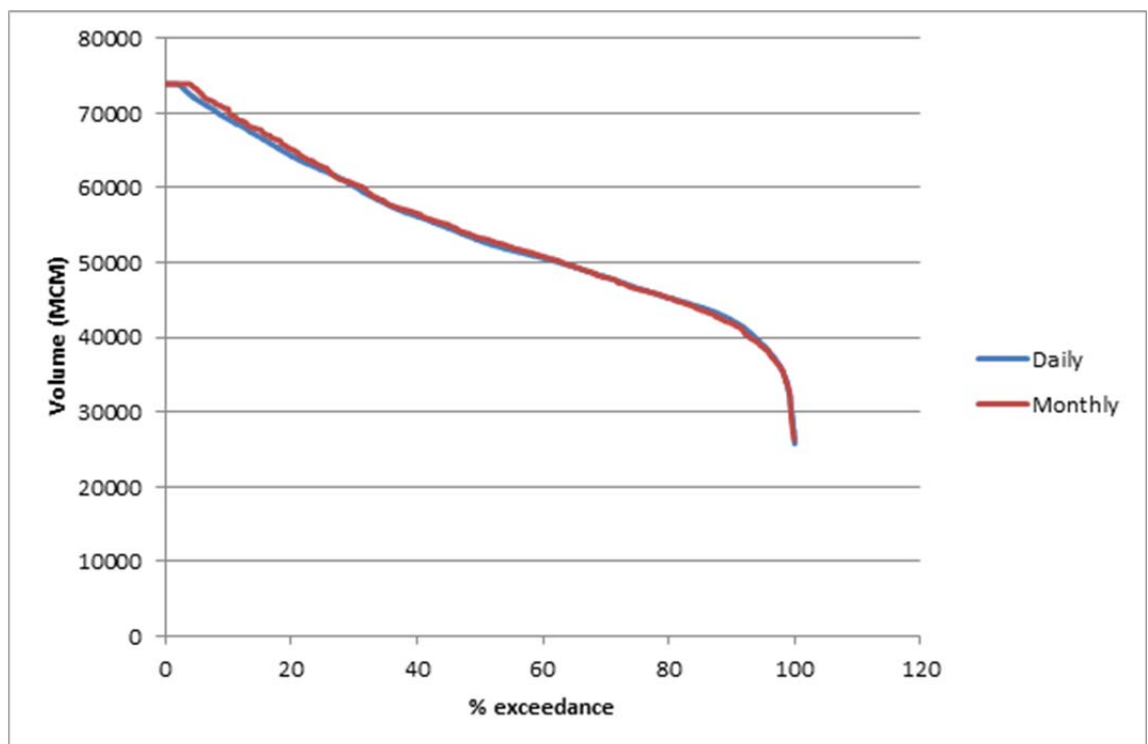


Figure 27 Tomago lower bucket volume distributions derived from daily and monthly WATHNET5 models

2.5 *Formulation of the Robust Optimisation Problem for the Lower Hunter System*

2.5.1 *Generalising the monthly WATHNET5 model*

In general, there are a range of water supply and demand management options available to secure the water supply for any region or locality. The National Urban Water Planning Principles adopted by the Council of Australian Governments (COAG) under the National Water Initiative state that optimal water planning should “*consider the full portfolio of water supply and demand options*”. Options can be characterised in various ways – supply/demand, short-term/long-term – however for modelling purposes it is most convenient to categorise options as:

- manufactured new supply options e.g. permanent desalination, temporary desalination, wastewater recycling
- climate dependent new supply e.g. dams, groundwater, stormwater harvesting, inter-regional transfers, domestic rainwater tanks
- demand management e.g. water efficiency, mandatory drought water restrictions

In the quest to secure water supply for the Lower Hunter against drought while catering for population growth, a mix of short- and long-term future options needs to be considered. For the purposes of this case study, which aims to demonstrate a methodology in an end user context, a limited number of options from each category were included in the monthly WATHNET5 model. Whilst these options are plausible they have been generalised and therefore are not a comprehensive reflection of any specific options under consideration through other water planning processes. Modifications to the WATHNET5 model were as follows:

1. Several infrastructure options were added to the model. These include a large scale permanent desalination plant, domestic rainwater tanks, a new dam, and expansion of the transfer capacity of the pipeline from Chichester to Newcastle.

Figure 28 presents the WATHNET5 schematic for the generalised model. A brief description of each infrastructure option follows:

- **Desalination**

There is potential to add a large scale permanent desalination plant at various locations. For ease of modelling it was assumed that the desalination plant would supply the central demand node (Node 3 Newcastle Demand). Node 20 introduces an optional desalination plant. The operation of the desalination plant would be triggered by a storage threshold.

- **Domestic rainwater tanks**

Domestic rainwater tanks experience frequent filling and drawdown cycles. By providing an alternative source of supply to the bulk water system, they offer the benefit of slowing down the drawdown of the bulk water system and thus delaying the triggering of drought contingency plans. Mass implementation of domestic rainwater tanks is incorporated into the model using the harvest node 26 in conjunction with node 23 and arcs (23,3). This is assumed to be a retrofit of new tanks to existing residential dwellings (because new dwellings have an alternative water source to meet BASIX).

The uptake of domestic rainwater tanks would likely depend on whether installation was mandatory or discretionary, and if discretionary, the level of subsidies offered (if any). For modelling purposes it is assumed that a subsidy equivalent to twice the NSW State Government rebate would be offered. It is expected that, at best, 100,000 5 kL tanks could be installed recognising that not all households would participate in discretionary installation of rainwater tanks due to space limitations, aesthetics or installation inconvenience.

- **New surface water source**

The Chichester River is regarded as HWC's most reliable source of water with an average streamflow of about 120 GL/year and a moderate annual coefficient of variation of 0.58. Currently, HWC gains access to only 25% of these flows (less than 10% of total Williams River flows), limited largely by the storage capacity of the existing Chichester Dam. A new dam complementing Chichester Dam would increase access to these flows through increased storage capacity.

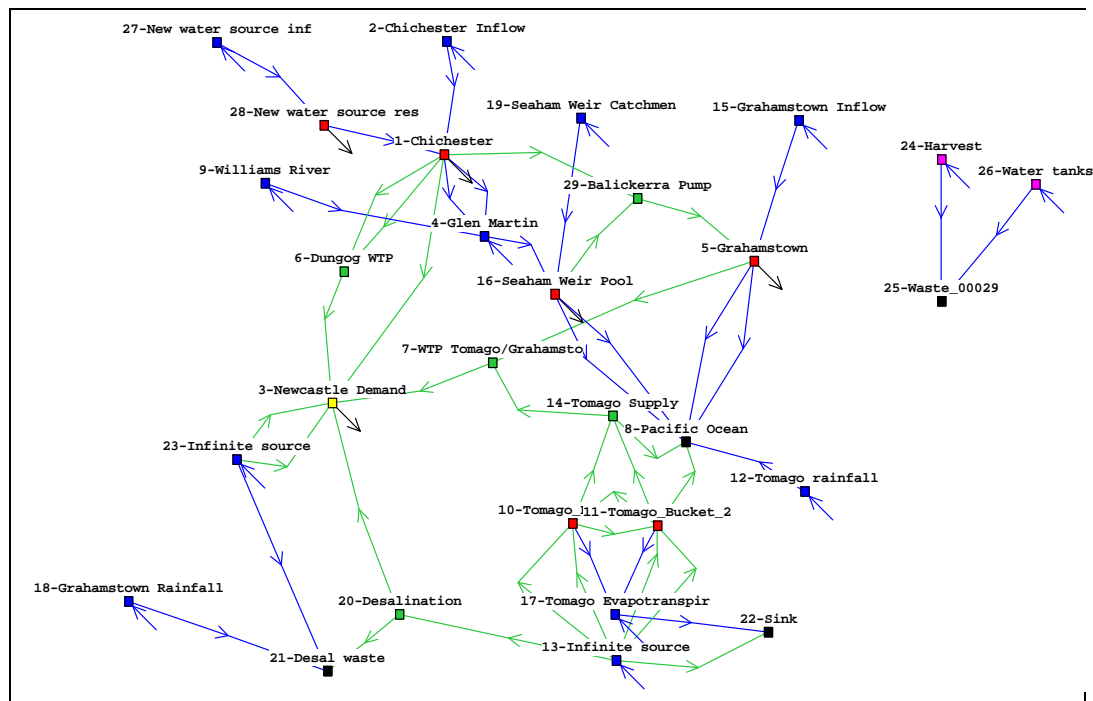


Figure 28 WATHNET5 schematic of the generalised Lower Hunter model

The new dam would serve the dual purposes of river flow regulation to improve the reliability of supply to Grahamstown Dam as well as providing water directly via the Chichester pipeline. Flows would be selectively released into the Williams River to be later collected at Seaham Weir and transferred to Grahamstown Dam via existing infrastructure. A new dam would increase supply reliability via the Chichester pipeline, delivering treated water to key growth areas west of Tarro and reducing reliance on the Grahamstown Scheme.

A new surface water source node 28 was added to the WATHNET5 model. It is noted that pumping from Seaham to Grahamstown is limited by natural flow in the Williams River. However, if the new surface water source is present, large steady controlled releases will enable the Balickerra pumps to work at capacity. This necessitated revising the Grahamstown subsystem. The natural flow

component arriving at Seaham Weir enters node 16 and can be transferred to Grahamstown using the k nearest neighbour sampling scheme. In contrast, when the new surface water source is present, controlled releases from the new dam are directed through arc (1,29). The capacity of arc (1,29) is set to zero for scenarios that do not include the new dam. The capacity of arc (29,5) is set at the maximum capacity of the Balickera pumps.

2. The current model implements fixed operational rules such as defining the trigger for transferring water from Seaham weir or how much water can be transferred from Chichester to Newcastle. Some of these rules are based on hydraulic constraints, while others are not. All the non-physical rules were removed to provide greater flexibility for the optimisation to explore different modes of operation.

Presently HWC limits transfers from Tomago sandbeds to 90 ML/day. However, the installed system is capable of pumping 110 ML/day when Tomago is more than 70 % full. If the storage is less than 70% then the pumping rate decreases linearly from 110 ML/day to 45 ML/day.

It is assumed there is no limitation on transfer capacity from Grahamstown reservoir to Tomago water treatment plant and from there to the Newcastle node. It is assumed that investment in transfer capacity will always be sufficient to meet demand.

Apart from introduction of restrictions the current model has no other strategies in place to manage severe drought. The development of a more comprehensive drought contingency plan (DCP) is the subject of the next section.

2.5.2 Decisions

A range of options are available to ensure a secure water supply for the Lower Hunter in the face of uncertain future climate change. In this study, fourteen options or decision variables, listed in Table 8, were identified as being potentially important. The decision variables fall into three categories:

1. Infrastructure

Infrastructure options refer to the construction and commissioning of physical assets such as dams, treatment plants, pipelines, desalination plants, water recycling plants, investment in water efficient technology and so on. It is assumed at the start of the simulation that any infrastructure asset is fully commissioned, except in the case of desalination. The desalination plant may be built up front (lead time equals zero) or it may be constructed during the simulation with a decision variable being the lead time.

2. Operational

Operational options refer to rules that control the operation of the bulk water system.

3. Drought contingency

Drought contingency options may be infrastructure or operational options. Collectively, they define a drought contingency plan (DCP). The purpose of a DCP is to ensure that the community served by the bulk water system can survive severe drought up to a specified return period without economic and social collapse.

In an industry position paper describing a framework for urban water resource planning, Erlanger and Neal [2005] state in their opening that:

“A safe and reliable water supply system is of utmost importance to the community. It is expected and understood that water utilities manage their water resources so that communities never run out of water.”

Erlanger and Neal recognise that failure to supply minimum water needs for an extended period would most likely result in disastrous social and economic losses that could conceivably threaten the very existence of the urban community. The notion of never running out of water should not be interpreted as meaning business-as-usual during severe drought. Rather it means the community should not be exposed to catastrophic shortages of water in the event of extreme drought. It does not preclude significant costs and hardship during severe drought.

The decisions are listed in Table 8 together with the lower and upper bounds imposed on the optimiser.

Decisions x_1 and x_2 define the first stage of the DCP, namely the imposition of restrictions primarily on outdoor water use. When the total storage fraction falls below the trigger x_1 , no restriction is imposed but actions are implemented to prepare the community for the imposition of mandatory restrictions. The second level of restrictions is imposed on outdoor domestic water use with an expected target total demand reduction of 3% when the total storage fraction falls below $(x_1 - x_2)$. The third level of restrictions is imposed when the total storage fraction falls below $(x_1 - 2x_2)$ with total demand expected to be reduced by 10%. If the total storage fraction falls below $(x_1 - 3x_2)$, then the fourth level of restrictions is imposed with outdoor domestic water use totally banned resulting in an expected 20% reduction in total demand. Finally, the last level of restrictions is imposed when the total storage fraction falls below $(x_1 - 4x_2)$ with total demand expected to be reduced by 28% as the community voluntarily cuts back on water use.

Decisions x_3 and x_4 define the second (and emergency) stage of the DCP. When the total storage fraction falls below the trigger $x_3^*(x_1 - 4x_2)$, emergency rationing is imposed with total water use reduced by $100*(1-x_4)\%$. The upper limit on x_4 is 70%, which corresponds to a demand reduction greater than the maximum reduction of 28% expected during level 5 restrictions. The imposition of emergency rationing would be expected to cause hardship within the community with significant economic and social costs. There is little precedent for such emergency measures. The experience of the city of Fukuoka in Japan in 1978 provides insight into such an emergency (Koga, 2012):

“Due to low rainfall since previous year, Fukuoka City had to restrict its water supply for 287 days from May 20, 1978 to March 24, 1979. Total hours of supply restriction was 4,054 hours (water supply was suspended an average of 14 hours a day), and a total of 13,433 water trucks were mobilised. Especially in summer, citizens can receive water only 5-6 hours in the evening of the day, and sometimes water supply was completely cut off in about 45,000 households. Citizens were not able to access to water which is indispensable to life, and even there were new words such as “Fukuoka desert” and “drought evacuation”. Civic life was disrupted, and the urban function could be ceased.

Families with infants and elementary school children who were on summer vacation evacuated from drought-stricken Fukuoka, and businesses which

require plenty of water experienced a drop in income due to menu restriction and reductions of business hours.

Households with water cut-off had difficulty carrying buckets of water to their homes; especially people living in apartments had to take the stairs. And flush toilets cannot be used without a bucket of water.

There were many complaints especially regarding “fair water supply”, especially in using water during no-water period by utilising water tanks.”

Table 8 List of decision variables

Decision x	Description	Lower limit	Upper limit	Category
1	Level 1 restriction storage trigger ¹	0.00	0.90	Drought contingency
2	Restriction trigger increment	0.05	0.25	
3	Emergency rationing trigger	0.0	1.0	
4	Severe rationing demand scaling factor	0.4	0.7	
5	Storage trigger to initiate desalination plant construction	0.0	1.0	
6	Desalination plant capacity (ML/day)	0	500	
7	Desalination plant construction lead time(month)	0, 12, 24, 36 or 60		
8	Desalination plant trigger	0.0	1.0	Operational
9	New surface water storage capacity (ML)	Either 0 or in range 100,000 to 230,000		Infrastructure
10	Chichester to Newcastle pipeline capacity expansion (ML/day)	0	50	Infrastructure
11	Grahamstown base gain ²	8000	12000	Operational
12	Grahamstown incremental gain ²	20	200	Operational
13	Grahamstown pumping trigger ³	0.0	1.0	Operational
14	Number of domestic rainwater tanks	0	100,000	Infrastructure

Notes:

1. Level 1 restriction storage trigger is the trigger for undertaking business readiness activities in advance of mandatory restrictions. The earliest this could occur is at a normal operating storage level, which is notionally 90%.
2. These variables drive water source selection, e.g. whether to draw water from Tomago Sandbeds or Grahamstown Dam.
3. This is equivalent to the storage level at which pumping water from Balickera into Grahamstown Dam must stop (1.0 is equivalent to Grahamstown Dam at 100% full).

It is assumed here that a series of measures such as pressure reduction, supply blackouts combined with community cooperation can produce sustained reductions in total demand ranging from 40 to 70%. The economic and social costs will be considerable, but importantly no collapse occurs as industry and commerce can continue to function.

Complementing emergency rationing is a parallel second stage of the DCP. Decisions x_5 to x_7 define options that will bring relief to emergency rationing by augmenting supply with a climate-independent source of water. When the total storage fraction falls below the trigger $x_5^*(x_1-4x_2)$, work commences on a desalination plant with capacity of x_6 to be commissioned x_7 months after commencement. The decision x_7 defines the pre-build investment in the desalination plant – the smaller x_7 , the higher the upfront investment in the desalination plant and the shorter the lead-time to commissioning and the sooner relief from emergency rationing can be obtained.

A special case occurs when x_7 is assigned 0. In that case, there is no pre-build investment – the desalination is assumed already constructed and operational at the

start of the simulation. This allows the optimisation to compare the building of an upfront desalination plant against deferring construction until triggered by the DCP.

Decision x_8 defines when the already-constructed desalination plant with daily capacity of x_5 ML/day is operated.

Decisions x_9 and x_{10} define the capacity of the new surface water source reservoir and additional pipeline transfer capacity from Chichester to Newcastle respectively. The capacity of the new surface water source can either be zero or lie in the range 100,000 to 230,000 ML.

Decisions x_{11} and x_{12} define the priority for storing water in Grahamstown. All the reservoirs in the WATHNET5 NFP were assigned 20 carryover arcs. Each carryover arc has a capacity equal to 1/20 of the reservoir capacity and a gain defined by equation (11). All reservoirs except Grahamstown were assigned a base gain of 10,000 and an incremental gain of 100 – this implements the so-called space rule which seeks to keep each reservoir with the same storage fraction. Decisions x_{11} and x_{12} define the base and incremental gain for Grahamstown reservoir respectively. Depending on the values assigned to x_{11} and x_{12} , water may be preferentially stored in Grahamstown or in the rest of the system.

Decision x_{13} defines the storage fraction that triggers the pumping of water from Seaham to Grahamstown reservoir.

Finally decision x_{14} defines the number of houses with rainwater tanks.

2.5.3 Objective Functions

A critical part of the case study involves definition of objectives. The following objectives were identified from a consultative process³ as being relevant and sufficient for the purposes of this study:

1. Minimise the expected present worth cost of capital, operating and restriction costs; and
2. Minimise the expected present worth cost of emergency rationing.

In reality water planning can involve more than two objectives reflecting social, environmental, financial, equity and risk values. The multi-criterion optimisation methodology can be applied using a greater number of objectives against which the performance of each option can be quantified (at least in relative terms).

In present worth evaluations, a 5% discount rate was used. The discounting was performed by first computing the expected value of a particular cost item and then multiplying by the discount factor.

The capital cost represents the cost of building new infrastructure, which in this case study, is the new surface water source, capacity expansion of the pipeline from Chichester to Newcastle and the desalination plant.

³ The final set of objectives and decisions was the product of a consultative process with staff from HWC and Sydney Catchment Authority, starting with a full-day workshop followed by multiple meetings to fine tune the formulation. The final set of objectives strikes a balance between the need for realism and working within the resource constraints of the project.

Table 9 summarises the capital costs for the new surface water source and the desalination plant. These costs are “indicative” and deemed sufficient for the purposes of this study – they should not be used in any other context. The capital cost model uses a binary function: if the asset is selected by the optimisation, then the total cost is the sum of a fixed setup cost and cost proportional to the size of the asset; however, if the asset is not selected, the capital cost is zero. For large desalination plants with installed capacity in excess of 20 ML/day, the construction time or lead time varies between 0 to 60 months depending on pre-build investment with shorter lead times requiring greater pre-build investment. In contrast, the small desalination plant costs are based on packaged plant designs and have short lead times.

Operating costs, summarised in Table 10, include the cost of pumping transfers from Seaham to Grahamstown reservoir and Grahamstown reservoir to Newcastle. It also includes cost of treating water in water treatment plants and operation of the desalination plant.

Table 11 summarises the estimated costs of restrictions to HWC and to the community. It is important when looking at the cost of implementing water restrictions to consider the economic and social costs involved. Costs of restrictions are real, affecting private individuals, the public sector and community as a whole.

The social impact of water restrictions was recently assessed through numerous studies. To estimate the social cost of water restrictions for the Lower Hunter the following process was used:

1. Studies examining the social costs of water restrictions around Australia were examined.
2. The maximum cost to the community per annum in Sydney 2006 was considered (Grafton and Ward, 2008).
3. The total loss from mandatory water restriction in Sydney over 12 month in 2004/2005 was considered (Grafton and Ward, 2008).
4. The willingness to pay to avoid restrictions estimated for SEQ was considered (Marsden Jacobs, 2006).
5. Differences and similarities between the restriction levels were examined and the estimated willingness to pay to avoid restrictions by the Lower Hunter community for each of the proposed restrictions was calculated.

The social cost of water restrictions in the Lower Hunter has been extrapolated to range from \$3/person/month to \$10.80/person/month for extreme restrictions, however the subject is widely debated as the impacts are not directly observable. The maximum value quoted in the literature is \$40,000 to \$80,000 gross value added per ML of water for certain industries. The social cost is therefore reported as a range with the values representing estimates of loss of consumer surplus.

Table 9 Capital cost summary

Decision variable	Fixed and Unit Cost	
New surface water source reservoir	\$150m + \$1300/ML storage in excess of 100,000 ML	
Small desalination plant (<20 ML/day installed capacity)	\$6m + \$3m/ML/day installed capacity Pre-build cost = \$0	
Large desalination plant (> 20 ML/day installed capacity)	\$150m + \$7.5m/ML/day installed capacity	
	Lead time months	Pre-build cost as % of total cost
	12	50%
	24	35%
	36	10%
	60	0
Chichester to Newcastle pipeline	\$1.45m/ML/day installed capacity	

Table 10 Summary of operating costs

Operations	Cost
Pumping from Seaham to Grahamstown reservoir	\$12/ML
Pumping from Grahamstown reservoir to Newcastle	\$76/ML
Tomago water treatment plant	\$80/ML
All other water treatment plants	\$50/ML
Desalination plant	\$1200/ML

Table 11 Restriction cost summary

Restriction level	Financial cost to water utility		Social cost (\$/person/month)
	Fixed(\$)	Variable (\$/month)	
Level 1	297,500	154,000	0
Level 2	70,500	229,000	3 – 15
Level 3	0	293,000	6 - 30
Level 4	18,000	305,000	8 - 40
Level 5	18,000	317,000	11 – 54

Emergency rationing is triggered after the imposition of level 5 restrictions which enforce a total ban on all outdoor water use and encourage other voluntary savings. Because emergency rationing would impose much severer cutbacks to water use, it is expected social costs would climb steeply. Table 12 summarises indicative costs which are deemed sufficient for the purpose of this case study but should not be used in any other context. The social cost is linearly scaled between the 40 and 70% demand reduction limits. A more considered approach to estimating such costs would involve carefully designed surveys of willingness-to-pay – this was beyond the scope of this study.

Table 12 Costs associated with emergency rationing

Reduction in total demand	Financial cost to water utility		Social cost (\$/person/month)
	Fixed(\$)	Variable (\$/month)	
40%	20,000	350,000	50 - 100
70%	100,000	500,000	150 - 300

The two objectives were evaluated for a particular set of decisions by simulating the Lower Hunter system using WATHNET5 using 10,000 50-year long replicates of representative climate. This represents a departure from the traditional simulation approach that uses a single 500,000-year replicate. This approach is necessary because it is not known when, in the future, a drought contingency plan will be triggered and whether the triggering of a such a plan will result in permanent changes to the system (e.g., a desalination plant may be built in response to the threat of a

severe drought; once built, it may be used as alternative source of water altering the risk profile of the system).

2.5.4 Constraints

In addition to meeting environmental flow requirements, two constraints were imposed on the optimisation :

1. No unplanned shortfalls are permitted in any replicate. An unplanned shortfall arises whenever restricted demand cannot be met. In this case study, an unplanned shortfall could only occur when emergency rationing is in effect and the reservoirs “run out of water”. This constraint implicitly secures the system against catastrophic collapse for droughts with expected return periods up to 1 in 500,000 years.
2. In any 50-year replicate the time spent in emergency rationing must be no greater than 10%. This constraint effectively puts a limit of a maximum of 5 years of emergency rationing within each replicate. It guides the optimisation away from solutions imposing a permanent state of emergency rationing.

These constraints represent value judgments on events that are beyond the community’s experience.

2.5.5 Improving Computational Performance

Equation (4) employs Monte Carlo simulation to evaluate objective functions scores. Multiple replicates of independent equally likely future streamflow time series are input to the WATHNET5 simulation model of the bulk water system to produce multiple replicates of responses from which the objective function scores are computed.

While Monte Carlo simulation represents undoubtedly the most general approach for evaluating objective function scores, the computational effort can be prohibitive particularly if maximising drought security is one of the objectives. To illustrate the practical significance of the problem, some typical figures for the Lower Hunter case study are considered. To simulate the dry and wet future climate scenarios, each consisting of 10,000 50-year replicates, takes approximately 1.5 CPU hours for a particular set of decisions. A minimum of 40,000 simulations (or objective function evaluations) is required to find an approximate solution to equation (4) using a MOEA. On a single high-performance desktop this would take about 2,500 days. In this study, a parallel cluster of 72 processors would reduce the turnaround time to approximately 34.8 days, which, nonetheless, is considered unacceptable.

The need for 10,000 replicates per future climate change scenario arises because a high level of drought security is required. If there were an insufficient supply of water over a prolonged period of time, the Lower Hunter would face social and economic collapse. The constraint that there can be no unplanned shortfalls in demand in any replicate effectively ensures that the Lower Hunter system can survive droughts with expected return periods up to nominally 1 in 500,000 years. The key point here is that this constraint will only be tested in replicates experiencing extremely severe droughts.

This insight offers an opportunity to reduce computational effort to a practicable level. The objective functions in this study take the form

$$f_i(x|Z_j) = \frac{1}{m} \sum_{k=1}^m \phi(Z_{kj}) \quad (13)$$

Where $\phi(\cdot)$ is a function of Z_{kj} , the simulated response for the k^{th} replicate of the j^{th} scenario and m is the number of replicates per scenario. This is an arithmetic mean in which each replicate is equally weighted.

A very considerable saving can be made by using a weighted average with a reduced number of replicates. The following scheme achieves this goal:

1. For each scenario rank the replicates using a suitable drought-related statistic to give the sequence $\{S_{(k),j}, k = 1, \dots, m\}$ where $S_{(k),j}$ is the $(k)^{th}$ ranked replicate in the j^{th} scenario where rank (1) denotes the replicate with the severest drought. In this study the minimum overlapping 2-year sum of streamflow at a key site was used as the statistic to rank the replicates.
2. For each scenario select a reduced scenario set defined as

$$S_j^R = \{S_{(k),j}, k = 1, \dots, m_d, m_d \ll m\} \cup \{S_{i(k),j}, i(k) \leftarrow U(1, m), k = 1, \dots, m_e, m_e \ll m\} \quad (14)$$

where $U(1, m)$ is a probability distribution that returns integers between 1 and m with equal probability. The reduced scenario set consists of two components. The first is the set of m_d replicates containing the m_d severest droughts in the scenario. This ensures the Monte Carlo simulation encounters the most severe droughts in S_j to ensure the no unplanned shortfall constraint is genuinely satisfied. The second is a set of m_e randomly selected equally likely replicates. This ensures a representative set of replicates is used to evaluate the expected present worth costs.

The objective function is approximated using the reduced scenario set as follows

$$f_i(x|Z(S_j^R)) = \frac{1}{m_d} \sum_{k=1}^{m_d} \phi(Z(S_{kj})) + \frac{1}{m_e} \sum_{k=1}^{m_e} \phi(Z(S_{i(k),j})) \quad (15)$$

The m_d severest drought replicates are weighted by $1/m_d$, while the randomly sampled replicates are weighted by $1/m_e \gg 1/m_d$.

In this study, m was set to 10,000, while m_d and m_e were set to 100. This reduces the computational effort by a factor of 50 with limited loss of information resulting in optimisation runs taking about 16 hours on a 72-processor Linux cluster.

3. RESULTS AND OUTPUTS

The results of the robust optimisation for the Lower Hunter bulk water system are organized into two parts. As a prelude to the main results the first section considers two population scenarios under the assumption of no climate change. This will provide a baseline for the second section which revisits the same two population scenarios under the assumption that the future climate in 2070 is spanned by the 2070 dry and 2070 wet scenarios described in Section 2.3.

3.1 *No-Climate-Change Optimisation*

This section considers two demand scenarios under a no-climate-change scenario. The first demand scenario uses HWC's current demand projection for between 2060 and 2070 in line with the timing of the future climate scenario. The 2060 demand is estimated to be around 92GL/year, which is around 28% higher than current demand. The second demand scenario considers a doubling (2 x) of current demand to 144 GL per annum to represent a much more stressed system than encountered in the 2060 demand scenario. The purpose of introducing the highly stressed demand scenario is to test the types of solutions found and the capability of the optimisation process under such stress. It would be incorrect to suggest that the double demand scenario is realistic in the sense that it is likely that the underlying bulk water system would have been expanded prior to such high demand occurring.

For each scenario the following two objectives were optimised:

1. Minimise the expected present worth (EPW) of capital, operating and restriction costs; and
2. Minimise the expected cost of emergency rationing expressed in \$/month.

The restriction and emergency restriction social costs were set at the upper limits reported in Table 11 and Table 12.

3.1.1 *No-Climate-Change 2060 Demand Scenario*

The Pareto frontier for the 2060 demand scenario (92GL/year) is presented in Figure 29. While there is trade-off between the two objectives, the cost range is very small. The emergency restriction cost ranges from \$0 to \$25,000, while the EPW of capital, operating and restriction costs ranges from \$224m to \$400m.

To better understand the solutions underpinning the Pareto set, Table 13 provides a detailed breakdown of the four solutions labelled in Figure 29. The following features warrant comment:

1. Common to all solutions on the Pareto front are the following:
 - a. No desalination plant is selected.
 - b. There is also no expansion of the pipeline from Chichester to Newcastle.
 - c. There is no or very limited use of rainwater tanks.
2. Solutions 1 to 3 do not opt for a new surface water source. The differences in performance arise from subtle differences in the restriction and emergency restriction triggers.
3. Solution 4 opts for the smallest new surface water source with a capacity just over 100,000 ML. The inclusion of the new reservoir reduces the frequency of

restrictions from a maximum of 3.30% to 0.80% and the frequency of emergency rationing from a maximum of 0.35% to 0.03%.

4. The main difference between the solutions is the emergency restriction trigger x_3 , which varies from 0 to 0.5. The frequency of emergency rationing (or the chance of emergency rationing in any month) ranged from 0.81% to 0.55%, while the frequency of restrictions ranged from 1.5% to 0.0%. To appreciate these differences, Figure 30 shows time series plots of supplied demand for the worst 50-year replicate for solutions 1 and 4; for solution 1, the emergency rationing, during which supplied demand is about 30% of normal demand, last for 26 consecutive months, while for solution 4, the period is 11 consecutive months.
5. All solutions opt for severe rationing scaling factors close to the upper limit of 70%. This is consistent with the strategy of minimising the chance of emergency rationing by enforcing the severest permissible reductions in demand should emergency rationing be triggered.

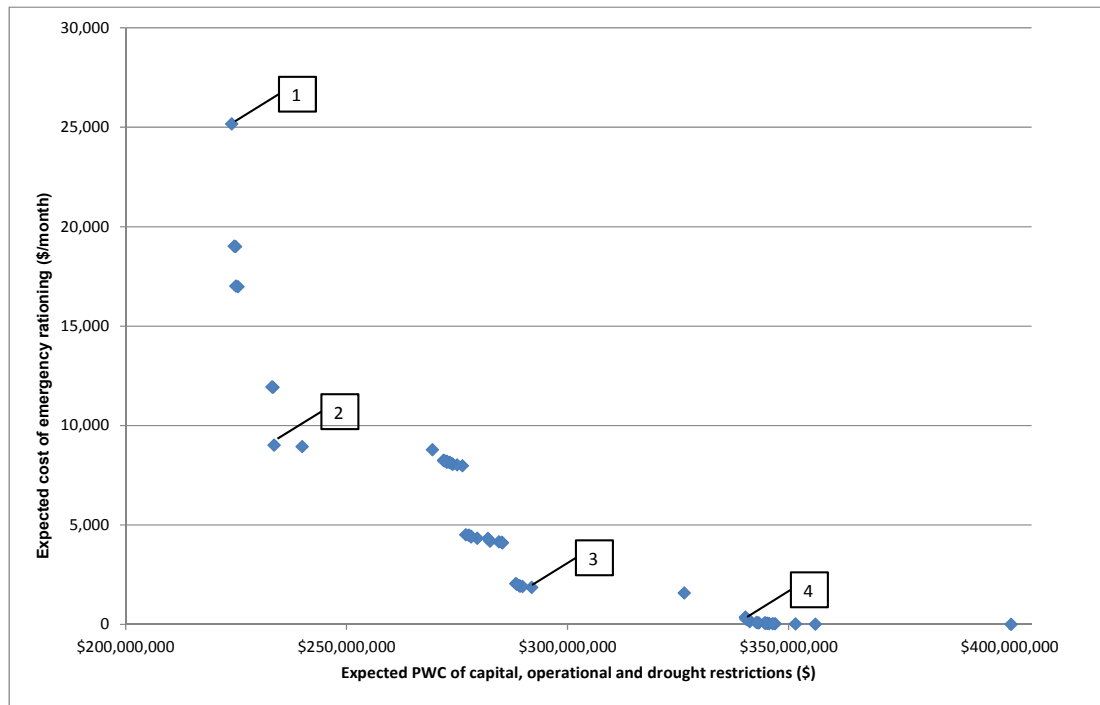


Figure 29 Pareto optimal solutions for the no-climate-change 2060 demand scenario (92GL/year)

Table 13 Summary of labelled solutions on Pareto front in Figure 29

Solution		1	2	3	4
Objectives	Expected PW cost of capital, operational and drought restrictions (\$m)	224	234	292	340
	Expected cost of emergency rationing (\$/month)	25167	9010	1856	368

Frequency	Chance of restrictions in any month (%)	2.60	3.31	2.56	0.80
	Chance of emergency rationing in any month (%)	0.349	0.270	0.126	0.029
Decisions	Level 1 restriction storage trigger	0.450	0.506	0.450	0.281
	Restriction trigger increment	0.060	0.053	0.066	0.052
	Emergency restriction trigger (expressed as percentage storage)	0.737 (15.6%)	0.502 (14.7%)	0.503 (9.3)	0.956 (7.0%)
	Severe rationing demand scaling factor	0.699	0.699	0.696	0.625
	Storage trigger to initiate desalination plant construction	---	---	---	---
	Desalination plant capacity (ML/day)	---	---	---	---
	Desalination plant construction lead time(month)	---	---	---	---
	Desalination plant trigger	---	---	---	---
	New surface water source capacity (ML)	---	---	---	101097
	Chichester to Newcastle pipeline capacity expansion (ML/day)	0.3	0	0.2	0
	Grahamstown base gain	8982	9889	8889	9979
	Grahamstown incremental gain	198	199	199	25
	Grahamstown pumping trigger	1.00	1.00	1	0.818
	Number of domestic rainwater tanks	18	48	12	0

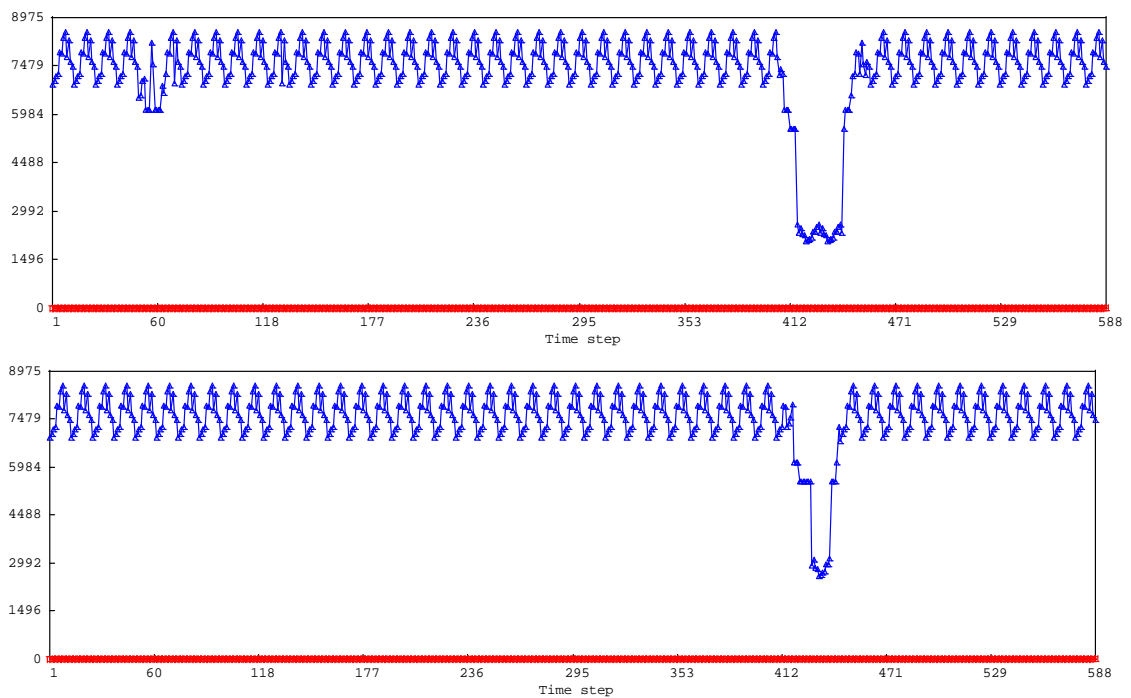


Figure 30 Time series plot of supplied demand for the worst 50-year replicate: Top panel corresponds to solution 1; bottom panel corresponds to solution 4

3.1.2 *No-Climate-Change 2 x Current Demand Scenario*

The Pareto frontier for the 2 x current demand scenario (144GL/year) displayed in Figure 31 reveals a behaviour very different to that of the 2060 demand scenario (92GL/year). There is a more pronounced trade-off between the objectives. The emergency restriction cost ranges from \$0 to \$160,000. To achieve this trade-off, the EPW of capital, operating and restriction costs ranges from \$635m to \$975m. Figure 31 shows a steep decline in emergency restriction costs between solutions 1 and 2 for a \$38m increase in the EPW of capital, operating and restriction costs. Beyond solution 2, however, a huge community investment of \$274m is required to reduce emergency restriction costs from \$4,700 to \$0. This insight highlights the value of exploring Pareto-optimal trade-offs.

Table 14 provides a detailed breakdown of the four solutions labelled in Figure 31:

1. Moving from solution 1 to 4 sees a large drop in the frequency of emergency rationing from 0.95% to 0.003% offset by an increase in restriction frequency from 5.48 to 10%. These trends result from an increasing level 1 restriction trigger and a falling emergency restriction trigger. For all solutions the severe rationing demand scaling factor is close to 70% indicating the most severe rationing has been selected when emergency rationing is in force.
2. Three solutions have a desalination plant with different lead times. However, only solution 4 has a large desalination plant.
3. The rainwater tank option has been largely ignored, a finding that occurs consistently in all the scenarios.

4. The new surface water source is selected in all solutions with the capacity growing from 142,000 ML for solution 1 to 230,000 ML for solution 4.
5. In all solutions, the pumping strategy for Balickera is to pump wherever there is air space in Grahamstown reservoir.

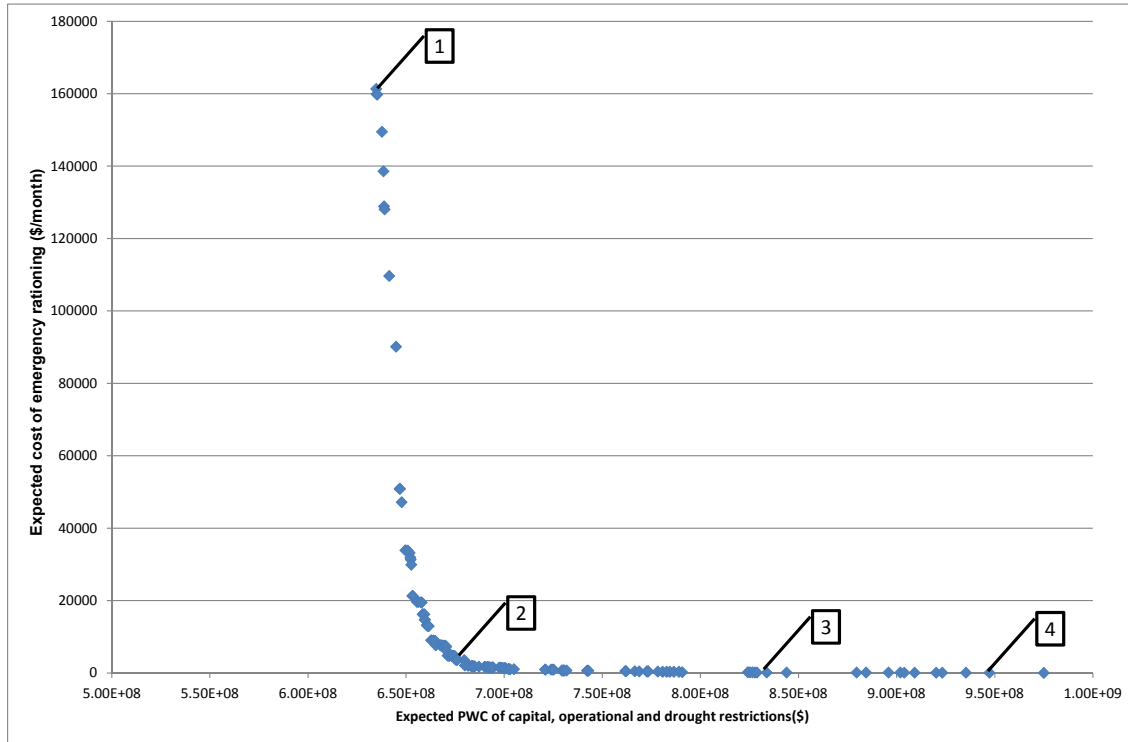


Figure 31 Pareto optimal solutions for the no-climate-change 2 x current demand scenario (144GL/year)

In summary, solution 1 minimises the EPW of capital, operational and restriction costs. As a result, it opts for the highest emergency restriction trigger. In contrast, solution 4 minimises the cost of emergency restrictions by investing in an expensive strategy to minimise the frequency of emergency rationing. It has opted for the largest desalination plant, the largest new water source capacity and the largest Chichester to Newcastle pipeline upgrade. Its emergency restriction trigger is much lower than the trigger to initiate desalination plant construction thus favoring use of desalination before imposition of emergency rationing.

Table 14 Summary of labelled solutions on Pareto front in Figure 31

Solution		1	2	3	4
Objectives	Expected PW cost of capital, operational and drought restrictions (\$m)	635	673	829	947
	Expected cost of emergency rationing (\$/month)	159914	4701	118	49
Frequency	Chance of restrictions in any month (%)	5.48	4.89	7.10	10.00
	Chance of emergency rationing in any month (%)	0.95	0.16	0.007	0.003
Decisions	Level 1 restriction storage trigger	0.450	0.451	0.563	0.616
	Restriction trigger increment	0.051	0.062	0.068	0.052
	Emergency restriction trigger (expressed as percentage storage)	0.954 (18.9%)	0.501 (9.5%)	0.126 (2.5%)	0.033 (2.6%)
	Severe rationing demand scaling factor	0.664	0.683	0.697	0.683
	Storage trigger to initiate desalination plant construction	0.837	0.989	0.997	0.994
	Desalination plant capacity (ML/day)	---	20	20	88
	Desalination plant construction lead time(month)	---	12	0	60
	Desalination plant trigger	---	0.516	0.648	0.482
	New surface water source capacity (ML)	142504	192624	229201	229736
	Chichester to Newcastle pipeline capacity expansion (ML/day)	0	0	0	37
	Grahamstown base gain	8351	8274	8067	8055
	Grahamstown incremental gain	27	35	21	43
	Grahamstown pumping trigger	1.00	1.00	1.00	1.00
	Number of domestic rainwater tanks	20	5	117	67

3.1.3 Sensitivity to Restriction Social Costs

In view of the uncertainty about the assignment of social costs incurred during restrictions, a sensitivity analysis was conducted on the social restriction costs quoted in Table 11. The restriction cost factor RF is defined as the ratio of the actual social cost and the lower bound social cost. As a result, RF spans a range of 1 to 5. In Figure 32 the Pareto-optimal fronts for RF values of 1, 3 and 5 are presented for the 2 x current demand scenario. It can be seen that for the same emergency restriction cost, the EPW of capital, operational and restriction costs increases as RF increases with the increase being the greatest when the emergency restriction costs are greatest.

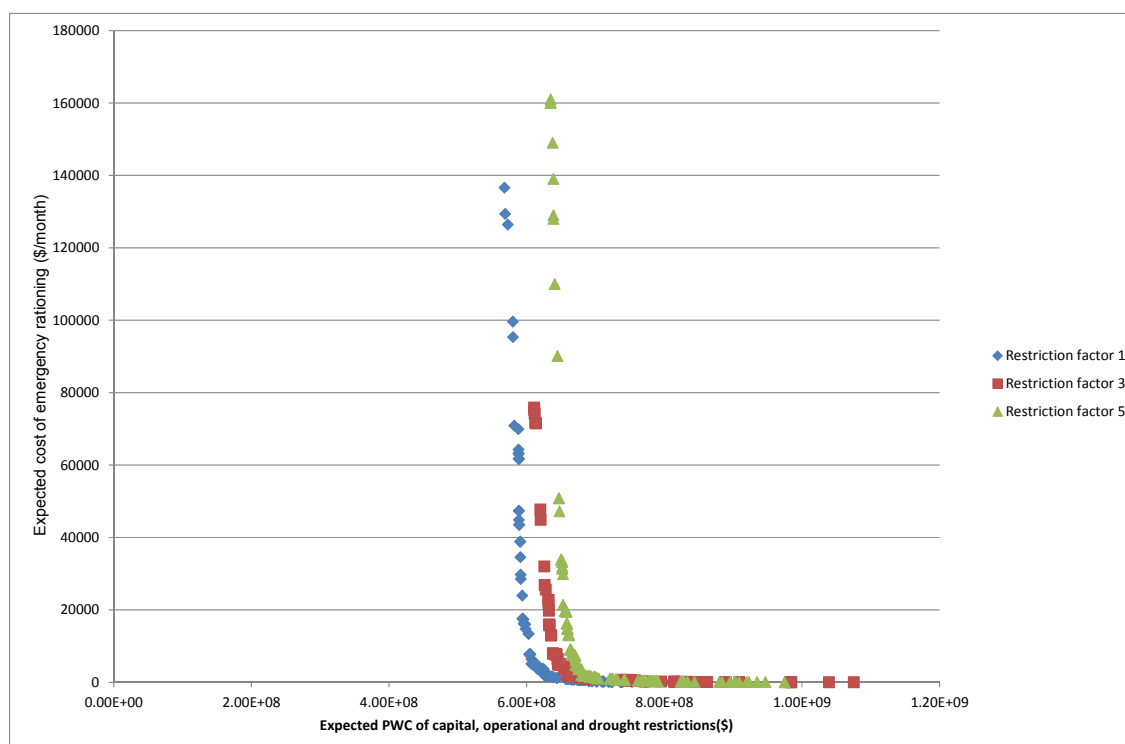


Figure 32 Pareto optimal solutions for different restriction cost factors for the no-climate-change 2 x current demand scenario (144GL/year)

To assess the sensitivity of the solutions to RF, Table 15 summarises three solutions each on a different Pareto front but with similar emergency restriction costs. As RF increases, the solutions change in the following ways:

1. The level 1 restriction trigger is reduced and the restriction trigger increment is increased to reduce the frequency of the more costly higher level restrictions.
2. The capacity of the new surface water source is increased to reduce the chance of entering restrictions.

While the solutions do change in response to an increase in RF, the EPW capital, operating and restriction cost only increases 6% and 10% as RF jumps from 1 to 3 and 1 to 5 respectively. These differences suggest that the social costs are sufficiently high, even at the lower level, to steer optimal solutions away from excessive reliance on higher level restrictions.

In a similar manner Figure 33 presents two Pareto fronts, one using emergency restriction social costs in the range of \$50 to \$150 and the other in the range \$100 to \$300 per person per month. The difference between the fronts is minimal with the emergency restriction costs taking values of the order of \$100,000 while the remaining costs take values of the order of \$600m. As before, this suggests that the lower bound social costs are sufficiently high to steer optimal solutions away from excessive reliance on emergency rationing.

Table 15 Summary of three solutions with similar expected emergency restriction costs on Pareto fronts in Figure 32

	Solution	Restriction factor RF		
		1	3	5
Objectives	Expected PW cost of capital, operational and drought restrictions (\$m)	618	655	675
	Expected cost of emergency rationing (\$/month)	3721	3716	3690
Decisions	Level 1 restriction storage trigger	0.535	0.453	0.451
	Restriction trigger increment	0.053	0.065	0.062
	Emergency restriction trigger (expressed as percentage storage)	0.315 (10.2%)	0.502 (9.7%)	0.500 (10.1%)
	Severe rationing demand scaling factor	0.682	0.691	0.686
	Storage trigger to initiate desalination plant construction	0.973	0.953	0.895
	Desalination plant capacity (ML/day)	18	20	18
	Desalination plant construction lead time(month)	12	12	12
	Desalination plant trigger	0.688	0.686	0.521
	New surface water source capacity (ML)	165784	195327	195969
	Chichester to Newcastle pipeline capacity expansion (ML/day)	0	0	0
	Grahamstown base gain	8104	8266	8075
	Grahamstown incremental gain	92	92	43
	Grahamstown pumping trigger	1	0.998	1
	Number of domestic rainwater tanks	53	2	2

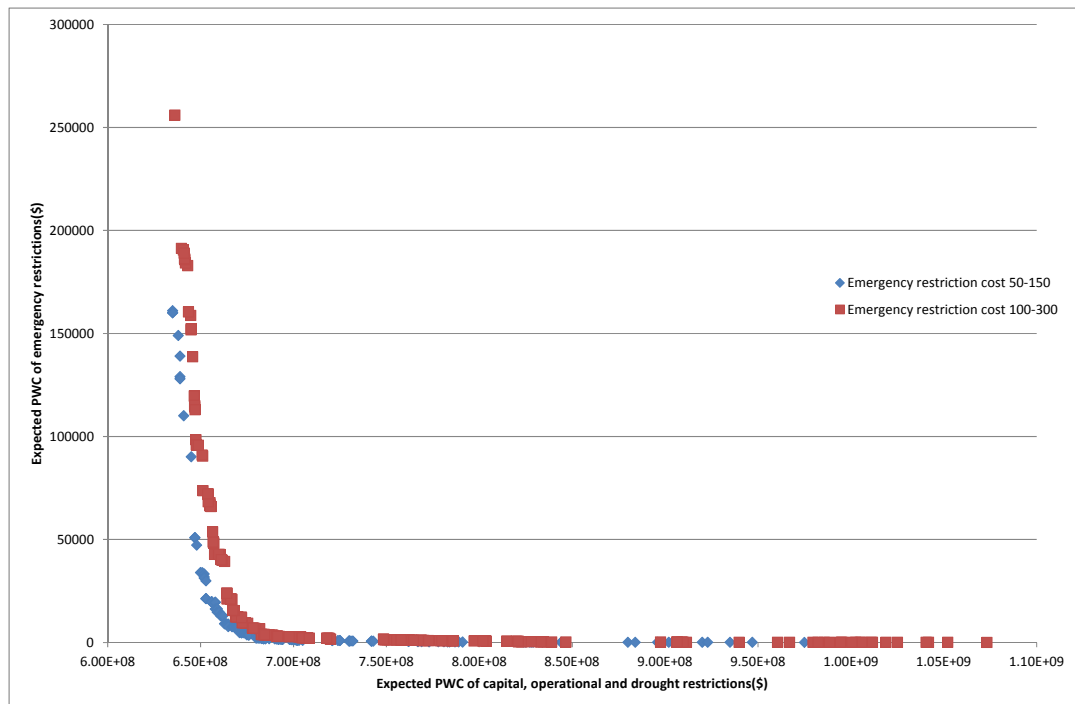


Figure 33 Pareto optimal solutions for different emergency restriction social cost ranges for the no-climate-change 2 x current demand scenario (144GL/year)

3.2 Robust Optimisation for an Uncertain Future Climate

This section considers two demand scenarios with an uncertain 2070 climate bounded by a dry and wet scenario this means it is likely that the 2070 climate will lie between the dry and wet scenarios. In the no-climate-change scenario analysis the trade-off between the cost of emergency rationing and all other costs was explored. For clarity of presentation, these two objectives will be combined to give the total EPW cost. The robust optimisation therefore seeks to:

1. Minimise the total expected present worth cost consisting of capital, operating, restriction and emergency restriction costs; and
2. Minimise the cost spread or the difference between the total EPW cost for the dry and wet climate scenarios.

By restricting the optimisation to two objectives, the Pareto optimal trade-offs are intuitively conveyed. As before, the restriction and emergency restriction social costs were set at the upper limits reported in Table 11 and Table 12.

3.2.1 Uncertain-2070-Climate, 2060-Demand Scenario

The Pareto frontier for the 2060 demand scenario (92GL/year) displayed in Figure 34 reveals a limited trade-off between total EPW cost and robustness. The total EPW cost ranges from \$360m to \$485m, while the cost spread across the dry and wet 2070 climate scenarios ranges from \$0.08m to \$13.4m. The proposition of increasing robustness by reducing the spread from \$13.4 to \$0.08m for an increased community investment of \$125m is not compelling.

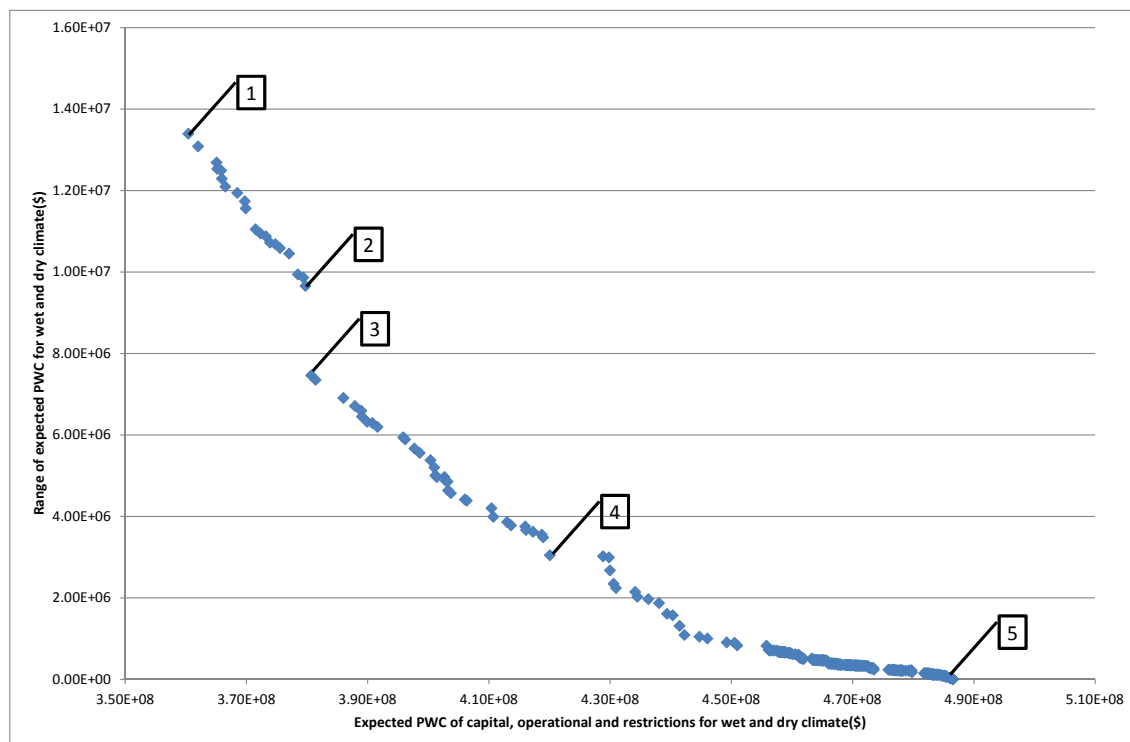


Figure 34 Robust Pareto optimal solutions for the 2060 demand scenario (92GL/year)

Table 16 provides a summary of the five solutions labelled on Figure 34. The chance of restrictions is less than 1.7% regardless of climate scenario and the chance of emergency rationing is at worst 0.08%. There is little difference between the solutions other than an increase in the new surface water source capacity. Overall, there is little sensitivity to climate uncertainty. It needs to be stressed that there is no opportunity to further improve the solutions. Figure 35 shows the total storage time series for the worst-drought replicate in solution 1. For a period of over 12 months, the total storage hovers around 1% - the system is on verge of an unplanned shortfall suggesting the optimisation algorithm has left little opportunity for further improvement.

Table 16 Summary of labelled solutions on Pareto front in Figure 34

	Solution	1	2	3	4	5
Objectives	Total expected PW of capital, operational and restriction costs (\$m)	360	378	381	420	485
	Spread of total expected PW cost (\$m)	13.39	9.65	7.46	3.04	0.08
Frequency	Chance of restrictions in any month (%) for dry and wet scenario	1.7 (dry) 0.83 (wet)	1.44 (dry) 0.67 (wet)	1.12 (dry) 0.48 (wet)	0.57 (dry) 0.21 (wet)	0.29 (dry) 0.11 (wet)
	Chance of emergency rationing in any month (%) for dry and wet scenario	0.082 (dry) 0.052 (wet)	0.043 (dry) 0.027 (wet)	0.043 (dry) 0.027 (wet)	0.017 (dry) 0.003 (wet)	0.0 (dry) 0.0 (wet)
Decisions	Level 1 restriction storage trigger	0.281	0.281	0.253	0.227	0.225
	Restriction trigger increment	0.050	0.054	0.050	0.050	0.051
	Emergency restriction trigger (expressed as percentage storage)	0.964 (7.8%)	0.932 (6.1%)	0.930 (4.9%)	0.902 (2.4%)	0.821 (1.7%)
	Severe rationing demand scaling factor	0.697	0.696	0.691	0.691	0.598
	Storage trigger to initiate desalination plant construction	---	---	---	---	---
	Desalination plant capacity (ML/day)	---	---	---	---	---
	Desalination plant construction lead time(month)	---	---	---	---	---
	Desalination plant trigger	---	---	---	---	---
	New surface water source capacity (ML)	100634	118300	120338	152672	207533
	Chichester to Newcastle pipeline capacity expansion (ML/day)	0	0	0	0	0
	Grahamstown base gain	8995	9728	9744	9744	9852
	Grahamstown incremental gain	32	20	21	20	25
	Grahamstown pumping trigger	0.987	0.987	0.995	0.988	1.000
	Number of domestic rainwater tanks	0.000	0.000	0.000	0.000	0.000

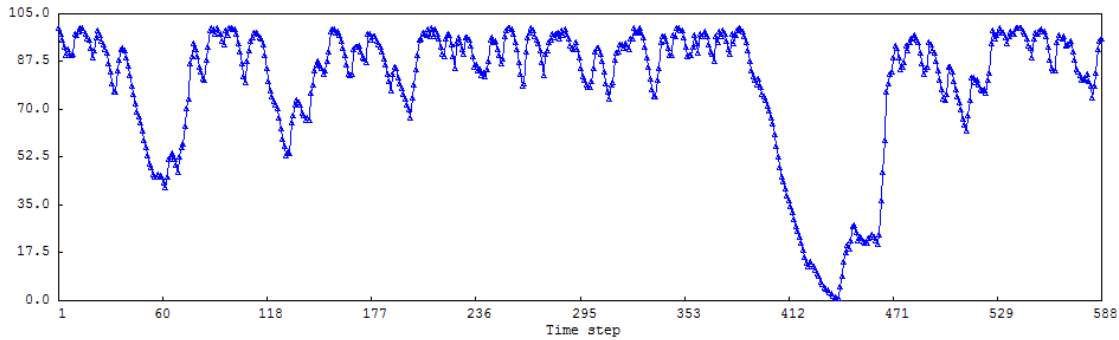


Figure 35 Total storage (%) time series for worst-drought replicate in solution 1 of Figure 34

The conclusion that there is relatively little sensitivity to uncertainty about future climate changes radically if the new surface water source is excluded from the options available to the optimiser. Figure 36 compares the Pareto fronts for two cases, one includes the new surface water source as an option and the other excludes it. With the new surface water source excluded as an option, the Pareto front shifts substantially to the right and exhibits a much larger trade-off between robustness and efficiency. All the solutions adopt a pre-built large desalination plant with capacities ranging from 50 to 350 ML/day together with rainwater tank installation ranging from 260 to 95,000 households. This comparison highlights the critical importance of defining the decision space – as the decision space becomes more constrained, the potential for optimisation is reduced and, as in this case, very substantially reduced.

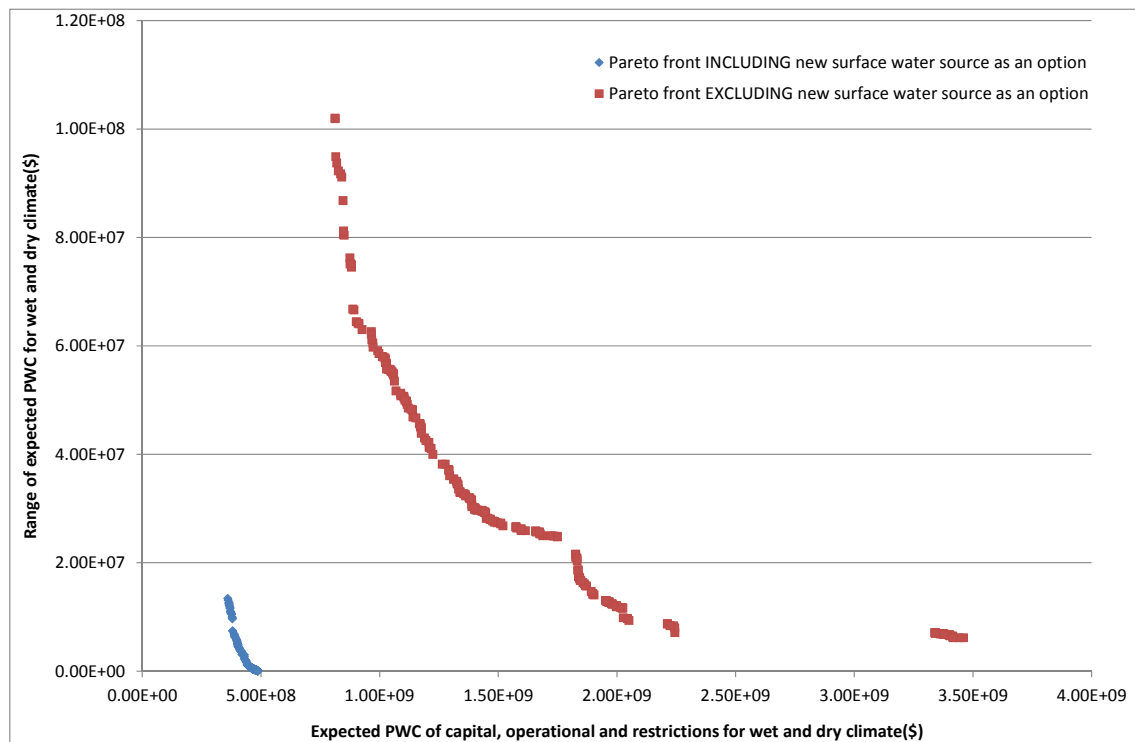


Figure 36 Robust Pareto optimal solutions for the 2060 demand scenario (92GL/year) for two cases: Including new surface water source as an option; and 2) excluding new surface water source as an option

3.2.2 Uncertain-2070-Climate, 2 x Current Demand Scenario

For the 2060 demand scenario (92GL/year), the Pareto optimal solutions showed little sensitivity to 2070 climate change uncertainty. However, a very different picture emerges for the 2 x current demand scenario (144GL/year). The Pareto frontier for the 2 x current demand scenario, displayed in Figure 37, reveals strong trade-offs between efficiency and robustness. The total EPW cost ranges from \$1092m to \$2943m, while the spread ranges from \$1m to \$455m. For solution 1 the spread represents 42% of the total EPW cost. Unfortunately reducing the spread requires a disproportionately large expected investment. The reduction of spread by \$53m when moving from solution 1 to 2 is offset by an increase in total EPW cost of \$73m, while moving from 4 to 5 reduces the spread a further \$174m in return for an increase in total cost of \$596m.

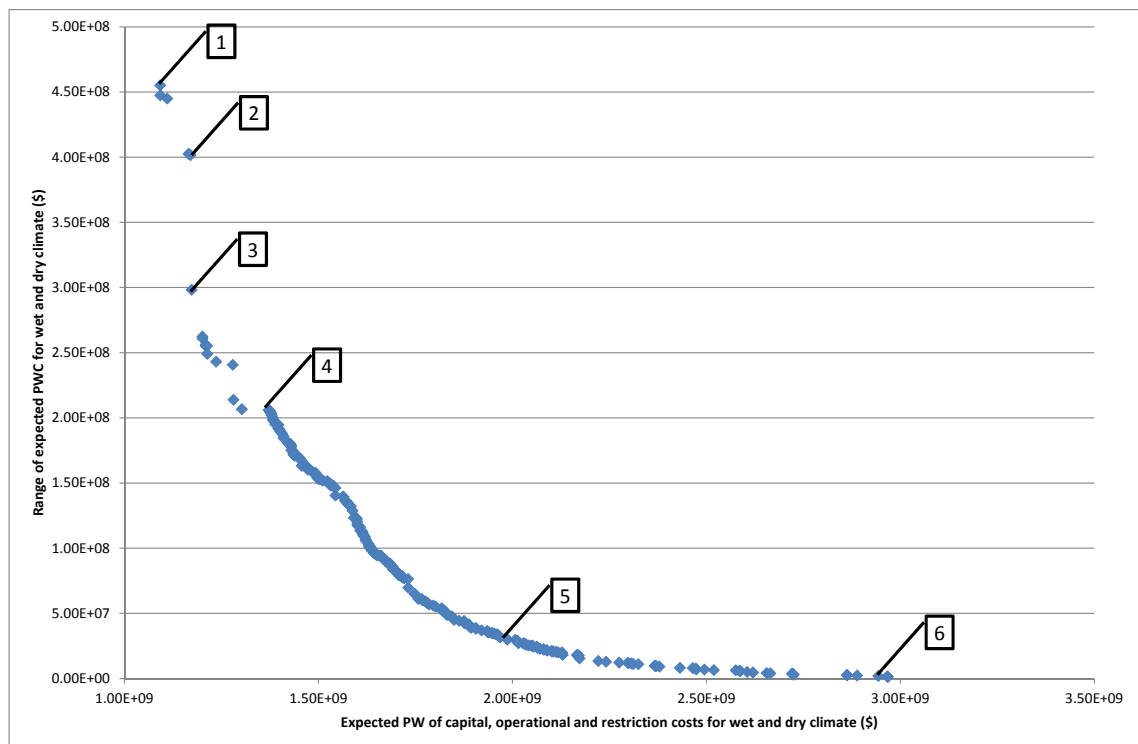


Figure 37 Robust Pareto optimal solutions for the 2 x current demand scenario (144GL/year)

Unlike the Pareto solutions for the 2060 demand scenario which eschew the desalination option, the Pareto solution set for the 2 x current demand scenario opts for desalination in all cases. Table 17 provides a summary of the 6 solutions labelled on Figure 37. The following features warrant comment:

1. All solutions opt for the maximum capacity of the new surface water source. This suggests that if the upper bound on the storage capacity were increased, the optimiser would exploit the additional capacity.
2. All solutions adopt desalination with zero lead time meaning the plant is commissioned at the start of the simulation and will supply water whenever total storage drops below the trigger. Solutions 1 to 3 opt for the small and cheap desalination option, while solutions 4 to 6 opt for the larger and more costly option.

Table 17 Summary of labelled solutions on Pareto front in Figure 37

Objectives	Solution	1	2	3	4	5	6
	Total expected PW of capital, operational and restriction costs (\$m)	1092	1165	1173	1372	1968	2943
	Spread of total expected PW cost (\$m)	455	402	298	205	31	1

Frequency	Chance of restrictions in any month (%) for dry and wet scenario	16.5 (dry) 6.3 (wet)	14.9 (dry) 5.6 (wet)	10.4 (dry) 3.4 (wet)	6.5 (dry) 2.0 (wet)	2.4 (dry) 0.82 (wet)	0.31 (dry) 0.13 (wet)
	Chance of emergency rationing in any month (%) for dry and wet scenario	1.0 (dry) 0.32 (wet)	0.91 (dry) 0.28 (wet)	0.71 (dry) 0.21 (wet)	0.32 (dry) 0.11 (wet)	0.055 (dry) 0.032 (wet)	0.0 (dry) 0.0 (wet)

Decisions	Level 1 restriction storage trigger	0.394	0.394	0.331	0.281	0.253	0.199
	Restriction trigger increment	0.057	0.054	0.051	0.051	0.051	0.051
	Emergency restriction trigger (expressed as percentage storage)	0.759 (12.6%)	0.751 (13.4%)	0.768 (9.7%)	0.681 (5.2%)	0.511 (2.5%)	0.641 (0%)
	Severe rationing demand scaling factor	0.678	0.677	0.696	0.686	0.697	0.546
	Storage trigger to initiate desalination plant construction	---	---	---	---	---	---
	Desalination plant capacity (ML/day)	17	17	17	50	74	125
	Desalination plant construction lead time(month)	0	0	0	0	0	0
	Desalination plant trigger	0.497	0.493	0.493	0.591	1.000	0.997
	New surface water source capacity (ML)	229918	229953	229934	229929	229918	222930
	Chichester to Newcastle pipeline capacity expansion (ML/day)	8	12	6	2	7	8
	Grahamstown base gain	8623	8101	8590	8719	8117	9623
	Grahamstown incremental gain	32	59	47	56	69	34
	Grahamstown pumping trigger	0.989	0.997	0.998	0.992	0.808	0.735
	Number of domestic rainwater tanks	36	25050	50232	91	245	50223

3. The increasing investment in desalination is accompanied by a decreasing level 1 restriction trigger resulting in a lower frequency of restrictions and emergency rationing.
4. Solution 1 exhibits the greatest difference in restriction frequency between the dry and wet climates. Only solutions 4, 5 and 6 produce restriction frequencies less than 10% for both the dry and wet climate scenarios.

It is instructive to examine the performance of the system during the worst-drought replicate. Figure 38 shows time series of total storage (%), desalination production and supplied demand for solution 1 for the worst replicate. The prolonged run of low/near-zero storage backed up by operation of the desalination plant and 33 consecutive months of emergency rationing illustrate the aggressiveness of the optimisation to make best use of available resources. Indeed many replicates exhibit similar prolonged periods of low storage confirming the aggressiveness of the optimisation. To avoid such solutions with extended periods of hardship close to the point of system failure it would be necessary to impose additional constraints on the duration and severity of emergency rationing – of course, satisfying such constraints would produce more costly solutions.

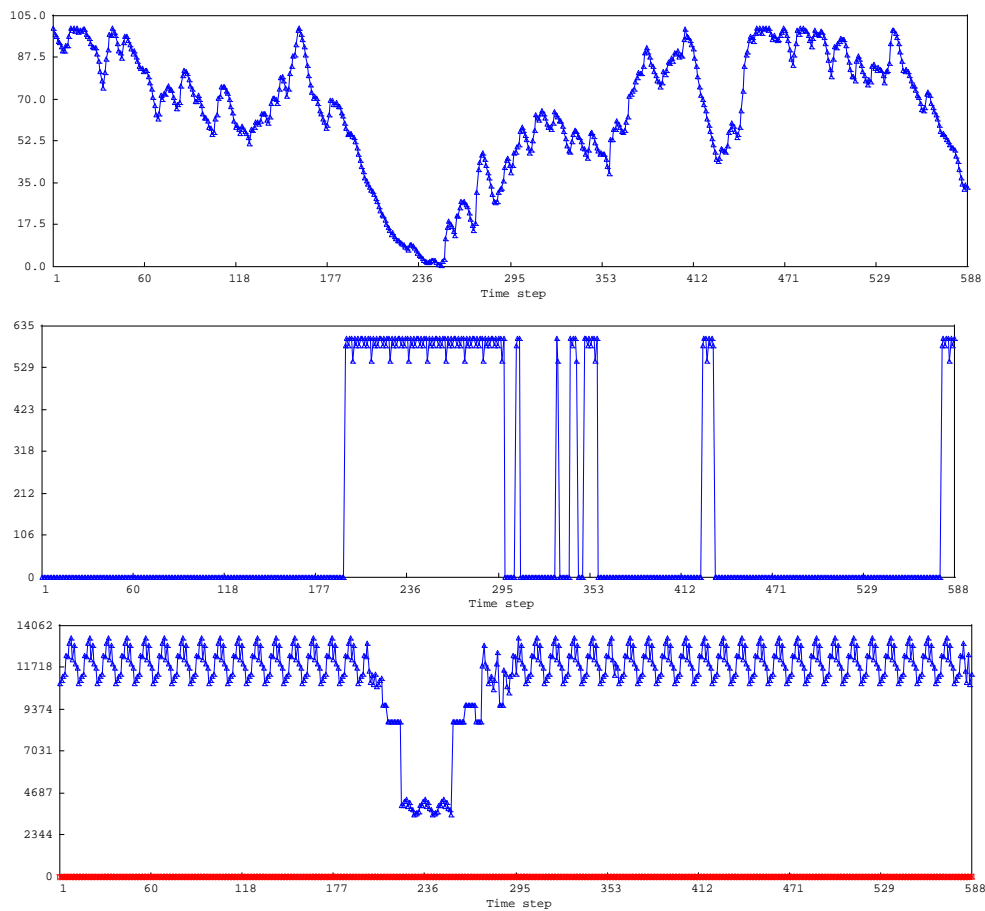


Figure 38 Time series plots for worst-drought replicate for solution 1 of Figure 37: Top panel – total storage (%); middle panel – desalination production (ML/month); bottom panel – supplied demand (ML/month)

3.3 *Concluding Remarks*

The Lower Hunter case study has demonstrated the capability of the robust optimisation formulation given by equation (4). The sensitivity of solutions to uncertainty about future climate varied considerably. For the 2060 demand scenario there was little sensitivity to the dry and wet climate scenarios resulting in a Pareto solution set spanning a narrow range of trade-offs. In contrast, for the 2 x current demand scenario, the trade-off between economic efficiency and robustness was considerable.

This variability in outcomes highlights the fact that (possibly large) uncertainty about future climate may not necessarily produce significantly different performance trajectories. The key concept is that of the exogenous stress imposed on the system. This is a subtle concept. It not only reflects the obvious stressors, namely population (and consequent demand) and climate change variability, but also the limits imposed on the feasible solution space which limits the possibilities explored by the optimisation search. For example, if the new surface water source option were not available to add more storage capacity to the system, Figure 36 shows that significantly inferior performance outcomes result. Likewise all the Pareto optimal solutions for the 2 x current demand scenario opted for the maximum new surface water source storage capacity suggesting that making available more opportunities for storage could produce better outcomes.

It is important to appreciate that the robust optimisation does not produce a single answer. Its purpose is to produce a range of “good” solutions that form the basis for negotiation between decision makers and stakeholders. It would be presumptuous to expect that a mathematical formulation could properly capture all the metadata that reflects the preferences of decision makers and stakeholders.

4. END USER PERSPECTIVE ON THE OPTIMISATION METHODOLOGY

This project has developed a methodology that identifies water resource planning and operational decisions that can be characterised as being optimal and also robust in the face of uncertain knowledge about future climate change. It has also demonstrated the application of the methodology in an end user context, with plausible but generalised decision variables, and two objectives relating to economic and social outcomes.

The methodology can be applied by other end users, to different locations and with more objectives. A generic process has therefore been developed to assist other end users in applying the research findings. The process steps are outlined in Figure 39 and described in the remainder of this section.

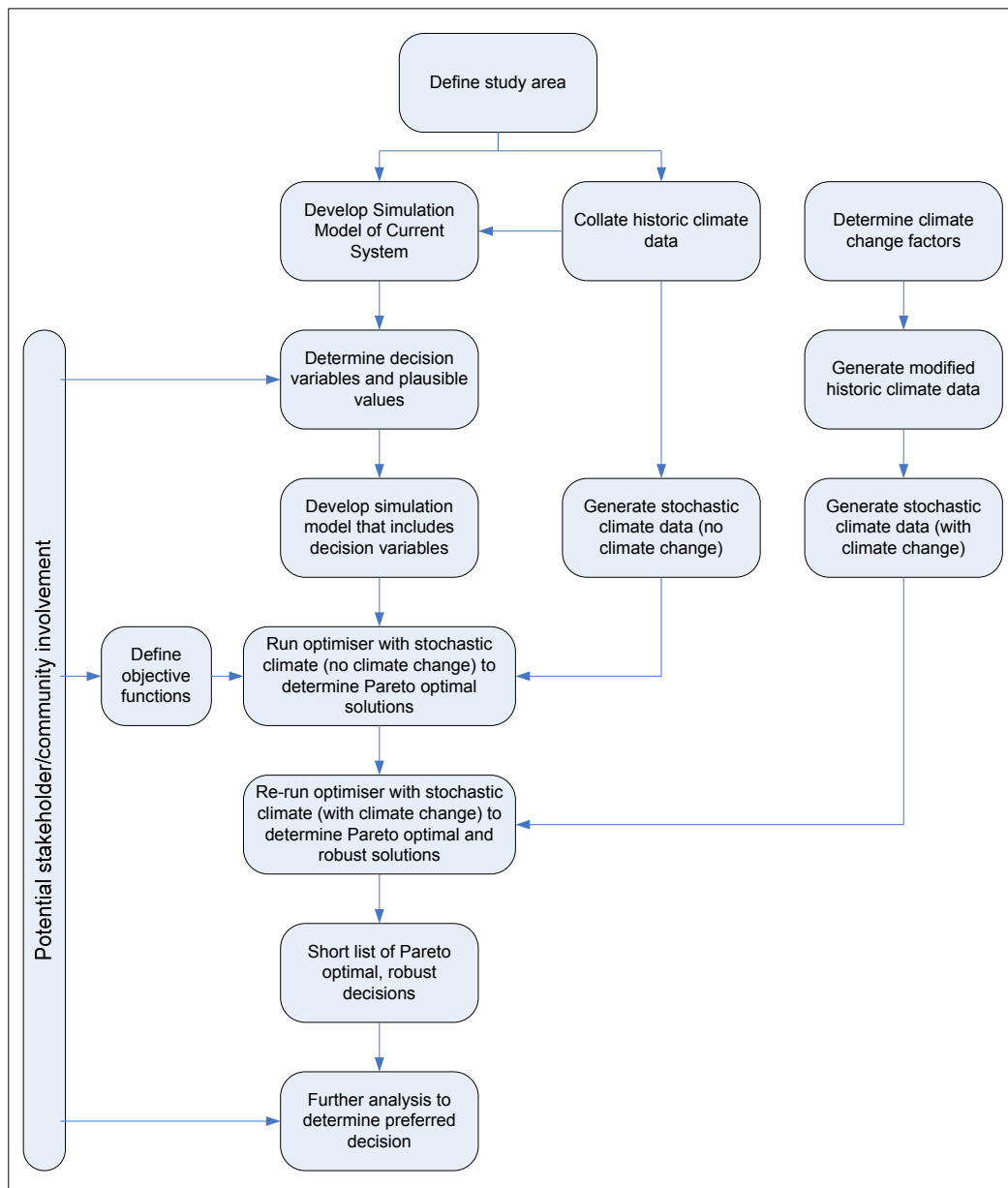


Figure 39 Process for applying the optimisation methodology

4.1 *Define the study area*

The methodology can be applied to any urban bulk water system. It may be useful to define study boundaries in terms of geographic boundaries relevant for administrative purposes e.g. Local Government Area or area of operations of a water utility.

4.2 *Develop a bulk water system simulation model*

The objective of the optimisation is to identify planning and operational decisions that are both optimal and robust in the face of uncertain knowledge about future climate change. Climate change is of greatest relevance to options that involve climate-dependent water sources such as surface water (dams, rivers) or groundwater.

A simulation model of the bulk water system is needed to determine the performance of climate-dependent water sources based on historic and stochastically generated climate data. A range of commercial-off-the shelf rainfall and runoff models are available or the user can custom build models relevant to the study area. The rainfall-runoff models must utilise climate inputs (such as rainfall and PET) that can be perturbed to describe changes in future climate (e.g. climate change factors derived from downscaling results from general circulation models).

4.3 *Augment the bulk water system simulation model with decision variables (e.g. water supply or demand management options)*

Planning and operational decisions need to be added to the simulation model. This may require developing additional rainfall-runoff models for proposed climate-dependent options.

For each decision variable logical boundaries and/or increments need to be defined from which the optimisation software can select possible “decisions”.

4.4 *Derive climate data*

Three types of data are required:

1. Historical data is used to calibrate the bulk water system simulation model.
2. Stochastic data (historical climate) – synthetic climate sequences are generated that preserve the statistical characteristics of historic climate records. Different synthetic climate generators are available such as the lag-1 Markov generation module that is used by the water resource modelling program WATHNET5.
3. Stochastic data (future climate) – for each future climate scenario, the historical data are modified using selected climate change factors (or equivalent) judged to represent plausible lower and upper limits on future climate change, the stochastic model is recalibrated and synthetic climate sequences regenerated.

4.5 *Define objective functions*

Water planning involves many objectives involving social, environmental, financial, economic and risk considerations. The multi-objective optimisation methodology could be applied, in principle, for any number of objectives against which the performance of each option can be quantified (at least in relative terms). It should be noted that the complexity of the Pareto front visualisation and explanation of optimiser results increases dramatically with the number of objectives. For this reason it is desirable to

keep the number of objectives to no more than three or four – this may require weighting of secondary objectives.

The end user is able to choose the time in the water planning process when a particular objective will be considered and the timing of stakeholder involvement. For example, an objective can be included in the optimisation or it could be addressed through alternative processes, such as community/stakeholder engagement on relative preferences from the options identified as Pareto optimal by the optimiser.

The end user is also able to involve stakeholders in defining the objectives and criteria, the metrics used to quantify the objectives. For example, stakeholders may be involved in defining an environmental objective such “minimise greenhouse gas emissions” and also involved in defining an appropriate criterion such as expressing greenhouse gas emissions as the present worth tonnes of CO₂e.

The end user will need to take into account the regulatory framework for their jurisdiction when developing objectives and criteria; for example, present worth calculations may need to use a state treasury endorsed discount rate.

4.6 *Environmental objectives*

Although the case study did not illustrate the use of environmental objectives, their inclusion in the modelling framework is no more complex than the inclusion of economic objectives in the case study. The main challenge lies in defining the environmental objectives in a robust way.

A simple example illustrates the principle. A widely used environmental flow rule is based on the concept of transparent and translucent flow releases. It is expressed as the U/V rule. When the natural flow q is less than U-percentile flow q_U , the flow release is q – this is referred to as a transparent flow in the sense that the reservoir’s presence does not affect the natural flow. When the natural flow exceeds the U-percentile flow, the release is q_U plus V% of the excess – this is referred to as a translucent flow in the sense the reservoir’s presence partly affects the natural flow. Formally the environmental flow release is

$$r = \begin{cases} q & \text{if } q < q_U \\ q_U + V(q - q_U) / 100 & \text{if } q \geq q_U \end{cases} \quad (16)$$

An intuitive environmental objective is to minimise the disruption of the natural flow regime by reservoir regulation. This is equivalent to maximising the variable V. Indeed when V equals 100% the reservoir system would be entirely transparent.

Mortazavi *et al.* (2012) provide a conceptually different example of formulating an environmental objective function. In a case study involving the Sydney bulk water system, they consider the regulation of flows in the Wollondilly river reach between Wingecarribee and Warragamba reservoirs. This reach has been identified as ecologically important. Field studies have identified potentially adverse impacts of altered flow regimes on platypus and water bird populations in the Wollondilly river. To avoid these impacts, the field studies recommended that the maximum monthly regulated flow be limited to 18,300 ML during the winter months from April to August, and to 12,200 ML during the summer months. The ecological impact of exceeding these recommended maxima is not well understood. Nonetheless, it is known that during the summer months, high flows have the highest impacts on the breeding of platypus and water bird populations, while the impacts of high flows are significantly less severe during the winter months. Accordingly, the following environmental stress metric was adopted to penalise the regulated flows exceeding the maximum low impact flows

$$Stress(m) = \begin{cases} \max \left[0, 5 \left(\frac{q_m - 12200}{12200} \right) \right] & \text{if } m \in \{\text{Sept}, \dots, \text{March}\} \\ \max \left[0, \left(\frac{q_m - 18300}{18300} \right) \right] & \text{if } m \in \{\text{April}, \dots, \text{August}\} \end{cases} \quad (17)$$

where q_m is the actual regulated release in the Wollondilly in month m and $Stress(m)$ is the penalty for exceeding the recommended flow limits in month m .

The environmental objective sought to minimise the total stress defined as the sum of the monthly stresses over the simulation. It needs to be stressed that this criterion is based on limited field data and relies on subjective judgments such as the impact in summer months is 5 times that of winter months and that the impact is cumulative.

The considerable epistemic uncertainty about the environmental impacts makes it challenging to formulate robust environmental objectives. Nonetheless, such objective functions need to be constructed if decision makers are to be aware of the trade-offs between environmental and other performance criteria.

4.7 Define constraints

Constraints are used to steer the optimisation away from solutions that are unacceptable or highly undesirable, such as solutions that would allow catastrophic water shortage or unacceptable social hardship.

4.8 Select an optimiser software package

The multi-objective evolutionary algorithm described in section 2.1 can interface with any simulation model. A range of computer codes implementing a range of multi-objective evolutionary algorithms are available. End users with sufficient expertise can link their simulation model to such an optimisation computer code. Ideally such a linkage would be implemented to exploit the inherently parallel architecture of evolutionary algorithms. Most end users will not have the required expertise and will therefore opt for a software package that provides this service. WATHNET5 is an example of such a package.

4.9 Run the optimiser

The optimiser searches through the set of feasible solutions. Each solution requires simulation of the bulk water system using stochastically generated climate data that incorporates the range of possible future climate change.

The optimiser augments the original objectives with the additional objective of minimising the difference in performance using the original criteria over possible climate change scenario(s). The Pareto-optimal solutions trade-off:

- Efficiency expressed as expected performance; and
- Robustness or sensitivity expressed as the difference in performance over the range of climate change scenarios.

4.10 *Further analysis*

The methodology identifies water resource planning and operational solutions (or portfolios) that can be characterised as being optimal and also robust in the face of uncertain knowledge about future climate. These solutions can be seen as a short-list from which to select the preferred planning or operational solution. This may involve further analysis, such as stakeholder/community engagement and fine tuning.

5. GAPS AND FUTURE RESEARCH DIRECTIONS

The technology (represented by software tools) to implement robust optimisation in the context of urban bulk water systems is relatively mature. Although considerable effort was expended in this study to make computations practicable, the most difficult task was associated with formulating the problem, namely what are the objectives, constraints and decisions. This, no doubt, reflects in part the lack of precedent for such studies. However, the deeper problem of capturing the values of decision makers and stakeholders in a way that can be codified should not be underestimated.

In this study, the end user's preference was to use objective functions based on economic and social costs. While there are significant issues valuing social costs, the use of costs ensured the robust optimisation problem was a two-objective problem. This has the advantage of communicating trade-offs in an easy-to-understand format. However, such an approach may hide trade-offs that are important to the decision making process. Moving to a many objective formulation offers one way to resolve this issue at the expense of making the search for the Pareto optimal set computationally and technically more challenging and, more importantly, making the interpretation of results more difficult.

The robust optimisation technology offers radically new opportunities and capabilities. There is a pressing need to test and adapt the technology in industry-relevant contexts.

The approach employed to obtain the climate change factors (i.e. the credible range of potential climate change impacts on rainfall and PET in the lower Hunter region) utilises the work summarised in the Climate Change in Australia study (CSIRO-BoM, 2007). It should be noted that while this approach and methodology is scientifically valid, is recognised as best practice at the time of writing, and satisfied the time and budget constraints of this project, there are other ways a credible range of climate change impacts could have been obtained. Importantly, there is also the possibility that these alternative methods could result in a bigger range of projected climate change impacts and, if this is the case, the optimisation modelling conducted here may not actually do as it is intended to do (i.e. cover the entire range of possible future climate scenarios). Therefore future work should focus on recent advances in climate modelling (e.g. new climate model output available as part of the latest IPCC update and CMIP5), research that evaluates the performance of GCMs and ranks them according to their ability to realistically simulate important aspects of Australian hydro-climatology, and new approaches for developing plausible climate change scenarios and providing climate change advice.

A parallel project of interest is the Eastern Seaboard Climate Change Initiative (ESCCI). In this project, all GCMs have been evaluated and the four "best" GCMs for the eastern seaboard region of Australia (including the Lower Hunter region) have been determined. Work is currently underway which applies three different dynamical downscaling models to the outputs obtained from the four "best" GCMs with the end result being 12 plausible scenarios for different emission scenarios, variables and time horizons. Once this ESCCI work has been completed the range of projected climate change impacts for around 2070 should be compared with the range employed in this study. If the upper (wet) or lower (dry) bound of the range is markedly different then the work conducted here should be repeated to assess the implications and practical benefits of advances in climate change advice – and also to test the robustness of the conclusions obtained here.

Another issue not explored in detail here is the utilisation of different stochastic models, in particular stochastic models that explicitly account for known drivers of interannual to multi-decadal variability and/or stochastic models that utilise pre-instrumental

information (i.e. palaeoclimate data) to put the period covered by the historically observed data into context (i.e. is it biased towards a dry or wet epoch) and to gain a better representation of the full spectrum of natural hydro-climatic variability that has occurred in the past – for example, see Henley *et al.* (2011). Table 2 and Table 3 show that the stochastic modelling approach used here is satisfactory. However, as with the climate change scenarios, future research could focus on utilising a variety of stochastic modelling approaches, assessing the sensitivities, strengths and weaknesses of each, and, importantly, determining what (if any) difference it makes for the optimisation modelling and resulting conclusions.

REFERENCES

- Argent, R.M., Murray, N., Podger, G.M., Perraud, J.-M. and Newham, L. (2007), E2 Reference Manual: Component Models.
- Australian Federal Treasury, 2005, Water and Australia's Future Economic Growth, available at http://www.treasury.gov.au/documents/1087/PDF/05_Water.pdf
- Barrico C. and C. H. Antunes (2006). "Robustness analysis in multi-objective optimisation using a degree of robustness concept". 2006 IEEE Congress on Evolutionary Computation. Sheraton Vancouver Wall Centre Hotel, Vancouver, BC, Canada July 16-2.
- Blöschl, G., and A. Montanari (2010), Climate change impacts—Throwing the dice?, Hydrol. Processes, 24, 374–381, doi:10.1002/hyp.7574.
- BMT WBM (2012), Derivation of Williams River Flow Datasets, prepared for Hunter Water Corporation, Andrew Grant and Philip Pedruco, R.M8248.001.01, Melbourne, Victoria
- Chiew, FHS and Siriwardena L (2005) Estimation of SIMHYD parameter values for application in ungauged catchments. In: MODSIM 2005 International Congress on Modelling and Simulation, Modelling and Simulation Society of Australia and New Zealand, Melbourne, December 2005, pp. 2883-2889, CDROM (ISBN 0-9758400-2-9).
- Cinque, K. (2009), A Quantitative Approach to Assessing the Effectiveness of Catchment Management for the Improvement of Drinking Water Quality, PhD thesis, RMIT University, Australia
- Coello, C. A., G. B. Lamont and D. A. V. Veldhuizen (2007). Evolutionary Algorithms for Solving Multi-Objective Problem, Springer
- CSIRO-BoM (2007), Climate Change in Australia: Technical Report, CSIRO Publishing. 141 pp. www.climatechangeinaustralia.gov.au.
- Cui, L. and Kuczera, G. (2010) coping with climate change uncertainty using robust multi-objective optimisation : application to urban water supply systems, Practical Responses to Climate Change National Conference 2010, Engineers Australia, Melbourne.
- Deb, K. (2001). Multi-objective optimisation using evolutionary algorithms, John Wiley & Sons, Inc.
- Deb, K., M. Mohan and S. Mishra (2003), A Fast Multi-objective Evolutionary Algorithm for Finding Well-Spread Pareto-Optimal Solutions, Rep. KanGAL Report No. 2003002, Indian Institute of Technology
- Deb, K. and H. Gupta (2006). "Introducing robustness in multi-objective optimisation ." Evolutionary Computation, 14(4): 463-494
- Dessai, S., Hulme, M., Lempert, R. and Piekle, Jr., R. (2009). Do we need better predictions to adapt to a changing climate, Eos, transactions of American Geophysical Union, 90(13).
- Dessai, S., Hulme, M., Lempert, R. and Piekle, Jr., R., "Do we need better predictions to adapt to a changing climate", Eos, transactions of American Geophysical Union, (2009). 90(13).
- Erlanger, P., and B. Neal (2005), Framework for Urban Water Resource Planning, Occasional Paper No. 14 - June 2005, Water Services Association of Australia, Melbourne.
- Grafton, R.Q. and M. Ward (2008). Prices Versus Rationing: Marshallian Surplus and Mandatory Water Restrictions, Economic Record, 84:S57-S65.

- Henley, B. J., M. A. Thyer, G. Kuczera, and S. W. Franks (2011) Climate-informed stochastic hydrological modelling: Incorporating decadal-scale variability using paleo data, *Water Resour. Res.*, 47, doi:10.1029/2010WR010003.
- HWC (2012), SoMo Documentation - Hunter Water Headworks Simulation Model, Version 2012.3c.
- Jin Y. and B. Sendhoff (2003). Trade-off between performance and robustness: An evolutionary multi-objective approach. *Evolutionary Multi-Criterion Optimisation*, pp.237 - 251, 2003. Springer-Verlag.
- Kiem, A. S., and D. C. Verdon-Kidd (2011), Steps toward “useful” hydroclimatic scenarios for water resource management in the Murray-Darling Basin, *Water Resour. Res.*, 47, W00G06, doi: 10.1029/2010WR009803.
- Koga, F. (2012) Aiming for a Water Conservation-Conscious City: Fukuoka City, www.urc.or.jp/summit/news/series1.pdf, viewed 28 Dec 2012.
- Kollat, J. B. and P. M. Reed (2006). "Comparing state-of-the-art evolutionary multi-objective algorithms for long-term groundwater monitoring design." *Advances in Water Resources*, 29(6): 792-807
- Koutsoyiannis, D., A. Efstratiadis, N. Mamassis, and A. Christofides (2008), On the credibility of climate predictions, *Hydrol. Sci. J.*, 53(4), 671–684, doi:10.1623/hysj.53.4.671.
- Koutsoyiannis, D., A. Montanari, H. F. Lins, and T. A. Cohn (2009), Climate, hydrology and freshwater: Towards an interactive incorporation of hydrological experience into climate research, *Hydrol. Sci. J.*, 54(2), 394–405, doi:10.1623/hysj.54.2.394.
- Kuczera, G. (1992). "Water supply headworks simulation using network linear programming." *Advances in Engineering Software*, 14(1): 55-60
- Kuczera, G., Cui, L., Gilmore, R., Graddon, A., Mortazavi, M. and Jefferson, C. (2009). Addressing the shortcomings of water resource simulation models based on network linear programming, *Proc. 31st Hydrology and Water Resources Symposium.*, Newcastle, Engineers Australia.
- Laumanns, M., L. Thiele, K. Deb and E. Zitzler (2002). "Combining Convergence and Diversity in Evolutionary Multiobjective Optimisation ." *Evolutionary Computation*, 10(3): 263-282
- Lim, W. H., and M. L. Roderick (2009), *An Atlas of the Global Water Cycle Based on the IPCC AR4 Climate Models*, ANU E Press, Canberra.
- Luo B. and J. Zheng (2008). “A New Methodology for Searching Robust Pareto Optimal Solutions with MOEAs”. *IEEE Congress on Evolutionary Computation*, pp 580-586
- Mahmoud, M., Liu, Y. *et al.*, (2009) A formal framework for scenario development in support of environmental decision-making, *Environmental Modelling & Software* 24 798–808.
- Marsden Jacob Associates (2006) *Economic Cost of Water Restrictions In South East Queensland*, For The Queensland Department Of Natural Resources & Water
- Matalas, N. C. (1967). Mathematical assessment of synthetic hydrology. *Water Resources Research* 3(4), pp. 937-945.
- Matalas, N. C. and M. B. Fiering (1977). Water-resource System planning. *Climate, Climatic Change, and Water Supply*, Natl. Acad. of Sci., Washington, D.C., 99–110.
- McMahon, T.A., Kiem, A.S., Peel, M.C., Jordan, P.W. and Pegram, G.G.S. (2008): A new approach to stochastically generating six-monthly rainfall sequences based on Empirical Model Decomposition. *Journal of Hydrometeorology*, 9, 1377-1389.

- Montanari, A., G. Blöschl, M. Sivapalan, and H. Savenije (2010), Getting on target, *Public Serv. Rev. Sci. Technol.*, 7, 167–169.
- Mortazavi, M., G. Kuczera, and L. Cui (2012), Multiobjective optimisation of urban water resources: Moving toward more practical solutions, *Water Resour. Res.*, 48, W03514, doi:10.1029/2011WR010866.
- Mulvey J.M., R.J. Vanderbei and S.A. Zenios (1995). Robust optimisation of large-scale systems. *Operations Research*, 43, pp. 264–281.
- National Climate Change Adaptation Research Facility (2010), National Climate change adaptation research plan: Water resources and freshwater Biodiversity, Southport, Queensland, Australia. [Available at www.nccarf.edu.au/national-adaptation-research-plan-water-resourcesfreshwater-Biodiversity.]
- Parry, M. L., O. F. Canziani, J. P. Palutikof, P. J. van der Linden, and C. E. Hanson (Eds.) (2007), Contribution of Working Group II to the Fourth Assessment Report of the Intergovernmental Panel on Climate Change, Cambridge Univ. Press, Cambridge, UK.
- Randall, D. A., *et al.* (2007), Climate models and their evaluation, in *Climate Change 2007: The Physical Science Basis. Contribution of Working Group I to the Fourth Assessment Report of the Intergovernmental Panel on Climate Change*, edited by S. Solomon *et al.*, chap. 8, pp. 589–662, Cambridge Univ. Press, Cambridge, U. K.
- SKM. (2003). Hunter Water - Water Resources Model Review, Sinclair Knight Merz.
- Verdon-Kidd, D. C., and A. S. Kiem (2010), Quantifying drought risk in a non-stationary climate, *J. Hydrometeorol.*, 11(4), 1019–1031, doi:10.1175/2010JHM1215.1.
- Watkins Jr, D. W., McKinney, D. C (1997). Finding Robust Solutions to Water Resources Problems. *Journal of Water Resources Planning and Management*, Vol. 123, No. 1, January/February, ISSN 0733-9496/97/0001-0049-0058. Paper No. 11872.

